



## P-T-t-deformation–fluid characteristics of lode gold deposits: evidence from alteration systematics

T. Campbell McCuaig<sup>1</sup>, Robert Kerrich \*

Department of Geological Sciences, University of Saskatchewan, Saskatoon, Saskatchewan, Canada S7N 5E2

Received 1 February 1997; accepted 8 April 1998

---

### Abstract

Structurally hosted lode gold-bearing quartz vein systems in metamorphic terranes possess many characteristics in common, spatially and through time; they constitute a single class of epigenetic precious metal deposit, formed during accretionary tectonics or delamination. The ore and alteration paragenesis encode numerous intensive and extensive variables that constrain the pressure–temperature–time–deformation–fluid (*P*–*T*–*t*–d–f) evolution of the host terrane and hence the origin of the deposits. The majority of lode gold deposits formed proximal to regional translithospheric terrane–boundary structures that acted as vertically extensive hydrothermal plumbing systems; the structures record variably thrust, and transpressional–transtensional displacements. Major mining camps are sited near deflections, strike slip or thrust duplexes, or dilatational jogs on the major structures. In detail most deposits are sited in second or third order splays, or fault intersections, that define domains of low mean stress and correspondingly high fluid fluxes. Accordingly, the mineralization and associated alteration is most intense in these flanking domains. The largest lode gold mining camps are in terranes at greenschist facies; they possess greenschist facies hydrothermal alteration assemblages developed in cyclic ductile to brittle deformation that reflects interseismic–coseismic cycles. Interseismic episodes involve the development of ductile S–C shear zone fabrics that lead to strain softening. Pressure solution and dislocation glide microstructures signify low differential stress, slow strain rates of  $\leq 10^{-13} \text{ s}^{-1}$ , relatively high confining stress, and suprathydrostatic fluid pressures. Seismic episodes are induced by buildup of fluid pressures to supralithostatic levels that induce hydraulic fracturing with enhanced hydraulic conductivity, accompanied by massive fluid flow that in turn generates mineralized quartz veins. Hydrothermal cementing of ductile fabrics creates ‘hardening’, lowers hydraulic conductivity, and hence promotes fault valve behaviour. Repeated interseismic (fault valve closed), coseismic (valve open) cycles results in banded and/or progressively deformed veins. Alteration during both interseismic and coseismic episodes typically involves the hydrolysis of metamorphic feldspars and Fe, Mg, Ca-silicates to a muscovite/paragonite–chlorite  $\pm$  albite/K-feldspars assemblage; carbonization of the metamorphic minerals to Ca, Fe, Mg-carbonates; and sulphidation of Fe-silicates and oxides to sulphides. Geochemically this is expressed as additions of K, Rb, Ba, Cs, and the volatiles H<sub>2</sub>O, CO<sub>2</sub>, CH<sub>4</sub>, H<sub>2</sub>S in envelopes of meter to kilometer scale. K/Rb and K/Ba ratios are close to average crustal values, potentially ruling out late stage magmatic fluids where K/Rb and K/Ba are respectively lower and higher than crustal values. Smaller deposits are present in subgreenschist, and amphibolite to granulite facies terranes. The former are characterized by subgreenschist facies alteration assemblages, vein

---

\* Corresponding author. Tel.: +1-306-966-5719; fax: +1-306-966-8593; e-mail: kerrich@pangea.usask.ca

<sup>1</sup> Present address: Steffen Robertson Kirsten Consulting, 25 Richardson Street, West Beach, W.A. 6005, Australia.

stockworks, brittle fracturing and cataclastic microstructures, whereas the latter feature amphibolite to granulite facies alteration assemblages, ductile shear zones, ductilely deformed veins, and microstructures indicative of dislocation climb during interseismic episodes. Hence the lode gold deposits constitute a crustal continuum of deposits from subgreenschist to granulite facies, that all formed synkinematically in broad thermal and rheological equilibrium with their host terranes. These characteristics, combined with the low variance of alteration assemblages in the higher temperature deposits, rules out those being metamorphosed counterparts of greenschist facies deposits. Deposits at all grades have a comparable metal inventory with high concentrations of Au and Ag, where Au/Ag averages 5, with enrichments of a suite of rare metals and semi-metals (As, Sb, ± Se, Te, Bi, W, Mo and B), but low enrichments of the base (Cu, Pb, Zn, Cd) and other transition (Cr, Ni, Co, V, PGE, Sc) metals relative to average crust. The hydrothermal ore-forming fluids were dilute, aqueous, carbonic fluids, with salinities generally  $\leq 3$  wt.% NaCl equivalent, and  $X_{(\text{CO}_2 \pm \text{CH}_4)}$  10–24 wt.%. They possess low Cl but relatively high S, possibly reflecting the fact that metamorphic fluids are generated in crust with  $\sim 200$  ppm Cl, but  $\sim 1$  wt.% S. Primary fluid inclusions are: (1)  $\text{H}_2\text{O}-\text{CO}_2$ , (2)  $\text{CO}_2$ -rich with variable  $\text{CH}_4$  and small amounts of  $\text{H}_2\text{O}$ , and (3) 2-phase  $\text{H}_2\text{O}$  (liquid–vapor) inclusions. Inclusion types 2 and 3 represent immiscibility of the type 1 original ore fluid. Immiscibility was triggered by fluid pressure drop during the coseismic events and possibly by shock nucleation, leading to highly variable homogenization temperatures in an isothermal system. A thermodynamic evaluation of alteration assemblages constrains the ore fluid pH to 5–6; redox controlled by the  $\text{HSO}_4/\text{H}_2\text{S}$  and  $\text{CO}_2/\text{CH}_4$  buffers; and  $X_{\text{CO}_2}$  that varies. The higher temperature deposits formed under marginally more oxidizing conditions. Stable isotope systematics of the ore and gangue minerals yields temperatures of 200–420°C, consistent with the crustal spectrum of the deposits, very high fluid rock ratios, and disequilibrium of the externally derived ore fluids with wall rocks. The ore fluid  $\delta\text{D}$  and  $\delta^{18}\text{O}$  overlap the metamorphic and magmatic ranges, but the total dataset for all deposits is consistent only with dominantly metamorphic fluids. Carbon isotope compositions of carbonates span –11 to +2‰ and show provinciality: this is consistent with variable proportions of reduced C (low  $\delta^{13}\text{C}$ ) and oxidized C (higher  $\delta^{13}\text{C}$ ) in the source regions contributing  $\text{CO}_2$  and  $\text{CH}_4$  to the ore fluids. In some instances, C appears to have been derived dominantly from proximal to the deposits, as in the Meguma terrane ( $\delta^{13}\text{C} \sim -22\text{\textperthousand}$ ). Sulphur isotope compositions range from 0 to +9‰, and are consistent with magmatic S, dissolution or desulphidation of magmatic sulphides, or average crustal sulphides.  $^{34}\text{S}$ -depleted sulphides occur in ore bodies such as Hemlo where fluid immiscibility led to loss of  $\text{H}_2\text{S}$  and consequent fluid oxidation. Gold is probably transported as an  $\text{Au}(\text{HS})_2^-$  complex. Relatively high S but low Cl in the hydrothermal fluid may explain the high Au slow base metal characteristic of the deposits. Gold precipitated in ore bodies due to loss of S from the ore fluid by sulphidation of wall rock, or immiscibility of  $\text{H}_2\text{S}$ ; and by oxidation or reduction of the fluid, or by chemisorption, or some combination of these processes. Most lode gold deposits have been brittle reactivated during uplift of host terranes, with secondary brines or meteoric water advecting through the structures. These secondary fluids may remobilize gold, generate retrograde stable isotope shifts, reset mineral geochronometers, and leave trails of secondary fluid inclusions. Data on disturbed minerals has led to invalid models for lode gold deposits. The sum of alteration data leads to a model for lode gold deposits involving a clockwise  $P-T-t$  evolution and synkinematic and synmetamorphic mineralization of the ‘deep later’ type. During terrane accretion oceanic crust and sediments are subcreted beneath the terrane boundary. Thermal equilibration generates metamorphic fluids that advect up the terrane structure, at lithostatic fluid pressure, into the seismogenic zone where the majority of deposits form. Thus many lode gold deposits are on intrinsic part of the development of subduction–accretion complexes of the high-T, low-P type. © 1998 Elsevier Science B.V. All rights reserved.

**Keywords:** lode gold; alteration; hydrothermal system; paragenesis; metamorphism, subduction–accretion

## 1. Introduction and scope

Alteration reflects numerous characteristics of hydrothermal systems that stem from open system chemical and isotopic exchange between an externally derived ore-forming fluid and rocks contiguous with an orebody. Conventionally, most alteration studies have addressed singular aspects of this alter-

ation process: examples include paragenesis, element budgets, chemical mass balance, regional or local lithgeochemistry, metasomatic and thermodynamic theory, activity relationships of alteration phases, fluid inclusion studies, and stable and radiogenic isotope systematics.

Viewed as a whole, hydrothermal alteration reflects an intricate interplay between rheological be-

haviour, fluid dynamics, and chemical and isotopic exchange. Alteration encodes information on intensive ( $P, T, X_{CO_2}$ ...etc.) and extensive (fluid flux, mass of ore or gangue) properties of the larger hydrothermal system within and external to orebodies, and the secular relationship of mineralization to regional deformation, magmatism and metamorphism. Similarly, different attributes of alteration may record equilibrium (fluid–mineral  $^{18}O/^{16}O$ ;  $a_K/a_H$  vs.  $a_{Na}/a_H$ —muscovite/albite) or disequilibrium conditions (hydraulic fracturing, fluid pressure transients, dynamic alteration fronts, partial overprinting by secondary fluids). Consequently, in this review we attempt a wholistic approach to alteration, in the recognition, for instance, that vein banding and paragenesis, gold grade, fluid phase separation, hydraulic fracturing, strain rate, and the coseismic–interseismic cycle are interrelated phenomena.

An emergent theme in research on lode gold deposits is an attempt rigorously to constrain the pressure–temperature–time–deformation–fluid ( $P-T-t-d-f$ ) characteristics of the hydrothermal system, and to place this in the context of the larger  $P-T-t-d$  evolution of the host terrane, collectively linked to the geodynamic setting (Clark et al., 1986, 1989; Craw and Koons, 1989; Kerrich, 1989a,b; Goldfarb et al., 1993; Groves et al., 1992; Phillips and Powell, 1993; Stüwe et al., 1993a,b; McCuaig et al., 1993). Accordingly, we attempt to synthesize those aspects of hydrothermal alteration associated with lode gold deposits that provide information on  $P-T-t-d-f$  characteristics of the ore-forming system.

The general characteristics of lode gold deposits, including their secular distribution, are first summarized. The architecture of the hydrothermal plumbing systems is then described from the terrane to intra-deposit scale. The range of tectonic fabrics that develop during alteration is discussed in terms of their significance for ambient  $P, T$ , stress, strain rate conditions, and the cyclic interaction of deformation, alteration, and fluid processes. Geochemical features of alteration are addressed for the metal inventory of the deposits and major- and trace-element distributions. The properties of the hydrothermal fluids inducing alteration and associated ore deposition are synthesized from fluid inclusion, phase equilibria, and stable and radiogenic isotope studies, including treatment of possible sources of the ore, fluid, and

gangue components. Transport and depositional mechanisms for gold are reviewed in light of alteration studies, and the timing of mineralization relative to deformation, magmatism, and metamorphism is considered from the geochronology of alteration minerals. In the summary, we draw the relevant lines of data together to synthesize a  $P-T-t-d-f$  scheme for lode gold deposits in their larger geodynamic setting.

## 2. Characteristics of lode gold deposits

Structurally hosted lode gold vein systems in metamorphic terranes constitute a coherent class of epigenetic precious-metal deposits; they are associated in space and time with accretionary tectonics (Kerrich and Wyman, 1990; Barley and Groves, 1992). Their origin, however, has been contentious for over a century, and there remain polarized views on both the timing and mode of their formation. This class of Au–Ag deposits has variously been named lode or reef type, terms that include veins in shear zones, through stockworks, to mineralized wall rocks. The term mesothermal or mesozonal has also been used in view of their predominance in mid-crustal, greenschist facies environments. However, the deposits are now known to have formed over a large range of crustal depths from > 25 km to the near surface environment; hence those terms are not appropriate (Groves, 1993; Groves et al., 1998). Gold only (Hodgson, 1982) is a misnomer inasmuch as the deposits contain significant Ag, with Au/Ag ratios averaging 5, and sporadically have enrichments of W and Te. Here, ‘turbidite’, or ‘slate’-belt hosted lode gold deposits are included with their greenstone-hosted counterparts, as they all share common metal budgets, ore-fluid characteristics, and geodynamic setting. Mother-lode type deposit is too parochial a label. The moniker ‘orogenic’ has recently been introduced for this class of lode deposit (Groves et al., 1998). This term captures the fact that the deposits are associated in space and time with collisional tectonic regimes. However, the Porgera deposit, Papua New Guinea, and other gold deposits in the southwestern Pacific, such as the epithermal Lahir deposit, also formed in collisional tectonic regimes, yet these have very different characteristics

than lode gold deposits, and did not form in metamorphosed terranes (Richards and Kerrich, 1993). Here we adopt the non-genetic term lode gold.

This class of precious metal deposit differs in terms of paragenesis, alteration style, metal budget, ore fluid chemistry, structural style, and geodynamic setting from Carlin-type, Porgera, epithermal or bonanza gold deposits, that collectively do not form coevally with metamorphism of the host terrane, and are associated with intracontinental extension or magmatic arcs (Bonham, 1989; Berger and Bagby, 1991; Henley, 1991; Richards and Kerrich, 1993; Kerrich, 1993).

Studies of lode gold deposits of all ages has revealed a number of common characteristics (Groves and Phillips, 1987; Kerrich, 1987, 1989a,b; Colvine et al., 1988; Böhlke, 1989; Colvine, 1989; Goldfarb et al., 1989, 1993, 1997; Rock et al., 1989; Ho et al., 1990a, 1992; Kontak et al., 1990; Cox et al., 1991; Groves and Foster, 1991; Poulsen et al., 1992; Foster and Piper, 1993; Phillips and Hughes, 1996). The principal characteristics are as follows:

1. Rich lode Au metallogenic provinces are associated with external supercontinent cycles, or external domains of internal supercontinent aggregation cycles.
2. The timing of mineralization is late-accretion, within the larger time frame of orogenic belts involving accretion of one or multiple allochthonous terranes.
3. Deposits are sited proximal to major accretionary structures within, or at the boundaries of, composite metamorphosed volcanic-plutonic or sedimentary terranes. Less commonly, deposits occur internal to terranes with no regional structure evident. In such cases outboard accretion likely leads to inboard lithosphere delamination.
4. Lode gold deposits are distributed in belts of great geological complexity, with gradients of lithology, strain, and metamorphic grade, reflecting an accretionary environment.
5. Supergiant lode gold metallogenic provinces are in greenschist facies metamorphic terranes.
6. Deposits are structurally hosted, associated with second or higher order splays of translithospheric faults.
7. Deposits are generally restricted to the brittle-ductile transition.

8. Gold precipitation is synkinematic, typically in a high-angle reverse fault regime, but with some examples in transcurrent fault regimes.
9. The alteration mineral paragenesis in greenschist facies domains is dominated by quartz, carbonate, mica, ( $\pm$  albite), chlorite, pyrite, scheelite and tourmaline.
10. There is a distinctive element association characterized by enrichment in Au, Ag( $\pm$  As, Sb, Te, W, Mo, Bi, B), with low enrichments of Cu, Pb, Zn relative to the background abundances. In Phanerozoic deposits Mo and Te are only enriched where veins cut felsic intrusions.
11. Ore forming hydrothermal fluids are dilute aqueous carbonic fluids, with uniformly low fluid salinities (typically  $\leq$  6 wt.% NaCl equivalent), and  $\text{CO}_2 \pm \text{CH}_4$  contents of 5–30 mole% and sporadic  $\text{H}_2\text{O}-\text{CO}_2$  unmixing.
12. Fluid pressures fluctuate from supra-lithostatic to sub-lithostatic within the brittle-ductile shear zones.
13. Lode systems may have vertical extents of up to 2 km, with a lack of zoning, or weak zoning, within deposits, albeit with some zoning of metal content at the scale of an entire mining district.
14. Primary stable and radiogenic isotope characteristics are uniform within deposits, albeit with interdeposit variations.
15. Mineralization is typically syn- to post-peak metamorphism.
16. Lamprophyres are closely associated in space and time with mineralization in many deposits.
17. Reactivation of the gold hosting structures is typical: reactivation may generate a secondary paragenesis, and reset some primary isotopic signatures.

Most of these deposits occur in terranes that experienced greenschist facies metamorphism, and the deposits feature greenschist-facies alteration assemblages. Recently, it has been recognized that Archean lode gold deposits in sub-greenschist, amphibolite, and granulite facies terranes share numerous characteristics, such as structural hosting, metal inventory, element association, and ore fluid properties and likely source, in common with greenschist hosted mesothermal counterparts (Colvine et al., 1988; Kerrich, 1989a,b; Ho et al., 1990b, 1992; Groves et al., 1992; Groves, 1993; Hodgson, 1993).

Accordingly, this class of structurally hosted Au–Ag vein deposits may be viewed as forming over a crustal depth range, or ‘crustal continuum’, extending from granulite to sub-greenschist facies environments (Groves et al., 1992; Groves, 1993). All lode gold deposits of this class are hosted in metamorphosed terranes, and this feature is arguably one of the most significant unifying characteristics. On this basis, and from the structural style of the host terranes, Polat and Kerrich (1997) argued that many lode gold provinces are an integral part of the development of high-*T*, low-*P* type subduction–accretion complexes.

This review is concerned with lode gold deposits that formed close in space and time with accretion and metamorphism of the host terranes (Kerrich and Cassidy, 1994; Kent et al., 1996). Smaller deposits may form later in the same terranes; these tend to have distinct mineral parageneses (Robert, 1994, 1995). Gold concentrations may also occur much later by secondary remobilization of primary ore, as in the Proterozoic gold orebodies at Chibougamau, Quebec (Guha and Kanwar, 1987).

### **3. Structural architecture of lode gold hydrothermal systems**

As hydrothermal alteration is intimately linked to deformation mechanisms and fracture/shear zone geometry in lode Au deposits, a brief synopsis of the structural architecture of their hydrothermal systems is warranted. Structural features common to lode gold deposits of all ages and geographic locations are listed below.

#### *3.1. Regional scale structure*

Deposits are associated with, or proximal to, first-order transcrustal generally terrane-bounding, or ‘docking’ structures that mark the boundaries of distinct, tectonically juxtaposed metamorphosed supracrustal sequences, or tectonostratigraphic terranes (Wyman and Kerrich, 1988; Colvine, 1989; Kerrich and Wyman, 1990, 1993; Groves and Foster,

1991; Goldfarb et al., 1993). Examples include the Destor–Porcupine and Kirkland Lake–Cadillac faults, that demarcate three distinct tectonostratigraphic terranes in the Archean Abitibi subprovince; the Boulder–LeFroy fault in the Archean Norseman–Wiluna belt associated with the giant Kalgoorlie Terrane lode gold deposits; The Hercynian suture in Uzbekistan to which the Muruntau deposit is proximal (Drew et al., 1996); the Melones fault in the Foothills Metamorphic Belt of California, that host the late Mesozoic Mother Lode gold province; and the Coast Range Megalineament along which the Cenozoic Juneau gold deposits are distributed (Fig. 1A, B; Clark et al., 1986; Böhlke and Kistler, 1986; Colvine, 1989; Hronsky et al., 1990; Poulsen et al., 1992; Goldfarb et al., 1993, 1997).

These first-order structures are typically characterized by megaboudinage; doubly plunging folds; complex anastomosing brittle–ductile shear zones; well-defined L–S tectonic fabrics with lineations ranging from steeply dipping to subhorizontal attitudes, and gradients of lithological type, metamorphic grade, and intensity of metasomatic alteration (Kerrich, 1986; Colvine et al., 1988; Hodgson, 1989; Swager, 1993). The geometry and displacement vectors in these complex structures indicate protracted histories of episodic movement and continued reactivation and are poorly understood. Many are high-angle reverse faults with later transcurrent motion (Hodgson, 1989; Swager, 1993). The geometry of these regional structures at depth is poorly constrained. There is some seismic evidence from the Abitibi greenstone belt that the high-angle structures that host the deposits become listric at depth (Fig. 1B). Local connection to depths of ~80 km in the mantle lithosphere is indicated by the syn-kinematic emplacement of lamprophyres along the structures, and the geochemistry of the lamprophyre dykes (Wyman and Kerrich, 1988).

Major mining camps are located on regional structures where there are large-scale discontinuities, such as dilational or antidilational jogs as at Kirkland Lake and Malartic (Fig. 1A); deflections with or strike-slip or thrust duplexes, for example, Timmins (Fig. 1A); or fault bifurcations or sharp changes in attitude exemplified by the Angel Camp and Jackson–Plymouth gold districts of the Foothills Metamorphic belt, CA.

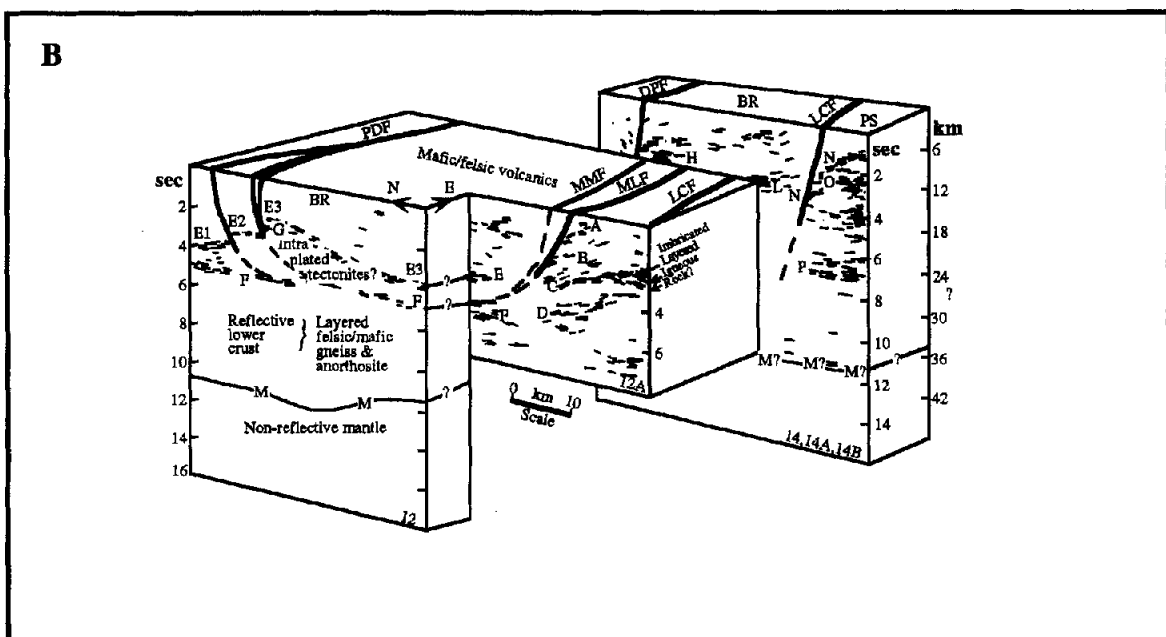
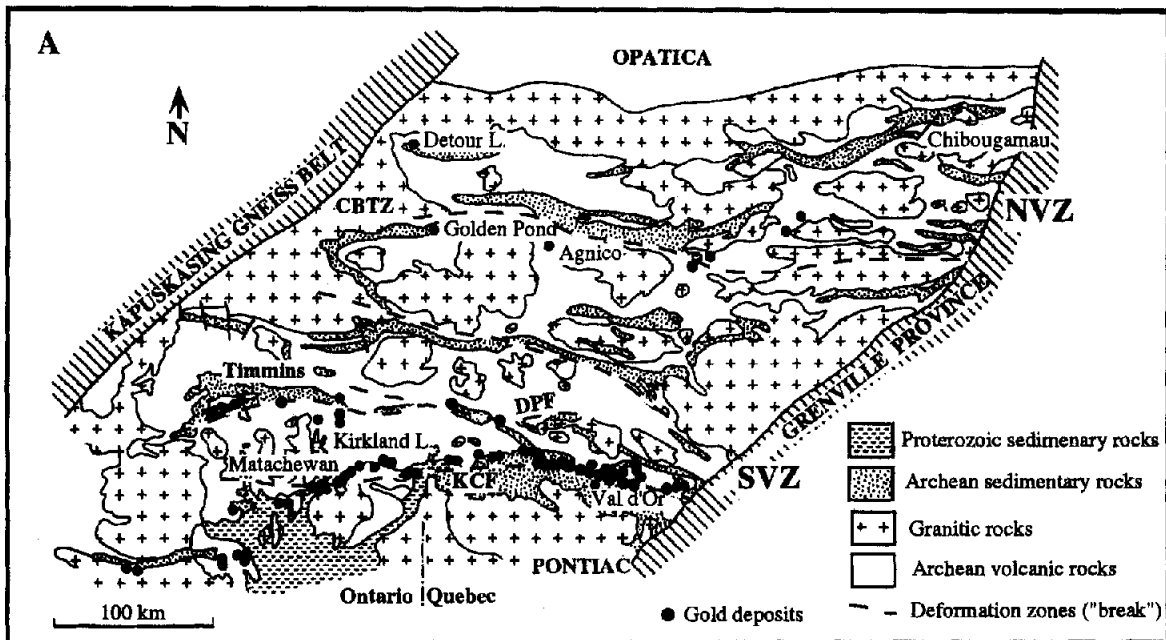


Fig. 1. (A) Distribution of lode gold deposits proximal to regional terrane bounding faults in the Archean Abitibi greenstone belt, Canada. In detail the orebodies are generally located north or south of the main east–west-trending structures. NVZ—Northern Volcanic Zone; SVZ—Southern Volcanic Zone; CBTZ—Casa–Baradi Tectonic Zone. DPF—Destor Porcupine Fault. KCF—Kirkland–Lake Cadillac Fault (Modified from Ludden et al., 1986, and Roberts, 1986). (B) Interpretation of major structures in the Abitibi belt in three dimensions, from vibroseis data. DPF as in A. LCF—Larder Lake Cadillac Fault. BR—Blake River Group. PS—Pontiac Subprovince. LCF of (B) is KCF of (A) (modified from Jackson et al., 1995).

### 3.2. Mine scale structure

Although spatially and temporally associated with structures of regional extent, lode gold deposits are rarely located within these first-order structures, but instead are hosted in second- or higher-order splays off of the regional structures. This geometrical relationship is particularly well developed in the Abitibi subprovince, where the majority of the deposits are located to the north or south of the two major east–west-trending structures; the Destor–Porcupine and Kirkland Lake–Cadillac faults (Fig. 1A). At Timmins, the giant Hollinger–McIntyre–Coniaunium and Dome vein systems (Fig. 2) are respectively on the Hollinger and Dome faults, second-order splays of the first-order Destor–Porcupine fault. Similarly, the Kirkland Lake and Val d'Or camps are north of the regional Kirkland Lake–Cadillac fault. The giant lode gold deposits of the Kalgoorlie–Kambalda trend, Western Australia, are distributed east and west of the Boulder–LeFroy fault on subsidiary splays (Travis et al., 1971).

The reasons why the deposits typically flank the first-order structures are not well understood. Three

hypotheses have been advanced: (1) that a temperature gradient exists laterally away from the first-order structure, inducing gold precipitation with decreasing temperature (Eisenlohr et al., 1989); (2) that the first-order structures, often developed in talc or mica schists, are more ductile in character and thus largely aseismic with more continuous deformation, whereas subsidiary splays in flanking brittle lithologies are more seismically active, leading to greater fluid-pressure fluctuations, enhanced fluid flow and physico-chemical conditions conducive to gold precipitation (Kerrich, 1989a,b); or (3) that the permeability and fluid flux are greater in the rocks flanking the first-order structures because these are zones of low mean stress (Ridley, 1993; Groves et al., 1995). These possibilities have yet to be adequately resolved, and processes (2) and (3) may be related; however, temperature gradients are unlikely to be a significant control given the lack of mineralogical, stable isotope or fluid inclusion evidence for temperature gradients between the deposits and barren structures (Section 9).

On the scale of individual deposits, the morphology of fracture and shear zone systems in these

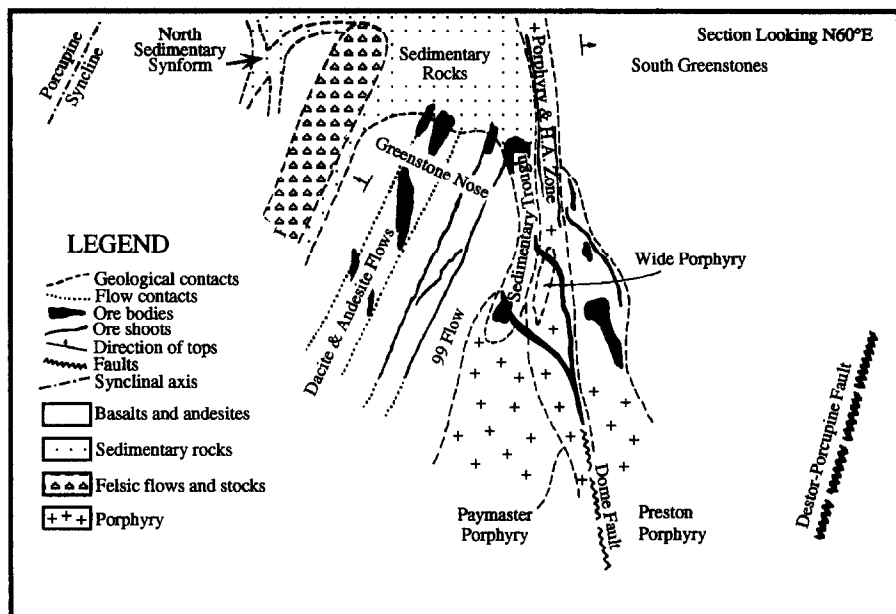
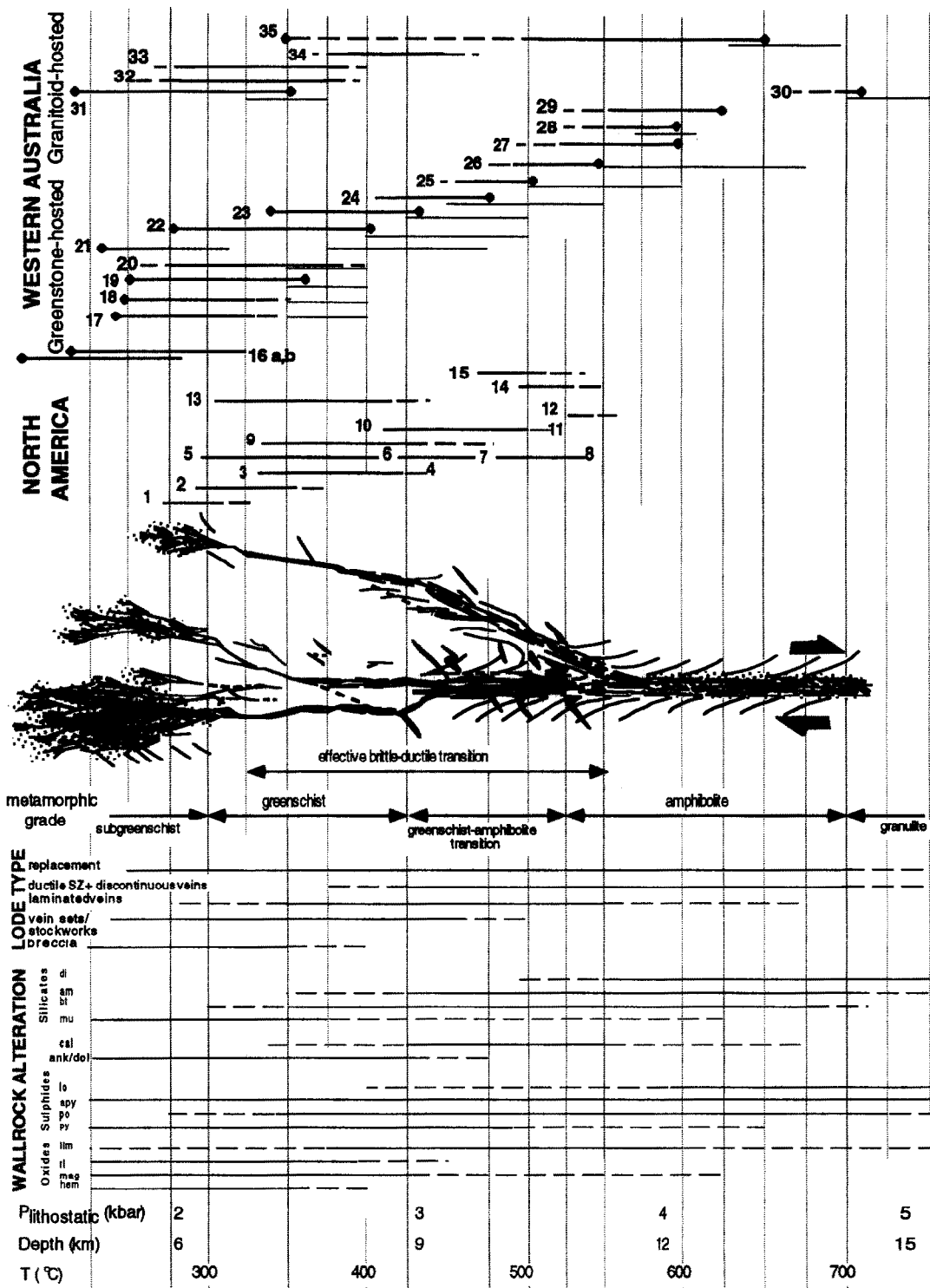


Fig. 2. Cross section of the Dome mine orebodies, Timmins, Abitibi SVZ. Note distribution of orebodies on the second-order Dome splay fault north of the regional Destor–Porcupine fault (Fig. 1A, B), and on third order splays north of the Dome fault (modified from Rogers, 1982).



second- and higher-order splays, which typically show displacements of 10's to a few hundred metres, may be grouped into four general structural styles: (1) breccias; (2) stockworks and vein sets; (3) laminated veins in shear zones; and (4) predominantly ductile shear zones hosting thin, discontinuous, highly attenuated and deformed veins (Fig. 3; Hronsky et al., 1990; Groves et al., 1992). Which of these geometries occur within any given deposit is a function of the rheological properties of the host lithologies and the pressures and temperatures at which deformation and concomitant fluid flow took place. However, two or more of these geometric styles often occur in a single deposit, given the numerous variables such as transients in fluid pressure and strain rate, that in turn govern structural style (Section 5). One style is typically dominant in a given deposit (Hronsky et al., 1990). These four structural morphologies represent a gradation from dominantly brittle to dominantly ductile conditions that likely reflect increasing crustal depths and temperature (Fig. 3). Where crosscutting relationships indicate a transition from one dominant plumbing geometry to another through time, the transition is invariably from a more ductile to a more brittle dominated end member (e.g., McCuaig et al., 1993; Vearncombe, 1993). This feature likely results from uplift of the host terrane following mineralization.

The fossil plumbing systems display vein geometries and kinematic indicators consistent with sub-lithostatic to transiently supralithostatic fluid pres-

sure cycling dominantly within high-angle reverse, or more rarely, oblique-reverse, or strike-slip faults in a tectonic regime with the far-field stress approximately orthogonal to the regional structures (Kerrich and Allison, 1978; Robert and Brown, 1986a; Sibson et al., 1988; Hronsky et al., 1990; Cox et al., 1991; Ridley, 1993; Sections 5 and 7). Consequently, fluid advection must have been directly up structures, within zones of low mean stress (Ridley, 1993).

### 3.3. Orebody scale controls

Orebodies within these lode-Au systems show a direct relationship to some combination of structural and lithological ‘traps’. Structural traps include: (1) dilational segments of fault systems, as in the Lachlan fold belt, Victoria, Australia (Cox et al., 1991); Norseman, Western Australia (McCuaig et al., 1993); and Timmins, Ontario (Phillips et al., 1997); (2) rheologically and chemically favourable lithologies, such as the Fe-basalt sequences at Kalgoorlie, Western Australia (Groves and Foster, 1991; Phillips et al., 1997); Norseman (McCuaig et al., 1993) and iron-formation hosted deposits in the Yilgarn Block, and Homestake, South Dakota (Groves and Phillips, 1987; Neall and Phillips, 1987; Caddey et al., 1991; Ford and Duke, 1993); (3) tectonic lineations; and (4) intersections of structures (e.g., Hronsky et al., 1990; Fedorowich et al., 1991; Peters, 1993a,b). In some mining camps, ore bodies appear to be con-

Fig. 3. Summary diagram illustrating the correlation of alteration mineralogy and orebody morphology with increasing metamorphic grade (bottom) for the crustal continuum of lode gold deposits with selected Archean deposits as examples (top). This is a composite section: no single crustal section is known to include the full range of deposit styles and metamorphic grades. For the deposits, the solid heavy line indicates the calculated temperature range of alteration and mineralization. Filled diamonds anchoring the low-temperature end indicate  $T$  (mineralization) calculated from fluid inclusion data; filled diamonds anchoring the high-temperature end indicate temperatures calculated from phase equilibria or isotope mineral pair geothermometry. Where both fluid inclusion and phase equilibria temperature estimates are available for a single deposit, the phase equilibria estimates are invariably higher (see text for discussion). Abbreviations: hem = hematite; mag = magnetite; rt = rutile; ilm = ilmenite; py = pyrite; po = pyrrhotite; apy = arsenopyrite; lo = löellingite; ank = ankerite; dol = dolomite; cal = calcite; mu = muscovite; bt = biotite; am = amphibole; di = diopside. Deposit key and data sources: North America (all deposits directly from Colvane, 1989, and references therein) 1 Ross; 2 Kirkland Lake; 3 Dome; 4 Hollinger-McIntyre; 5 Couchenon-Williams; 6 Campbell; 7 Dickenson; 8 Madsen; 9 Geralton; 10 Doyon; 11 Bousquet; 12 Musselwhite; 13 Sigma-Lamaque; 14 Lupin; 15 Detour. Western Australia: 16a, b Wiluna (a = early, b = late, Hagemann et al., 1993); 17 Lance field (Ho et al., 1990b); 18 Golden Mile (Ho et al., 1990b); 19 Mt. Charlotte (Ho et al., 1990b); 20 Harbour Lights (Ho et al., 1990b); 21 Sons of Gwalia (Ho et al., 1990b); 22 Hunt (Clark et al., 1986); 23 Victory-Defiance (Clark et al., 1989); 24 North Royal (McCuaig et al., 1993); 25 Crown-Mararoa (McCuaig et al., 1993); 26 Scotia (McCuaig et al., 1993); 27 Fraser's (Ho et al., 1990b); 28 Nevoria (Ho et al., 1990b); 29 Marvel Loch (Mueller et al., 1991b); 30 Griffin's Find (Ho et al., 1990b); 31 Lady Bountiful (Cassidy and Bennett, 1993); 32 Granny Smith (Cassidy, 1992); 33 Porphyry (Cassidy, 1992); 34 Great Eastern (Cassidy, 1992); 35 Westonia (Cassidy, 1992).

trolled by transitions in regional metamorphic grade as for the greenschist–amphibolite transition at Red Lake, Ontario (Andrews et al., 1986); and Yellowknife, Northwest Territories (Boyle, 1961); and in South Island, New Zealand (Craw and Koons, 1989). The mechanisms that may be operating to create ore bodies in these structural and chemical traps are discussed in Section 11 on gold transport and precipitation.

Gold may be contained dominantly within quartz veins, as ‘replacement’ within altered wall rocks bounding veins and shear zones, or as some combinations of these two styles. Examples of vein dominated gold mineralization are the QT and QF vein systems of the Dome mine, Timmins; the Laramie and Sigma deposits Val d’Or, Abitibi belt; the Norseman deposits, Western Australia; and deposits of the Meguma terrane, Nova Scotia (Rogers, 1982; Robert and Brown, 1986a,b; Kontak et al., 1990; McCuaig et al., 1993). Notable replacement-dominated gold deposits are iron-formation hosted deposits, the Kalgoorlie deposit of the Yilgarn block, and vein selvage-related gold mineralization of the Hollinger–MacIntyre deposit, Timmins, Ontario (Wood et al., 1986; Neumayer et al., 1993a,b).

#### 4. Hydrothermal alteration

Hydrothermal alteration assemblages contiguous with quartz-dominated veins in shear zones, faults or fracture systems (fluid conduits) reflect open system chemical and isotopic metasomatic interaction of fluids with adjacent wall rocks. The fluids approach chemical, isotopic, and thermal equilibrium, or locally show disequilibrium, as they advect upwards through the crust (Fig. 4; see Korzhinskii, 1970, for a general treatment of metasomatic theory). In this section the mechanisms of hydrothermal alteration are reviewed, and their interrelationship to other controls such as tectonics and architecture of the hydrothermal system. Effects of host rock composition on alteration assemblages, and the development of alteration parageneses are described, as are variations of mineral type and composition with temperature and pressure. Finally, lateral zonation is discussed.

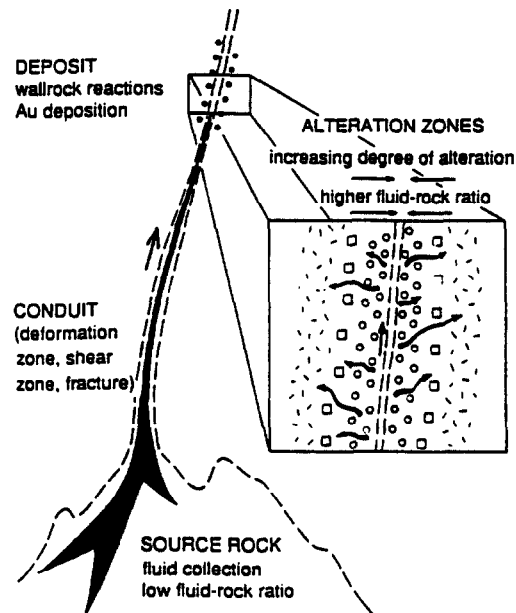


Fig. 4. Schematic diagram of process of fluid sourcing, focussed flow, infiltration into wall rocks and resultant hydrothermal alteration as envisioned for lode gold systems, from Ridley (1990).

#### 4.1. Alteration mechanisms

Variables that control alteration associated with lode gold orebodies and their hydrothermal plumbing systems include: (1) the tectonic regime and resultant stress field in which the deposits are formed, i.e., dilational jog versus high-angle reverse faults; (2) fluid/rock ratios; (3) composition of the host lithologies, i.e., felsic, mafic, ultramafic; (4) composition of the hydrothermal fluid, including Eh, pH, and activities of H, K, Na, S, H<sub>2</sub>O, CO<sub>2</sub>, and salinity; (5) the temperatures, and (6) pressures at which hydrothermal alteration and gold mineralization occur; and (7) equilibrium or disequilibrium conditions. Complex interplay of these seven variables influence the rheologies of rock units, effective fluid pressures, the mechanisms of deformation, fluid/rock interaction, and the metasomatic reactions that operate.

Metasomatic alteration due to fluid/wall rock interaction occurs by two main processes: advection of fluids along fractures/microcracks from the scale of laterally extensive quartz veins to the migration of fluids along mineral grain boundaries, and diffusion of ions through static pore fluids (advective versus

dispersive terms of chemical mass transport). Which of these processes dominates is determined by the permeability of the conduit versus diffusion rates along grain boundaries in wall rock; however, fluid infiltration is much faster than ionic diffusion along grain boundaries during hydrothermal alteration in lode gold systems (cf., Ridley, 1990; Fig. 4). As alteration mineralogy is dependent upon fluid/rock ratios, it follows that alteration is also dependent upon the geometry of the hydrothermal plumbing system and the deformation mechanisms operating within it, which collectively dictate fluid access into the wall rocks.

#### 4.2. Mineral paragenesis

Paragenetic diagrams summarize: (1) the relative timing of ore and gangue minerals; (2) the relative abundance of minerals; and the (3) secular relationship of the alteration mineral assemblages to evolving deformation style and fluids. Accurate knowledge of paragenetic development is essential for geochemical studies; only minerals associated with gold can provide information on the ore-depositing fluid. Paragenetic development in veins and wall rocks is relatively consistent in lode gold deposits worldwide. Quartz and carbonates are precipitated over a relatively wide temporal range, whereas other silicates (plagioclase, chlorite, mica), sulphides (pyrite, arsenopyrite, sphalerite, galena), oxides (ilmenite, rutile), and gold have more restricted periods of deposition. Typical paragenetic diagrams for greenschist facies hosted deposits of the Timmins and Val d'Or camps are illustrated in Fig. 5. Paragenetic schemes in subgreenschist or amphibolite and granulite facies hosted deposits are less well documented.

Compositions of two or more minerals can potentially yield information on cation (Ca, Na, K) and anion (F<sup>-</sup>, Cl<sup>-</sup>) activities in the hydrothermal fluids, and appropriate assemblages may yield thermometric or barometric data (Sections 8 and 9). Single, robust minerals may constrain the isotopic composition of the ore-fluid, or the age of mineralization (Kerrich and Cassidy, 1994). For example, tourmaline and fine-grained white scheelite are paragenetically associated with gold in the Timmins mining camp, On-

tario, whereas coarse-grained honey-coloured scheelite is later than gold and precipitated from a different fluid. Accordingly, tourmalines provide primary information, such as the <sup>87</sup>Sr/<sup>86</sup>Sr ratios of the ore-forming fluid, whereas coarse scheelites yield Sm-Nd ages 260 Ma post-mineralization (Bell et al., 1989; King and Kerrich, 1989b; Kerrich and Cassidy, 1994; Section 12).

Gold may show one or more stages of deposition, but the last stage is invariably in late brittle fractures. Collectively, these observations have given rise to three opposed hypotheses: (1) that late gold is largely paragenetically early gold that has been remobilized, with potentially some additional gold added (McCuaig et al., 1993; Kerrich and Cassidy, 1994); (2) that the majority of gold is introduced later than main-vein forming hydrothermal event (Jemielita et al., 1990; Hanes et al., 1994); or (3) late and unrelated to the bulk of the vein it is hosted in (Fayek and Kyser, 1995). The issue of gold timing is discussed further in Section 12.

The paragenetic sequence of mineral assemblages and structures identified in both the least-altered wall rocks and fluid-dominated shear zones in many lode gold deposits indicate that many deposits have evolved through a number of pressure-temperature-time-deformation regimes, and fluid events [(P-T-t-d-f) (see discussion of timing relationships below)]. Therefore, it is imperative that hydrothermal wall rock alteration envelopes be examined in both a spatial and temporal framework. The former involves lateral zonation away from the veins and shear zones, and differences in alteration assemblages between deposits, whereas the temporal framework concerns changes in alteration mineralogy and deformation mechanisms with time.

#### 4.3. Alteration zonation and mineralogy in lode gold deposits

The mineralogy of alteration assemblages associated with lode gold deposits is varied, and zonation occur over a range of scales: (1) between host lithologies of differing bulk composition; (2) with increasing distance orthogonally away from the fluid conduit(s); and (3) regionally with temperature and pressure of formation.

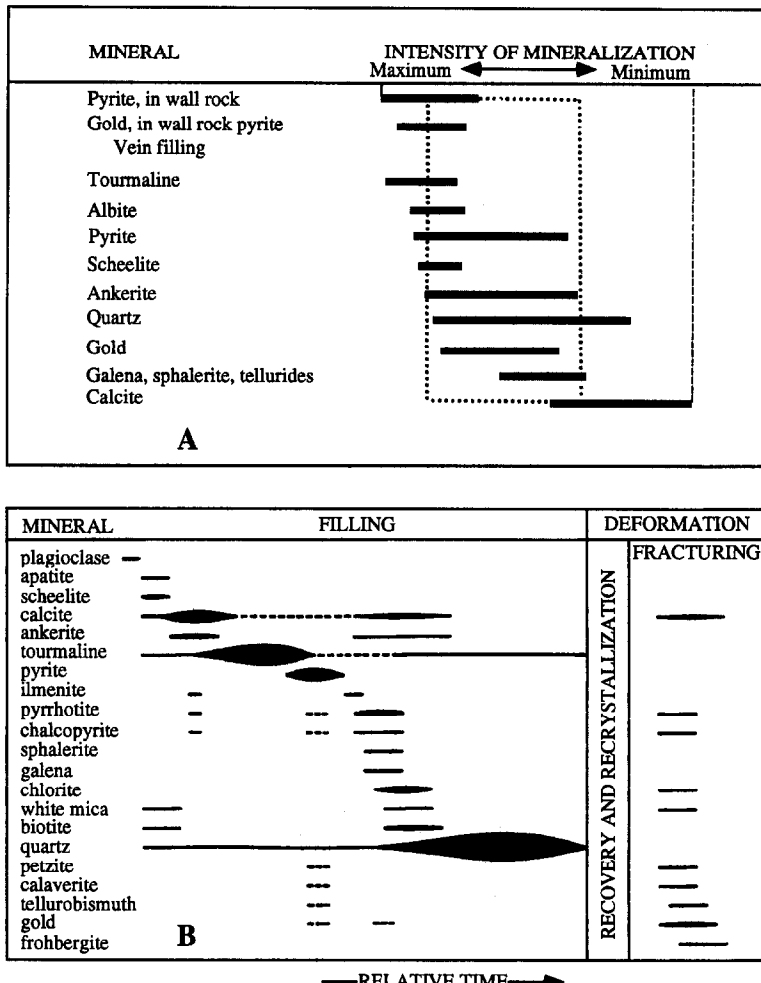


Fig. 5. Generalized paragenetic development of gold-bearing quartz veins. (A) Timmins mining camp and (B) Val d'Or mining camp, in the Archean Abitibi greenstone belt, Canada. (A) modified after Hurst (1935), and (B) after Robert and Brown (1986a,b).

#### 4.3.1. Alteration parallel to fluid conduits

Within a single lithology the alteration zones may be traced parallel to the fluid conduits, both down dip and along strike, for hundreds of metres showing little variation in mineralogy within individual structural conduits. These observations imply relatively isothermal conditions of vein emplacement and metasomatism (Kerrich, 1987, 1989a,b). Thus alteration zones are often described as *alteration envelopes* surrounding fluid conduits. In a given lithology, the alteration paragenesis, and  $\delta^{18}\text{O}$  quartz change little over more than two vertical kilometres in the Hollinger-MacIntyre and Kirkland Lake deposits, of the Abitibi belt (Bain, 1933; Kerrich,

1989b). This uniformity is in contrast to the marked lateral variations in alteration away from fluid conduits. However, a fluid conduit in a single deposit that transects two lithologies of contrasting bulk composition will have very different mineral assemblages in the different lithologies (Fig. 6; Table 1; cf., Böhlke, 1989).

#### 4.3.2. Lateral zonation perpendicular to fluid conduits

The most marked changes in alteration mineralogy occur perpendicular to the fluid conduits. Innermost alteration zones are restricted to fault/fault, or

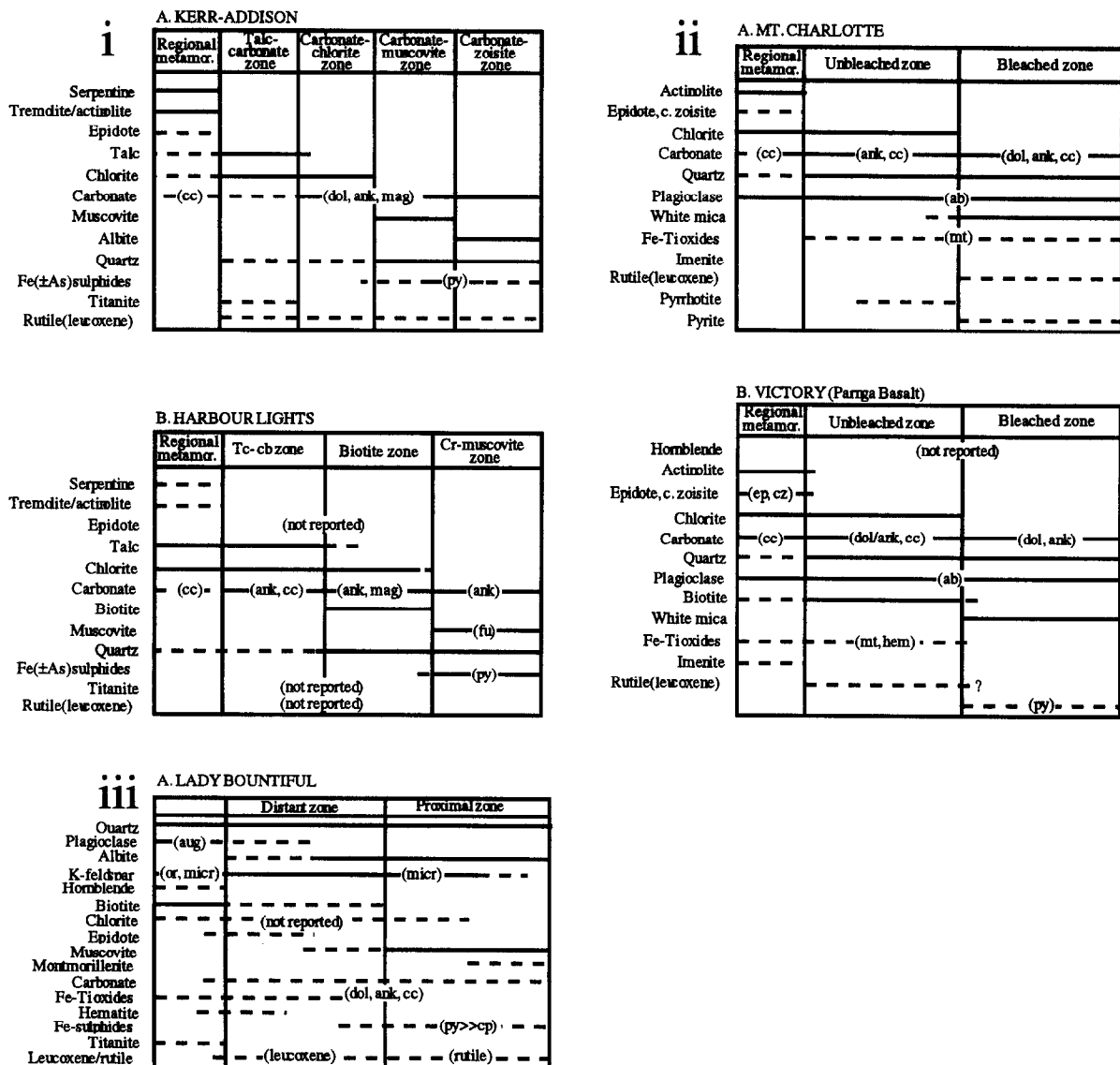


Fig. 6. Examples of lateral zonation of hydrothermal alteration associated with greenschist facies deposits hosted in differing lithologies. (i) ultramafic lithologies, (ii) mafic lithologies, (iii) granodiorite (from Kishida and Kerrich, 1987, and Mikucki et al., 1990, where original data sources are given).

fault/lithological-contact intersections, and vein-wall rock boundaries, dilatational flexures in structures, or other such areas of extremely high fluid flux (e.g., Peters, 1993a,b; Fig. 7A), whereas distal alteration zones are generally ubiquitous throughout the hydrothermal plumbing system. Inner zones may range from millimetres to tens of metres or more in

thickness, and are defined by the presence of diagnostic mineral assemblages. Inner, or proximal alteration zones immediately adjacent to quartz veins, are areas of greatest fluid flux, reflecting fluid-dominated metasomatic reactions. The mineralogical zones distal to the vein reflect a gradient of decreasing fluid/rock ratio, as well as diminishing chemical

Table 1

Summary table of silicate hydrothermal alteration assemblages from proximal alteration zones of the four dominant host lithologies of Archean lode-gold deposits in the Yilgarn Craton

Temperature and depth ranges—metamorphic grade	Mafic	Ultramafic	Granitoid	BIF
225°–400°C < 1–3 kbar (< 5 to 10 km) sub- to mid-greenschist	ALBITE ANKERITE/dolomite Muscovite ( $\pm$ V-mica) Chlorite Biotite Paragonite Clinozoisite Tourmaline	Cr-muscovite MAGNESITE/dolomite Mg-chlorite Mg-biotite Muscovite Tremolite	ALBITE MUSCOVITE CHLORITE Ankerite/calcite Biotite Tourmaline	ANKERITE/siderite CHLORITE ALBITE Muscovite
375°–550°C 2–4 kbar (7–14 km) Greenschist–amphibolite transition	Ca-AMPHIBOLE BIOTITE Ca-PLAGIOLASE Calcite/ankerite Clinozoisite/epidote Chlorite K-feldspar Titanite	TREMOLITE PHLOGOPITE Mg-CHLORITE Calcite/dolomite Ca-amphibole Talc	Ca-AMPHIBOLE BIOTITE Ca-PLAGIOLASE Calcite K-feldspar Titanite Muscovite Epidote/clinozoisite	Fe-AMPHIBOLE ANKERITE/calcite Chlorite Feldspar Muscovite
525°–700°C 3–5 kbar (10 to 18 km) amphibolite–granulite	DIOPSIDE GARNET (grandite) Ca-amphibole Biotite Calcite Ca-plagioclase K-feldspar Cordierite Clinozoisite Sillimanite/ andalusite	DIOPSIDE OLIVINE (forsterite) Tremolite Phlogopite Calcite Cordierite Garnet (grandite) Anthophyllite Spinel (hercynite)	DIOPSIDE (Act)-HORNBLENDE Ca-plagioclase Biotite K-feldspar Calcite Titanite Garnet Cordierite Sillimanite/ andalusite	HEDENBERGITE Fe-AMPHIBOLE Fe-garnet Olivine (fayalite) Biotite Calcite/siderite

Sources of data: Clark et al. (1989), Ho et al. (1990b), Mueller and Groves (1991) and Cassidy (1992). Note that quartz is present in all deposits in all host rock lithologies, and is not diagnostic of alteration style and therefore is not listed in the table. Where non-specific mineral names are listed (e.g., Ca-amphibole, Fe-amphibole), mineral groups characterized by solid-solution series are implied. Temperature ranges are approximate only, and correspond to temperature ranges, lode style and metamorphic grade as indicated on Fig. 3. Hydrothermal minerals in uppercase lettering typically characterize the range of temperature of formation. Assemblages are varied and one or more minerals may be a minor component or even absent in some deposits. Modified from Cassidy (1992). Ankerite includes ankerite and ferro-dolomite.

gradients as fluids approach equilibrium with country rock (discussed below), and represent progressive infiltration of the fluid into the wall rock by advection and diffusion. Examples of chemical gradients are decreasing K, Rb, CO<sub>2</sub>, S contents, and X<sub>CO<sub>2</sub></sub> of fluid inclusions away from orebodies of the Kerr Addison mine and Val d'Or deposits (Kishida and Kerrich, 1987; Guha et al., 1991). Boundaries between alteration zones may be knife sharp or gradational over centimetres to meters: sharp boundaries are common in proximal alteration zones, whereas,

diffuse boundaries predominate in distal alteration zones. The most distal alteration zones grade into least-altered regional metamorphic assemblages.

Examples of such lateral alteration zonation are illustrated in Figs. 5 and 6. Note that the greatest complexity usually occurs in inner alteration zones due to narrow zone widths and the episodic nature of deformation and fluid infiltration, which act in concert to produce alteration zones with complex cross-cutting relationships (Fig. 7B). These zones are progressive in nature, such that proximal alteration zones

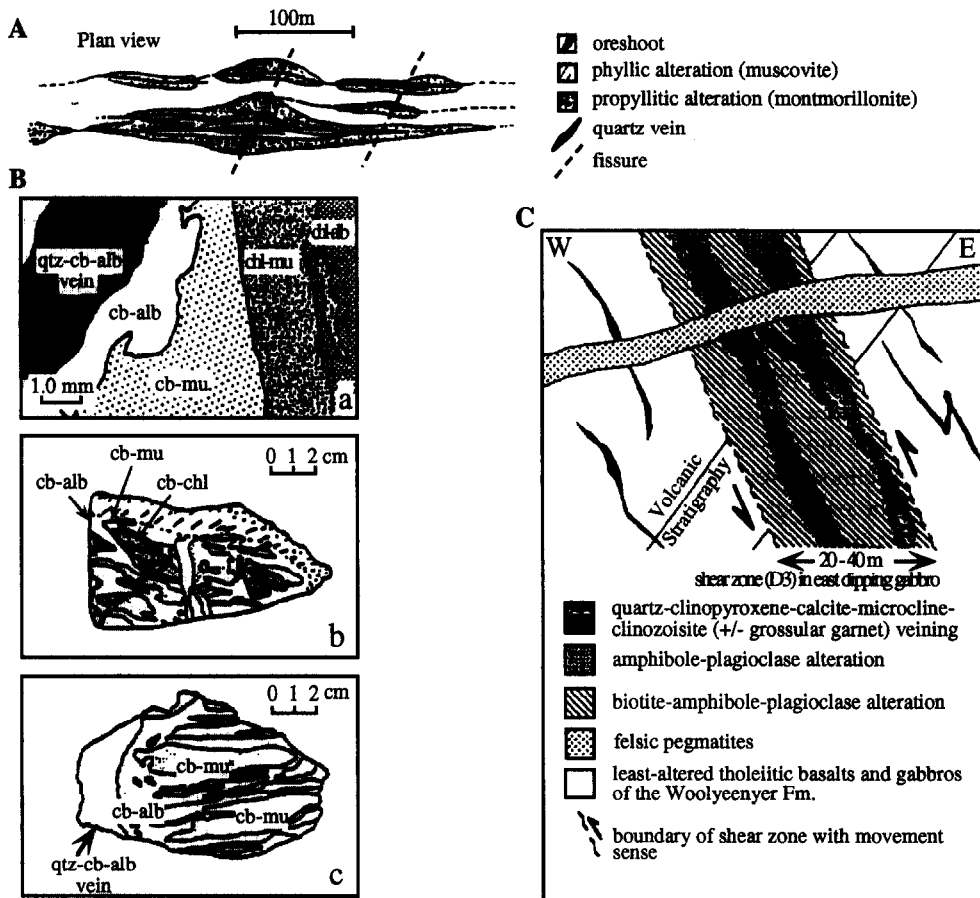


Fig. 7. Lateral zonation of alteration assemblages associated with lode gold deposits. (A) Schematic diagram of alteration envelopes in the sub-greenschist facies Charter's Towers gold district, Queensland. Notice how gold lodes and inner alteration envelopes are restricted to intersection of structures, the areas of highest fluid flux (from Peters, 1993b). (B) Line drawings of innermost alteration selvages surrounding quartz veins in the greenschist facies Kerr-Addison mine, Abitibi belt, Ontario. Note the complexity of alteration assemblages due to multiple fracturing episodes and variable fluid infiltration (from Kishida and Kerrich, 1987). (C) Alteration associated with the amphibolite facies Scotia mine, Yilgarn Block, Western Australia (from McCuaig et al., 1993).

overprint their distal counterparts. At the Archean Mount Charlotte deposit, Kalgoorlie, hosted by the Golden Mile dolerite, Mikucki and Heinrich (1990) report two alteration zones. An inner zone of quartz, albite, abundant muscovite, ankerite, pyrite, and rutile, and an outer zone of quartz, albite, minor muscovite, abundant chlorite and ankerite, with minor pyrite, and ilmenite, and rutile. The Charters Towers gold deposit, Queensland, is hosted in a mid-Palaeozoic metamorphic terrane of the Cambro-Ordovician Tas-

man fold belt. Peters and Golding (1989) described a phyllitic alteration zone proximal to veins, and an outer polyphytic zone of montmorillonite and illite. Thus the zonation of mineral assemblages away from the fluid conduits can be viewed as metasomatic reaction fronts (e.g., Korzhinskii, 1970; Kishida and Kerrich, 1987; Clark et al., 1989).

#### 4.4. Variations in alteration assemblages and mineral compositions with temperature and pressure

Deposits formed at significantly different temperatures, but within similar lithologies, feature distinct

alteration assemblages (Andrews et al., 1986; Colvine et al., 1988; Mueller and Groves, 1991; Cassidy, 1992; Groves et al., 1992; McCuaig et al., 1993). The variation in key alteration minerals with temperature and pressure for various lithologies is summarized in Fig. 3 and Table 1, and generally relates directly with the metamorphic grade of the host rocks.

There are relatively few studies of the composition of silicates and carbonates from lode gold deposits, and the majority are for Archean deposits hosted in greenschist facies rocks. In many examples mineral compositions show a strong control by host rock composition and temperature. Chlorites are typically ripidolite to clinochlore, with compositions reflecting those of the original host rock. For example, chlorites in ultramafic rocks at the Kerr-Addison deposit, Ontario, are less aluminous (17.4–17.6 wt.%) and more magnesian ( $MgO = 21\text{--}26$  wt.%) than counterparts in basalts. Chromium contents may reach 1.3 wt.% in ultramafic hosted deposits (Fryer et al., 1979; Kerrich, 1983).

With increasing temperatures of hydrothermal alteration, amphiboles predominate over chlorite. Amphiboles are generally of the Ca-type, ranging from tremolite–actinolite through actinolitic hornblende to hornblende, with Fe/Mg ratios reflecting those of the host rock (Mueller and Groves, 1991; Cassidy, 1992; McCuaig et al., 1993). Variations are also noted with temperature. In basalt-hosted deposits, for example, amphiboles are generally actinolite at upper greenschist facies, but in higher-temperature deposits are hornblende. Exceptions are noted in some high-temperature BIF-hosted deposits, where Ca-poor grunerite is common (McCuaig et al., 1993, and references therein).

Micas are compositionally variable: greenschist facies deposits are characterized by K or Na mica. Compositions can vary substantially: in the Hoyle Pond deposit, Timmins, Rye (1987) documented compositions ranging from 90% muscovite to 90% paragonite. Chromium contents range up to 3 wt.% (Kerrich, 1983). Biotite is the prevalent mica in the higher temperature deposits that formed in upper greenschist to granulite facies terranes, although margarite, the Ca-equivalent of biotite, has been reported from the Dumagami deposit, Quebec (Eliopoulos, 1982). Vein feldspars are typically al-

bit in greenschist facies deposits, although sparse orthoclase has been reported, for example at the Canadian Arrow deposit, Abitibi belt (McNeil and Kerrich, 1986; Colvine et al., 1988). Calcic feldspars are predominant in the higher-temperature deposits. K-feldspars are also commonly present in inner alteration zones of high-temperature deposits (Cassidy, 1992; McCuaig et al., 1993, and references therein).

Tourmaline is generally in the schorl–dravite solid solution series irrespective of host lithology. Rare green-coloured Cr-dravites have been reported for veins in ultramafic rocks (King, 1988; King and Kerrich, 1989a). The tourmalines are low-Cl, F, hydroxy varieties, signifying low Cl and F activities in the ore fluids, consistent with fluid inclusion evidence presented below for low-salinity fluids (Section 7).

Carbonates show a strong control by wall rock composition, from siderite, through dolomite, to calcite in Fe-, Mg- and Ca-rich host lithologies respectively, and MnO contents also reflect host rock control. In greenschist facies deposits, quartz and carbonate (ankerite, Fe-dolomite) generally constitute the principal gangue minerals, and carbonate is also present in the alteration assemblages that envelop the vein systems (Fryer et al., 1979).

For deposits formed in amphibolite facies terranes, carbonate is generally restricted to vein assemblages and is invariably calcite. Deposits hosted in upper-amphibolite facies host rocks are characterized by abundant Ca-bearing minerals, predominately in the inner zones of these high-temperature deposits, including amphibole, clinopyroxene in the diopside–hedenbergite series, epidote, and grossular garnet (Colvine et al., 1988; Mueller and Groves, 1991; McCuaig et al., 1993). At the Scotia deposit in the southern Norseman camp, a calc silicate assemblage locally overprints hydrothermal biotite and occurs independently of gold zones. Both are late but locally share the same structure as gold zones (S. Peters, personal communication).

With increasing pressure and temperature, dominant Fe-sulphides and arsenides change from pyrite and arsenopyrite in subgreenschist to greenschist facies hosted deposits, to pyrrhotite and arsenopyrite to löellingite in granulite facies hosted deposits, reflecting lower sulphur activities at higher temperatures (Fig. 3; Section 8).

## 5. Relative timing of alteration, deformation, metamorphism, and fluid flow: Textural evidence

Tectonic fabrics and microstructures that form in quartz veins and contiguous alteration haloes surrounding lode gold deposits have been much under-used in assessing hydrothermal alteration processes and conditions. Such fabrics can reveal information on: (1) the deformation mechanisms that operated, and hence intensive variables such as temperature, fluid pressure, confining stress and strain rate; (2) changes in deformation mechanisms over time, such as a coseismic to interseismic cycle; (3) the relative timing of hydrothermal alteration, mineralization, and quartz vein emplacement to deformation mechanism, and metamorphism; and (4) reactivation of ore-hosting structures during post mineralization uplift.

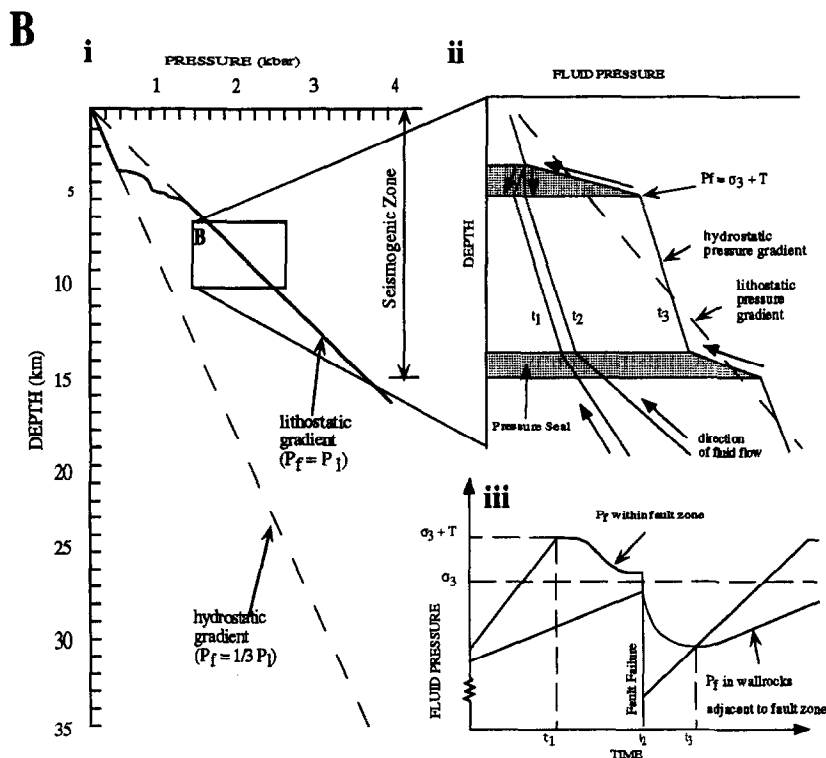
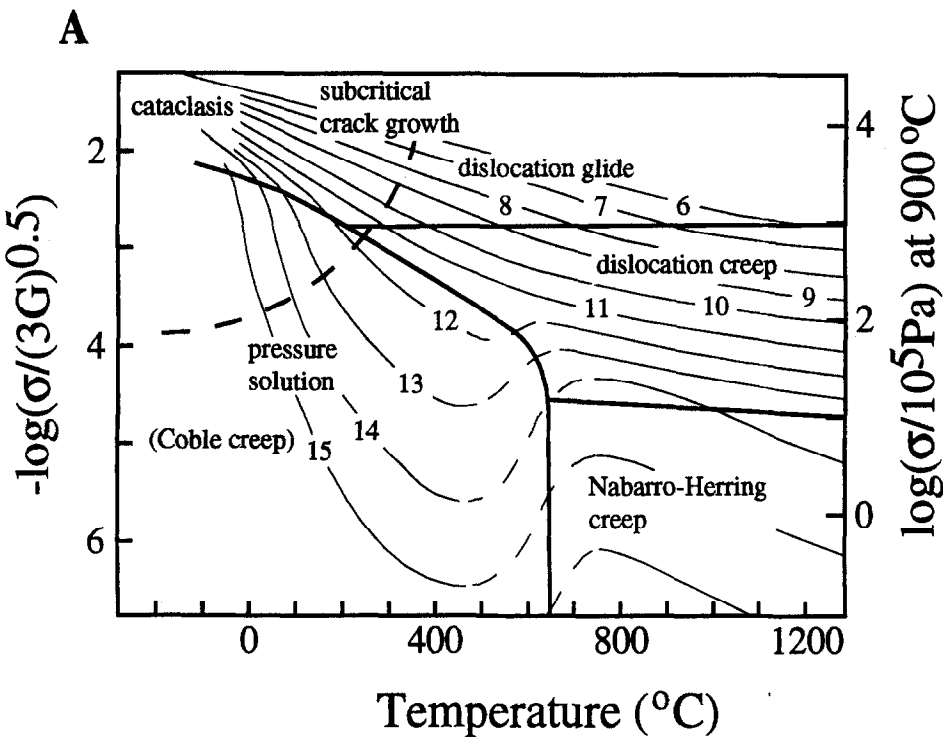
### 5.1. Deformation mechanisms

The development of petrofabrics within mineral assemblages is dependent upon: (1) the original rheological properties of the rock such as grain size and the relative susceptibility of minerals within the assemblage to adopt anisotropic or isotropic fabrics (e.g., mica/chlorite/amphibole possess high susceptibility, whereas quartz/feldspar/carbonate/clino-pyroxene are characterized by low susceptibility); (2) the precipitation of anisotropic and/or isotropic hydrothermal minerals, and their modal abundance; and (3) the intensive variables such as confining stress, fluid pressure, temperature (homologous  $T = T/T_{\text{melt}}$ ) and strain rate. Collectively, these variables control the deformation mechanisms that are operating, and hence the tectonic fabrics that develop.

Steady-state deformation of mineral grains under geological conditions may occur by one, or some combination, of the following processes: (1) cataclasis, involving repeated transgranular fracturing and frictional sliding of rock particles; (2) intercrystalline or grain boundary diffusive mass transport, termed pressure solution or Coble creep; or (3) dislocation mechanisms, involving the glide of solid-state defects (dislocations) in crystal lattices, or glide and climb of dislocations (Rutter, 1976; Kerrich and Allison, 1978). These are competing processes that are dependent on the intensive variables as illustrated in Fig. 8A.

At low confining stresses and temperatures, rocks deform by brittle-dominated macroscopic and microscopic fractures, expressed as faults and cataclasites respectively; strain rates are also relatively high. Increasing confining stress with depth promotes the transition from brittle to ductile behaviour. However, fluid pressure may act to counter confining stress (effective confining stress = confining stress  $- P_{\text{fluid}}$ ) by promoting the dilation associated with fracture propagation. Tensile failure is possible only at shallow depths in the crust, where confining stress is low. At greater depths tensile fractures cannot open, as confining stress inhibits dilation (Fig. 8A). However, if fluid pressure exceeds confining stress (effective confining stress), hydraulic fractures may propagate. The positive volume changes associated with metamorphic dehydration reactions generates metamorphic fluids at lithostatic- to suprastatic pressure, that will promote hydraulic fracturing (Fyfe et al., 1978; Connolly, 1997). Many of the vein systems in lode gold deposits have the characteristics of hydraulic fractures, signifying that the ore-forming fluids were transiently at supralithostatic fluid pressure (Figs. 8B and 9; Kerrich and Allison, 1978; Sibson et al., 1988). Consequently, the broad association of lode gold deposits with metamorphosed terranes, and fluid flow near-peak metamorphism, taken with the field evidence for hydraulic fractures that require lithostatic or greater fluid pressures, may signify a genetic relationships between the two (Kerrich, 1990a,b).

At intermediate temperatures and pressures in the crust, steady-state deformation of rocks is by pressure solution; differential stresses and strain rates are low. At higher temperatures and pressures, corresponding to upper greenschist through amphibolite to granulite facies, rocks deform ductilely by dynamic recrystallization. Dynamic recrystallization by dislocation glide involves the progressive formation of undulose extinction, mortar texture, and successive generations of subgrains and sub-subgrains (etc.), in which dislocations have self-organized into new (sub)grain boundaries. Recovery of deformed mineral grains occurs by two basic processes: the migration of subgrain boundaries, and the formation of new grain boundaries, which can combine in a number of ways to return strained grains to states of low free energy, with coarser grain size, straight grain



boundaries, and triple junction (foam texture) microstructure. These mechanisms dominantly involve dislocation migration and boundary diffusive processes (Drury and Urai, 1990). Dynamic recrystallization and recovery are competing processes, with the former dominating at  $\leq 300^\circ\text{C}$  and the latter dominating at  $\geq 400^\circ\text{C}$ .

Distinct macro and microtextures result from a complex interplay of these processes and can be used to constrain the  $T-t-d-f$  evolution of hydrothermal alteration associated with lode gold deposits. Examples are detailed below for quartz veins and wall rock alteration assemblages. In general, cataclasis and brittle fracture predominate in deposits hosted in sub-greenschist facies rocks; pressure solution, and dynamic recrystallization by dislocation glide predominate in deposits within greenschist facies rocks; whereas deposits developed in amphibolite or in granulite facies rocks feature ductily deformed veins in ductile shear zones reflecting dynamic recovery by dislocation climb. This transition in microscopic deformation mechanisms and texture with increasing depth and temperature in the crust parallels the trend in macroscopic style of shear zone vein system (Fig. 3).

### 5.2. Strain softening and hydrothermal hardening: The interplay of deformation and fluid flow

Numerous studies have demonstrated that the deformation of wall rocks, fluid pressure fluctuations and intermittent fluid flow, metasomatic alteration, and mineralization are inextricably linked in lode gold deposit systems, and operate cyclically, (e.g., Kerrich, 1986; Sibson et al., 1988; Cox et al., 1990, 1991; Abraham and Spooner, 1995). There is abundant field evidence for cyclic transitions between supravhydrostatic and supralithostatic fluid pressure. The three most compelling lines of field evidence

are: (1) sigmoidal veins in ductile shear zones (Fig. 9A, C, E); (2) vertical dilation in flat veins; and (3) reactivation of high angle reverse faults.

Sigmoidal quartz veins developed in ductile shear zones are common in many gold deposits, particularly those developed in mid-greenschist to lower amphibolite facies, exemplified by the Yellowknife gold camp, Northwest Territories, and the Kambalda camp of the Yilgarn Block. The veins are not 'born' sigmoidal, but rather reflect alternating episodes of high-strain rate hydraulic fracturing at high fluid pressure where crack tips propagate parallel to the maximum principal stress, with intervening slow strain rate and ductile creep at lower fluid pressure, during which the veins progressively rotate (Kerrich and Allison, 1978; Fig. 9A, C, E; see caption for explanation). In the Yellowknife and Val d'Or camps, and Norseman, Western Australia (Robert and Brown, 1986a,b; Fig. 9B, F) veins in all orientations, including flat, may dilate together. For crustal depths of 8 to 12 km corresponding to the greenschist and amphibolite facies, this requires fluid pressure to exceed the lithostatic load, and for differential stress to be small. Banding of such veins indicates many fluid pressure cycles from hydrostatic to supralithostatic conditions (Fig. 8B; Kerrich and Allison, 1978; Fryer et al., 1979; Robert and Brown, 1986a,b). The boudinaged banded flat vein from the Victory mine, Kambalda requires switching of maximum effective stress orientations: fluid pressure was supralithostatic and the maximum principal stress horizontal for successive open-fill events and the maximum principal stress vertical in intervening events to boudinage the vein (Fig. 9F). Many deposits, such as at the Yellowknife and Val d'Or, occur in reactivated high angle reverse faults. Sibson (1985) has shown that reactivation of such faults is mechanically inhibited, except under conditions of lithostatic fluid pressure. Details of this cycle are given below. Hydraulic

Fig. 8. (A) Deformation mechanism map for quartz (grain size = 100  $\mu\text{m}$ ), showing variations in deformation mechanisms with temperature, differential stress, and strain rate (modified from Rutter, 1976). Contoured numbers represent  $-\log$  strain rate, vertical axis approximates  $-\log$  differential stress. (B) Fluid pressure fluctuations associated with lode gold deposits. (i) Fluid pressure vs. depth (solid line), after Thompson and Connolly (1992). Seismogenic zone from Sibson (1990). (ii) Details of fluid ( $P_f$ ) pressure fluctuations with time ( $t_1$ ,  $t_2$ ,  $t_3$ ) along the lithostatic pressure gradient during episodic seismic failure, hydraulic fracture, catastrophic fluid flow, vein emplacement and mineral deposition (Cox et al., 1990). Pressure seals may be relatively impermeable lithologies, or mineralized segments of faults.

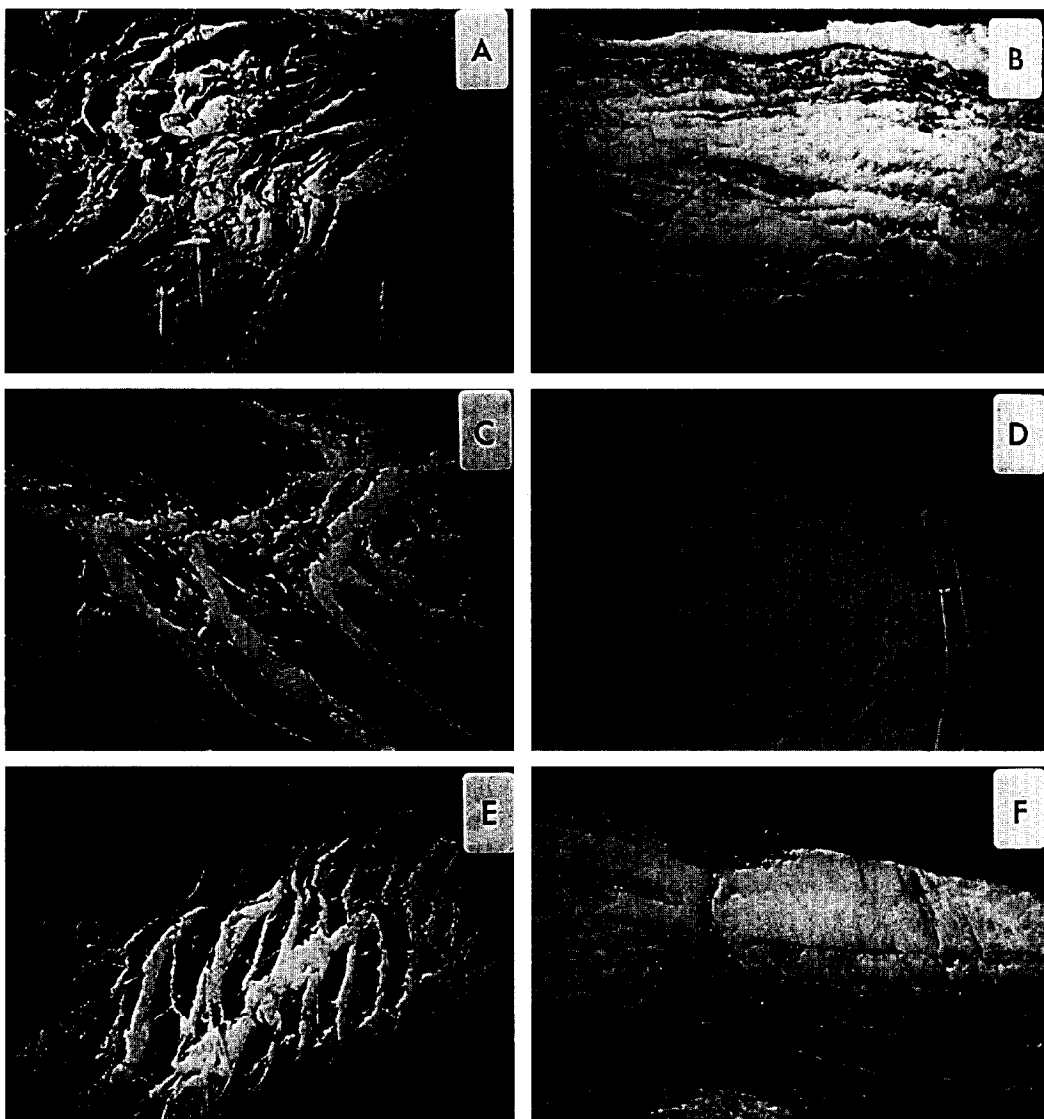


Fig. 9. Photographs of gold-bearing quartz veins. (A) Sigmoidal veins in a ductile shear zone, Con Mine, Archean Yellowknife greenstone belt. Vein tips propagate parallel to the maximum principal stress during hydraulic fracture. Between fracture events the veins are rotated in the shear zone by ductile creep. (B) Flat veins in the Con mine. (C) Sigmoidal vein arrays, Dome mine, Archean Abitibi greenstone belt. (D) Laminated veins, Dome mine. The laminae are fragments of wall rock progressively fractured off the vein-wall contact during successive hydraulic fracturing events. (E) Sigmoidal vein arrays, Victory Mine, Archean Norseman-Wiluna belt. (F) Flat laminated and boudinaged veins, Victory Mine. Boudinage signifies switching of the principal stress directions from horizontal during hydraulic fracturing, to vertical during boudinage.

conductivity may increase by eight orders of magnitude during hydraulic fracturing, promoting very high fluid fluxes (Fyfe et al., 1978).

Progressive alteration of wall rock causes new minerals to form, which affects the wall rocks' resul-

tant permeability and response to stress. The formation of phyllosilicate minerals such as chlorite, biotite, and muscovite, by hydrolysis during alteration and deformation may impart a fabric to the rocks, decreasing wall rock competency and generating me-

chanical anisotropy. In combination, these two attributes focus deformation in the structures. The increased anisotropy will increase permeability, allowing greater infiltration of hydrothermal fluids, and thus further alteration, which in turn leads to progressive deformation. This cycle is referred to as the process of 'strain softening'. The anisotropic fabric has an additional effect in that the tensile strength orthogonal to the fabric is less than parallel to the fabric. Consequently, hydraulic fractures preferentially open parallel to the fabric generating fabric-parallel vein systems rather than stockworks (Kerrich and Allison, 1978).

Conversely, the precipitation of various anhydrous minerals with prismatic crystal habits such as quartz, carbonate, and albite will increase the competency of the wall rocks, cementing anisotropic fabrics. This 'strain hardening' process increases the competency, but concurrently lowers the hydraulic conductivity, of the wall rocks and can inhibit further fluid infiltration and hydrothermal alteration. Therefore, the alteration produced can have a profound effect on the extent of alteration haloes through the competitive nature of the strain softening and hardening processes. There may also be an interplay between increasing fabric development (anisotropy) with progressive shear, and fabric cementation by hydrothermal mineral precipitation. These features are notable in the Yellowknife deposits (Kerrich et al., 1977).

The cycle between strain softening by fabric development and strain hardening by hydrothermal mineral precipitation contributes to fault-valve behaviour in the fluid conduits (Fig. 8B) and is manifested in the development of banded (laminated) veins. During successive hydraulic fracture events, vein-wall rock systems tend to break outside of the veins beyond the zone of wall rock cementation, such that successive selvedges of wall rock become rafted into the veins, generating a banded structure (Fig. 9B,D; cf., Cox et al., 1991, and references therein). Spectacular examples of banded veins occur in the Timmins and Val d'Or camps, Canada (Fryer et al., 1979; Robert and Brown, 1986a,b), and the Norseman camp of Western Australia (McCuaig et al., 1993).

Between brittle failure events, ductile mechanisms operate, imparting ductile fabrics to wall rocks and

previously deposited quartz. This cyclic brittle-ductile behaviour, so characteristic of lode gold deposits, indicates that the hydrothermal fluids responsible for alteration and mineralization varied from sub-, to supralithostatic fluid pressures (Fig. 8B).

### 5.3. Quartz vein fabrics

Comparison of quartz textures from veins in lode gold deposits allows variations in deformation and recrystallization mechanisms, with both temperature and time, to be recognized. At low temperatures and effective confining stress, but relatively fast strain rates (sub-greenschist facies), brittle deformation by cataclastic processes dominate, producing abundant fault gouge, breccia, and stockworks. Microstructures observed in such environments include fractured grains, stylolites and fault gouge along discrete planes with little dynamic recovery of grains. Stylolites developed by pressure solution indicate periods of slow strain rate. Between these planes of strain accommodation, the quartz veins will be relatively undeformed so that primary depositional textures and primary fluid inclusions will commonly be preserved (Gebre-Mariam et al., 1991; Peters, 1993b).

At intermediate temperatures and confining stress in greenschist facies hosted deposits, vein geometries comprise breccias through to laminated veins in ductile shear zones and sigmoidal vein arrays with abundant evidence of hydraulic fracturing (Sibson, 1990; McCuaig et al., 1993). Under these conditions brittle and ductile deformation mechanisms operate with intervening hydraulic fractures and dislocation mechanisms, plus grain-boundary diffusive mass transport and pressure solution. However, rates of dynamic recrystallization exceed recovery rates producing undulose extinction and serrated grain boundaries with variable subgrain formation (Fig. 10A). Primary depositional features are destroyed in this variety of quartz, which often contains abundant secondary and pseudosecondary fluid inclusions along intragranular and transgranular fractures, although primary inclusions may be preserved in least-deformed grains.

At high temperatures and confining stress in amphibolite and granulite facies hosted deposits, ductile deformation dominates. Deformation is accommodated in broad shear zones that may contain discon-

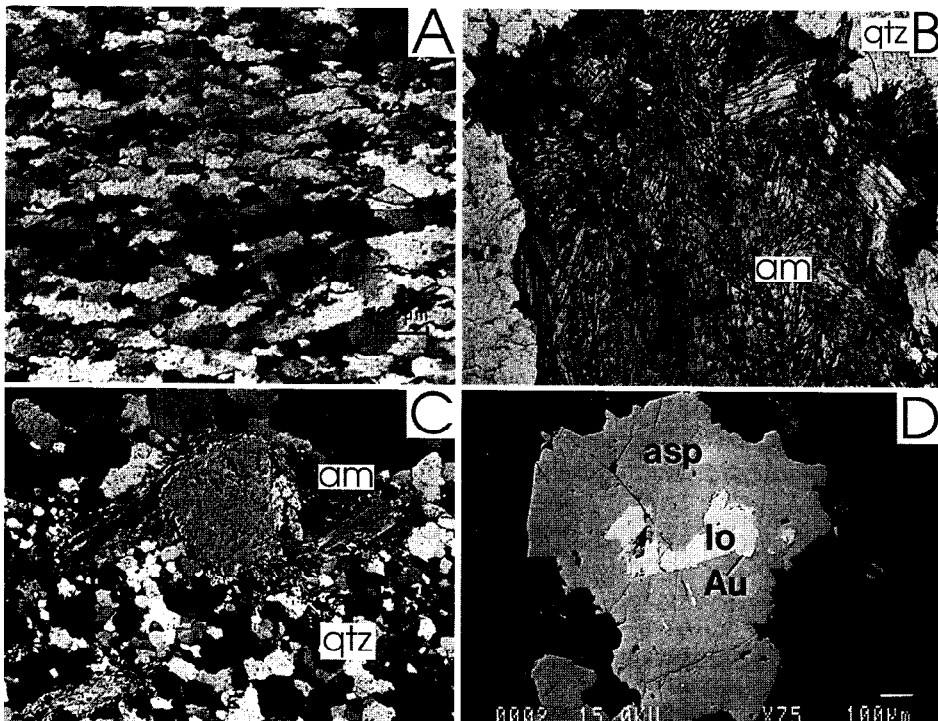


Fig. 10. (A) Typical quartz fabric found in greenschist grade deposits. Dynamic recrystallization rates exceed recovery producing elongate grains with undulose extinction, subgrains, and serrated grain boundaries (from Kerrich and Allison, 1978). (B) Monomineralic selvedge of amphibole in quartz. Earlier formed amphiboles towards the center of the selvedge are coarser and deformed, while undeformed rosettes of amphibole are intergrown with the quartz (Crown Reef, Regent Mine, Norseman, field of view = 1.4 cm). (C) Amphibole in quartz vein that has been deformed. Fibrous tails on rotated amphibole grain are also amphibole of exact same composition (actinolitic hornblende). Note the recovered nature of the quartz, which displays 120° grain boundaries and minimal undulose extinction (Mararoa reef, Ajax mine, Norseman). (D) Loellingite ( $\text{FeAs}_2$ ) grain rimmed by arsenopyrite with gold occurring at the contact between the two phases (Scotia mine, Norseman).

tinous and highly deformed quartz veins (Figs. 3 and 9; Hronsky et al., 1990; Sibson, 1990; McCuaig et al., 1993). Microstructures in these veins are produced by dislocation climb mechanisms: recovery rates of mineral grains will equal or exceed those of deformation and dynamic recrystallization, such that quartz veins may possess equant crystals with little or no undulose extinction, and 120° grain boundary intersections (Fig. 10C). As recrystallization processes destroy or alter fluid inclusions (Drury and Urai, 1990), primary fluid inclusions are only rarely preserved in this variety of quartz.

Multiple quartz micro-textures may be found in a single lode gold deposit. Microscopic textures such as intragranular fractures in quartz grains with undulose extinction or subgrain mantles indicate cyclical

variation in deformation mechanisms. These micro-textures are consistent with macroscopic features such as variably deformed quartz veins, mutually crosscutting laminated, massive, and brecciated quartz, and ductile fabrics in alteration haloes surrounding brittlely-emplaced veins, that collectively indicate transient fluid overpressuring leading to cyclic fluctuations between brittle hydraulic fracturing (fast strain rate) and ductile behaviour (slow strain rate) within the plumbing systems of lode gold deposits (Drew et al., 1996). The cyclic behaviour may well be related to the coseismic-interseismic cycle of seismogenic faults (Sibson et al., 1988; Sibson, 1990), and there is fluid inclusion evidence for this phenomenon (Section 7; Guha et al., 1991; Bouillier and Robert, 1992).

Variations in deformation mechanisms within individual lode gold quartz veins with time has also been documented. Quartz from high-*T* deposits showing significant degrees of dynamic recovery can be crosscut by later stage quartz that shows more undulose extinction and less recovery, and both may be cut by later stylolites or brittle fractures containing fault gouge (McCuaig et al., 1993). These features record the uplift and cooling of the host terranes after the thermal peak of metamorphism. Uplift of the host terrane and refracturing of the vein system may lead to populations of secondary fluid inclusions, and resetting of some primary chemical and isotopic signatures (Goldfarb et al., 1989; Kyser and Kerrich, 1991; Kerrich and Cassidy, 1994; Kent and McCuaig, 1997; Sections 7 and 12).

#### 5.4. Wall rock alteration fabrics

Within the wall rocks and vein selvedges, deformation and recrystallization processes operate in the same manner, but are complicated by the presence of multiple mineral phases with contrasting rheological properties and by the variable transmission of strain through fault/shear zones. In brittle-dominated plumbing systems formed at lower temperatures, strain accommodation occurs on discrete planes, and fabrics in the wall rock alteration haloes may not be extensively developed. In contrast, ductile-dominated plumbing systems accommodate strain in broad shear zones, imparting well developed tectonic fabrics to wall rock alteration assemblages (Fig. 3; Kerrich and Allison, 1978; Hronsky et al., 1990, and primary references therein).

Lode gold deposits formed at low and intermediate temperatures (below upper-greenschist facies) possess alteration assemblages with preferred dimensional orientations of alteration minerals, particularly phyllosilicate phases, which overprint metamorphic assemblages and fabrics. These deposits are generally considered as forming syn-late deformation and post-peak metamorphism. However, deposits formed at high temperature ( $\geq$  lower-amphibolite facies) show large degrees of dynamic recovery in alteration assemblages. In these cases, it becomes difficult to distinguish between deposits that formed at these high temperatures (cf., Barnicoat et al., 1991; Mueller

and Groves, 1991; Knight et al., 1993; McCuaig et al., 1993; Neumayer et al., 1993a,b) and deposits which formed at lower temperatures and then were subsequently metamorphosed during a later thermal event (cf., Golding and Wilson, 1982; Hamilton and Hodgson, 1986). For example, the Big Bell deposit of the Yilgarn Craton with cordierite–sillimanite–K-feldspar–garnet–biotite–quartz assemblages, was interpreted by Phillips and de Nooy (1988) to be a deposit that developed at greenschist facies conditions, and was subsequently metamorphosed to amphibolite grade. In contrast, Wilkins (1993) interprets this deposit as post-peak metamorphic on the basis of microstructural studies.

The micro- and meso-structural observations of alteration assemblages associated with these high-*T* deposits is crucial to resolving this dilemma. Variable deformation of veins and their contiguous alteration assemblages in the shear zones indicate synkinematic formation of deposits. Specifically, minerals such as amphibole and biotite in these deposits may be both aligned with and overprint the tectonic fabric on the scale of a single thin section, and while extensive dynamic recovery is apparent in the vein and alteration assemblages, rosettes of fibrous minerals, such as amphibole and chlorite, are also present (Fig. 10B, C; McCuaig et al., 1993). Multiple generations of sulphides are often apparent with deformed crystals overgrown by or coexisting with less deformed or pristine crystals (Bain, 1933). Alteration selvedges immediately adjacent to the veins are often mono- or bi-mineralic in nature (Fig. 10B). These fibrous and monomineralic assemblages have a high thermodynamic variance, indicative of formation within an open hydrothermal system (Korzhinskii, 1970; Ridley, 1990; Barnicoat et al., 1991; McCuaig et al., 1993; Mikucki and Ridley, 1993). If the deposits had been subsequently metamorphosed, more equigranular, polymetallic assemblages reflecting lower thermodynamic variance would be expected. Another key observation is that in these high-*T* deposits, löellingite, where present, is always rimmed by arsenopyrite (Fig. 10D). If the deposits had been subsequently metamorphosed, arsenopyrite would be rimmed by löellingite due to desulphidation reactions that occur during prograde metamorphism (Barnicoat et al., 1991; McCuaig et al., 1993; Neumayer et al., 1993a,b).

### 5.5. Synthesis of textural observations

In summary, vein and wall rock microstructures and fabrics provide complementary information to mineral paragenesis on the conditions of mineralization. Microstructural, macrostructural, and metamorphic observations collectively signify that these high-temperature deposits formed synkinematically, and at syn- to post-peak metamorphic conditions, in gross rheological and thermal equilibrium with the host terranes and are not metamorphosed lower temperature deposits. This has profound implications for both the timing and causes of mineralization, and hence exploration models. One of the clearest demonstrations of this characteristic is at Red Lake, Ontario, where Andrews et al. (1986) mapped out the transition from deposits in greenschist facies rocks with greenschist grade alteration assemblages to counterparts in amphibolite facies rocks with amphibolite grade alteration assemblages. Similar transitions of metamorphic grade between deposits have been identified in the lower- to mid-amphibolite facies, Coolgardie Domain, (Knight et al., 1993); in the upper-greenschist to lower-amphibolite facies Norseman Terrane of the Yilgarn Block (McCuaig et al., 1993); and the Yellowknife gold camp of the Slave Province, Canada (Boyle, 1979).

The observation that hydrothermal alteration assemblages typically overprint peak regional metamorphic assemblages does not necessarily imply a timing of mineralization significantly post-peak metamorphism. Rather, there is compelling evidence in high-*T* lode gold deposits that the mineralizing event occurred under *P-T* conditions close to peak regional metamorphism, but that the hydrothermal fluids imposed greater activities of H<sub>2</sub>O, CO<sub>2</sub>, and S in fluid conduits than in distal metamorphic rocks. Lower temperature deposits in greenschist or subgreenschist facies terranes appear to have formed during the waning stages of regional metamorphism.

Over the crustal range from subgreenschist to amphibolite and granulite facies, where the deposits form, mineralization was syn- to post-peak metamorphism and synkinematic. Cyclic fluid pressure fluctuations drive a cycle of brittle hydraulic fracturing and vein emplacement, with intervening periods of slow ductile deformation, all in the framework of the coseismic–interseismic cycle of active faults. Hence

the cyclicity of deformation style, fluid pulses, vein formation, and gold deposition are dynamically and genetically linked (Fig. 8; Kerrich and Allison, 1978; Sibson et al., 1988; Sibson, 1990; Miller et al., 1994; Robert et al., 1995; Ridley et al., 1996; Smith et al., 1996).

Possible exceptions to the post-peak metamorphic timing of lode gold deposition may occur in the Val d'Or camp of the Abitibi subprovince, where there is evidence for two distinct periods of gold mineralization: one preceding peak metamorphism that is cross-cut by metamorphosed felsic intrusions, and a second more typical post-peak metamorphic mineralization event that crosscuts later unmetamorphosed intrusions (Couture et al., 1994). However, this appears to be an exception to the rule.

## 6. Whole-rock geochemistry

In this section we first describe the distinctive metal inventory of lode gold deposits, and reasons for high gold/base metal ratios. The question of mobile vs. immobile elements is then addressed, and on this basis the results of chemical mass balance during alteration is summarized. In conclusion local and regional patterns of alteration that correlate with gold grade, or siting of deposits are described.

Whole-rock geochemistry of hydrothermal alteration assemblages associated with lode-gold deposits has been addressed by various authors (Kerrich, 1983; Kishida and Kerrich, 1987; Böhlke, 1989; Clark et al., 1989; Mikucki et al., 1990; Lesher et al., 1991). In all cases, geochemical variations, like patterns of alteration and mineralogical assemblages, show marked variations laterally away from the fluid conduits, but little variation within an individual lithology along strike or down dip within any given deposit. However, the chemical changes within a deposit are strongly dependent upon host rock composition (see Section 4).

### 6.1. Metal and rare element inventory

Lode gold deposits are characterized by a metal and trace-element inventory consisting of high en-

richments of rare elements Au, Ag, As, Sb  $\pm$  Te  $\pm$  Se  $\pm$  W  $\pm$  Mo  $\pm$  Bi  $\pm$  B, with generally low level enrichments of abundant base metals Cu, Zn, Pb relative to background abundances, and Au/Ag ratios averaging 5 (Fig. 11; Kerrich, 1983; Groves and Phillips, 1987; Colvine et al., 1988; Mueller and Groves, 1991). Sporadic enrichments of galena and sphalerite occur in the Yellowknife and Hollinger deposits respectively, but do not reach economic grades (Fig. 11). Reasons for the enrichment of rare elements, yet absence of enrichment of relatively abundant base metals are likely due to differences in transport of the elements by the hydrothermal fluid. Sulphur will readily complex Au and associated elements, but not the base metals Cu, Pb, Zn, which form complexes with Cl (Seward, 1973). Hydrother-

mal fluids associated with lode gold deposits possess generally low salinities (see fluid inclusion Section 7), which would not be conducive to base-metal transport, but significant contents of reduced sulphur, given that the source rocks (average crust) have more abundant S than Cl ( $\sim 0.1\%$  S vs. 200 ppm Cl). In addition, the source regions likely evolved fluids under low water/rock ratios (0.05). Under these conditions, rare elements will not exceed their solubility in the ambient fluid, whereas contents of abundant elements may be constrained by saturation (Kerrich and Fryer, 1981). Dehydration reactions at the greenschist–amphibolite transition will generate dilute aqueous fluids, with low Cl, relatively high dissolved S, and a carbonic component, at lithostatic fluid pressures. Collectively, these characteristics are

## Archean Lode Gold and Archean and Proterozoic VMS Deposits

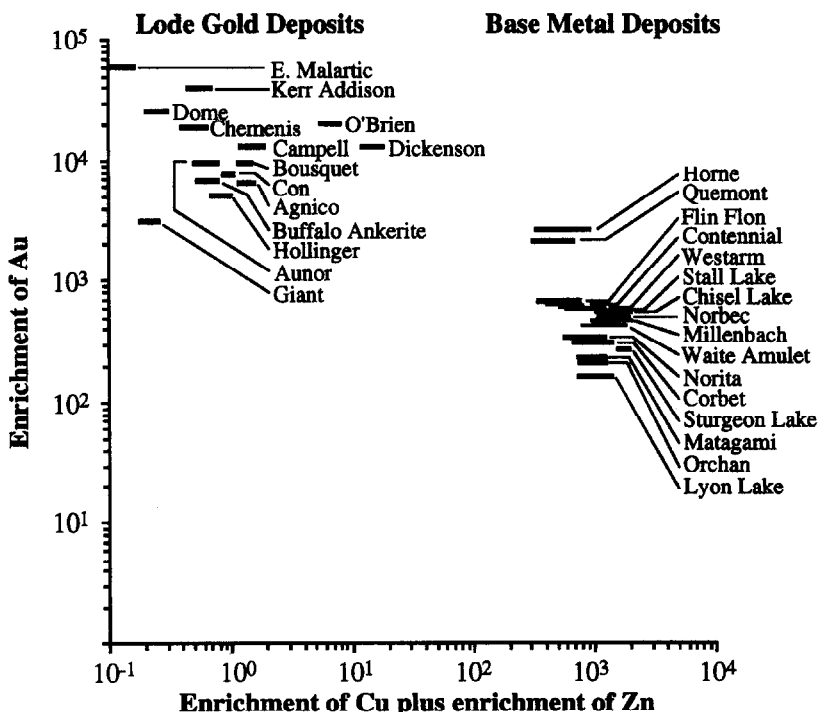


Fig. 11. Concentrations of Au vs. Cu + Zn for Archean lode gold deposits of Canada, and Archean and Paleoproterozoic volcanic hosted massive sulphide (VMS) deposits. Concentrations are relative to average crustal abundances of Au, Cu and Zn (modified from Kerrich, 1983).

Table 2

Dehydration and decarbonation reactions generating metamorphic fluids in the crust, and hydration and carbonatization reactions in lode gold deposits

*Dehydration and/or decarbonation reactions proceeding under diagenetic through upper greenschist facies conditions*

1.  $3\text{Ca}(\text{Mg},\text{Fe})(\text{CO}_3)_2 + 4\text{SiO}_2 + \text{H}_2\text{O} \rightarrow (\text{Mg},\text{Fe})_3\text{Si}_4\text{O}_{10}(\text{OH})_2 + 3\text{CaCO}_3 + 3\text{CO}_2$   
ferroan dolomite      quartz      talc      calcite
2.  $5\text{Ca}(\text{Mg},\text{Fe})(\text{CO}_3)_2 + 8\text{SiO}_2 + \text{H}_2\text{O} \rightarrow \text{Ca}_2(\text{Mg},\text{Fe})_5\text{Si}_8\text{O}_{22}(\text{OH})_2 + 3\text{CaCO}_3 + 7\text{CO}_2$   
ferroan dolomite      quartz      actinolite      calcite
3.  $3\text{Al}(\text{Mg},\text{Fe})_3\text{AlSi}_3\text{O}_{10}(\text{OH})_8 + 10\text{CaCO}_3 + 21\text{SiO}_2 \rightarrow 3\text{Ca}_2(\text{Mg},\text{Fe})_5\text{Si}_8\text{O}_{22}(\text{OH})_2 + 2\text{Ca}_2\text{Al}_3\text{Si}_3\text{O}_{12}(\text{OH}) + 8\text{H}_2\text{O} + 10\text{CO}_2$   
chlorite      calcite      quartz      actinolite      epidote
4.  $15\text{KAl}_3\text{Si}_3\text{O}_{10}(\text{OH})_2 + 9(\text{Mg},\text{Fe})_5\text{Al}_2\text{Si}_3\text{O}_{10}(\text{OH})_8 + 32\text{CaCO}_3 + 21\text{SiO}_2 \rightarrow 16\text{Ca}_2\text{Al}_3\text{Si}_3\text{O}_{12}(\text{OH}) + 15\text{K}(\text{Mg},\text{Fe})_3\text{AlSi}_3\text{O}_{10}(\text{OH})_2 + 32\text{CO}_2 + 28\text{H}_2\text{O}$   
muscovite      chlorite      calcite      quartz      epidote      biotite
5.  $6\text{Fe}_2\text{O}_3 + \text{C} \rightarrow 4\text{Fe}_3\text{O}_4 + \text{CO}_2$  reduction of hematite coupled with oxidation of carbon  
hematite      magnetite
6.  $3\text{FeS}_2 + \text{Fe}_3\text{O}_4 + 2\text{C} \rightarrow 6\text{FeS} + 2\text{CO}_2$  reduction of magnetite coupled with oxidation of carbon  
pyrite      magnetite      pyrrhotite
7.  $\text{C} + \text{O}_2 \rightarrow \text{CO}_2$  oxidation of carbon
8.  $2\text{C} + 2\text{H}_2\text{O} \rightarrow \text{CO}_2 + \text{CH}_4$  hydrolysis of carbon
9.  $\text{CH}_4 + 2\text{H}_2\text{O} \rightarrow \text{CO}_2 + 8\text{H}^+ + 8\text{e}^-$

*Hydration and/or carbonate forming reactions proceeding within domains of mineralization (hydrolysis of Fe,Ca,Mg-silicates to Fe,Ca,Mg-carbonates and muscovite)*

10.  $3\text{NaAlSi}_3\text{O}_8 + \text{K}^+ + 2\text{H}^+ \rightarrow \text{KAl}_3\text{Si}_3\text{O}_{10}(\text{OH})_2 + 6\text{SiO}_2 + 3\text{Na}^+$   
albite      muscovite
11.  $3(\text{Mg},\text{Fe})_4\text{Al}_2\text{Al}_2\text{Si}_2\text{O}_{10}(\text{OH})_8 + 6\text{Ca}_2\text{Al}_3\text{Si}_3\text{O}_{10}(\text{OH}) + 6\text{SiO}_2 + 24\text{CO}_2 + 10\text{K}^+ \rightarrow 10\text{KAl}_3\text{Si}_3\text{O}_{10}(\text{OH})_2 + 12\text{Ca}(\text{Mg},\text{Fe})(\text{CO}_3)_2 + 10\text{H}^+$   
aluminous chlorite      epidote      muscovite
12.  $3\text{Ca}_2(\text{Mg},\text{Fe})_5\text{Si}_8\text{O}_{22}(\text{OH})_2 + 2\text{Ca}_2\text{Al}_3\text{Si}_3\text{O}_{12}(\text{OH}) + 10\text{CO}_2 + 8\text{H}_2\text{O} \rightarrow 3(\text{Mg},\text{Fe})_5\text{Al}_2\text{Si}_3\text{O}_{10}(\text{OH})_8 + 10\text{CaCO}_3 + 21\text{SiO}_2^a$   
actinolite      epidote      chlorite      calcite
13.  $19\text{Ca}_2(\text{Mg},\text{Fe})_5\text{Si}_8\text{O}_{22}(\text{OH})_2 + 6\text{Ca}_2\text{Al}_3\text{Si}_3\text{O}_{12}(\text{OH}) + 100\text{CO}_2 + 14\text{H}_2\text{O} \rightarrow 9(\text{Mg},\text{Fe})_5\text{Al}_2\text{Si}_3\text{O}_{10}(\text{OH})_8 + 50\text{Ca}(\text{Mg},\text{Fe})(\text{CO}_3)_2 + 14\text{SiO}_2^a$   
actinolite      epidote      chlorite
14.  $3(\text{Mg},\text{Fe})_5\text{Al}_2\text{Si}_3\text{O}_{10}(\text{OH})_8 + 19\text{CaCO}_3 + 11\text{CO}_2 \rightarrow 15\text{Ca}(\text{Mg},\text{Fe})(\text{CO}_3)_2 + 2\text{Ca}_2\text{Al}_3\text{Si}_3\text{O}_{12}(\text{OH}) + 3\text{SiO}_2 + 11\text{H}_2\text{O}^a$   
chlorite      calcite      ankerite      epidote
15.  $\text{Ca}_2(\text{Mg},\text{Fe})_5\text{Si}_8\text{O}_{22}(\text{OH})_2 + 3\text{CaCO}_3 + 7\text{CO}_2 \rightarrow 5\text{Ca}(\text{Mg},\text{Fe})(\text{CO}_3)_2 + 8\text{SiO}_2 + \text{H}_2\text{O}^a$   
actinolite      calcite      ankerite

*Production of carbonate and sodium-bearing minerals within domains of mineralisation (hydrolysis of Fe,Ca,Mg-silicates to Fe,Ca,Mg-carbonates and albite + paragonite)*

16.  $(\text{Mg},\text{Fe})_4\text{Al}_2\text{Al}_2\text{Si}_2\text{O}_{10}(\text{OH})_8 + 2\text{Ca}_2\text{Al}_3\text{Si}_3\text{O}_{12}(\text{OH}) + 22\text{SiO}_2 + 8\text{CO}_2 + 10\text{Na}^+ \rightarrow 10\text{NaAlSi}_3\text{O}_8 + 4\text{Ca}(\text{Mg},\text{Fe})(\text{CO}_3)_2 + 10\text{H}^+$   
aluminous chlorite      epidote      quartz      albite      ferroan dolomite
17.  $(\text{Mg},\text{Fe})_4\text{Al}_2\text{Al}_2\text{Si}_2\text{O}_{10}(\text{OH})_8 + 6\text{Ca}_2\text{Al}_3\text{Si}_3\text{O}_{12}(\text{OH}) + 6\text{SiO}_2 + 24\text{CO}_2 + 10\text{Na}^+ \rightarrow 10\text{NaAl}_3\text{Si}_3\text{O}_{10}(\text{OH})_2 + 12\text{Ca}(\text{Mg},\text{Fe})(\text{CO}_3)_2 + 10\text{H}^+$   
aluminous chlorite      epidote      paragonite
18.  $\text{KAl}_3\text{Si}_3\text{O}_{10}(\text{OH})_2 + 6\text{SiO}_2 + 3\text{Na}^+ \rightarrow 3\text{NaAlSi}_3\text{O}_8 + \text{K}^+ + 2\text{H}^+$   
muscovite      albite
19.  $\text{KAl}_3\text{Si}_3\text{O}_{10}(\text{OH})_2 + \text{Na}^+ \rightarrow \text{NaAlSi}_3\text{O}_{10}(\text{OH})_2 + \text{K}^+$   
muscovite      paragonite

Modified from Kerrich (1983); <sup>a</sup>Equations after Whitehead et al. (1981).

in common with the ore fluids that formed lode gold deposits (Tables 2 and 3; Fyfe et al., 1978; Phillips, 1993; Phillips and Powell, 1993; Sections 7–9).

Significant variations in rare element and metal inventory are common. For example, the Kerr–Adison and O'Brien deposits, Abitibi subprovince, are As-rich; the Aroya lode, Kalgoorlie, and Macassa deposit, Abitibi, possess abundant tellurides; The

Dome and MacIntyre deposits, Timmins, and Norseman deposits, Western Australia, have some ore shoots rich in scheelite (Kerrich, 1983; Mueller et al., 1991a); and the Hemlo deposit is noted for high Mo contents (Pan and Fleet, 1995). Such variations on the scale of a terrane may be related to the local crustal budget of these elements (Pan and Fleet, 1995). However, such variations are noted even on

Table 3  
Summary of *P-T-X* characteristics of lode gold ore-forming fluids

Characteristic		Notes
Pressure	0.7 kbar (generally 1–3 kbar)	<ul style="list-style-type: none"> <li>transient supralithostatic to sublithostatic cycling in fluid conduits accompanied by episodic catastrophic fluid flow and hydraulic fracturing controlled by fault–valve mechanisms at high fluid/rock ratios</li> </ul>
Temperature	160°–700°C (generally 250°–400°C)	<ul style="list-style-type: none"> <li>isothermal conditions prevail within a given deposit, but broad temperature gradients noted on the terrane scale, that correlate with regional metamorphic isograds</li> <li>fluids maintain approximate thermal equilibrium with contiguous wall rocks along advection path</li> </ul>
Composition		
Volatiles	H–C–O–S–N H <sub>2</sub> O–CO <sub>2</sub> ± CH <sub>4</sub> ± H <sub>2</sub> S ± N <sub>2</sub>	<ul style="list-style-type: none"> <li>X<sub>CO<sub>2</sub></sub> ≈ 0.05–0.3, trend to higher CH<sub>4</sub>/CO<sub>2</sub> ratios with increasing temperature and pressure</li> </ul>
Solutes	Na > K ≥ Ca ≥ Mg	<ul style="list-style-type: none"> <li>rare primary saline inclusions recognized in some deposits, origins</li> </ul>
Salinity	0–35 wt.% NaCl equiv. (generally ≤ 6 wt.%)	<ul style="list-style-type: none"> <li>controversial. Possibly fluid unmixing, or secondary fluid</li> </ul>
pH	near neutral	<ul style="list-style-type: none"> <li>controlled by hematite–magnetite buffer at all crustal levels</li> </ul>
Redox state	generally reducing	<ul style="list-style-type: none"> <li>transient oxidation may occur at depositional site</li> </ul>
Metasomatism	LILE (K, Rb, Ba, Cs, Ti), S, CO <sub>2</sub>  Au, Ag, (± As, Sb, W, Sb, Te, Se, Mo, Bi, B)	<ul style="list-style-type: none"> <li>dependent on bulk composition of host rocks, but generally SiO<sub>2</sub>, CO<sub>2</sub>, S, K + LILE added at all-T, Ca added at high-T, and Na added at all-T</li> <li>higher-T deposits may contain greater abundances of Ag, W, Cu and Pb relative to lower-T deposits</li> </ul>
Fluid source	metamorphic ± magmatic ± mantle surface	<ul style="list-style-type: none"> <li>isotopic data requires large source rock volumes</li> <li>fluids dominantly metamorphic, from devolatilization of greenstones</li> <li>radiogenic isotopes require input from deep (sub-greenstone) reservoir, this deep signature more prominent proximal to greenstone margins</li> <li>surface waters possibly present in shallow-level deposits</li> </ul>
Gold transport	sulphide ligands ± chloride ligands	<ul style="list-style-type: none"> <li>dominantly Au(HS)<sub>2</sub><sup>-</sup> at sub-greenschist, Au(HS)<sup>0</sup> at amphibolite facies</li> <li>arsenic complexes may also contribute significantly to gold solubility, chloride complexes may be important gold carriers at high-T</li> </ul>
Gold deposition	(1) wall rock reactions (2) phase immiscibility (3) fluid mixing (4) chemisorption	<ul style="list-style-type: none"> <li>replacement lodes controlled by wall rock reaction; vein lodes by phase immiscibility due to transient large-scale decreases in fluid pressure</li> <li>fluid mixing potentially important in (a) high-level deposits, (b) interaction with reducing carbonaceous rocks</li> </ul>

See text for references.

the scale of single deposits. The reasons for these variations are not fully understood, but likely stem either from wall rock control and/or differing physicochemical conditions of the fluid and depositional mechanisms that operated at the sites of mineralization (see Section 11). For example Bi, W, Mo and Te are enriched in veins where they cut granites, in the Victorian gold province of South Australia. Empirically, many ore bodies with abundant tellurides are characterized by alteration assemblages that include barite and/or V-mica, signifying a relatively higher redox state of the hydrothermal fluid, as at Hemlo.

The fineness of gold in lode deposits of all ages, including slate belt equivalents, is high averaging 900, with low variability, whereas gold in porphyry, volcanogenic, and epithermal deposits is lower and more variable. Morrison et al. (1991) suggest that if the  $\text{AgCl}_2^-$  complex dominates for silver, and  $\text{Au}(\text{HS})_2^-$  dominates for gold, then sulphidation reactions, or other reactions involving decreased  $a_{\text{SO}_4}/a_{\text{H}_2\text{S}}$ , would promote gold but not silver precipitation whereas in the other types of deposits precipitation mechanisms destabilize chloro and bisulphide complexes. The high reduced S to Cl ratio of lode gold ore fluids may also play a role in fineness. Higher-*T* deposits may tend to have greater Ag, Sb, W, Cu, and Pb abundances than their lower-*T* counterparts (Perring et al., 1990; Mueller and Groves, 1991).

### 6.2. Element mobility

Calculations of chemical mass balance conducted on suites of rocks representing a wide range of alteration intensities, from numerous lode gold deposits, have shown that high-field-strength elements (HFSE: Th, Nb, Ta, Zr, Hf, Ti, Y, P, Al, Ga), rare-earth elements (REE: La through Lu), and compatible transition elements such as Sc and V, are usually alteration insensitive, or isochemical. Accordingly, variations in absolute abundances arise from volume changes during hydrothermal alteration, with ratios of these elements, and patterns on chondrite- or mantle-normalized diagrams largely unchanged from those of the precursor host rock (Kerrich, 1983; Lesher et al., 1991). This observation is

consistent with experimental data and observations on other hydrothermal systems which indicate that REE are only significantly mobilized in zones of high water/rock ratios ( $> 10^5$ , Kerrich and Fryer, 1979; Humphries, 1984; Michard and Albarade, 1986; Michard, 1989; Bau, 1991; Wood and Williams-Jones, 1994), or F-rich fluids (King and Kerrich, 1987; Pan and Fleet, 1996) and HFSE under even higher ratios (Campbell et al., 1984; Pan et al., 1994). Chromium and Ni appear to be mobile at a local scale from the presence of Cr-muscovite and Ni-rich chlorite in ultramafic and adjacent felsic rocks (Kerrich, 1983).

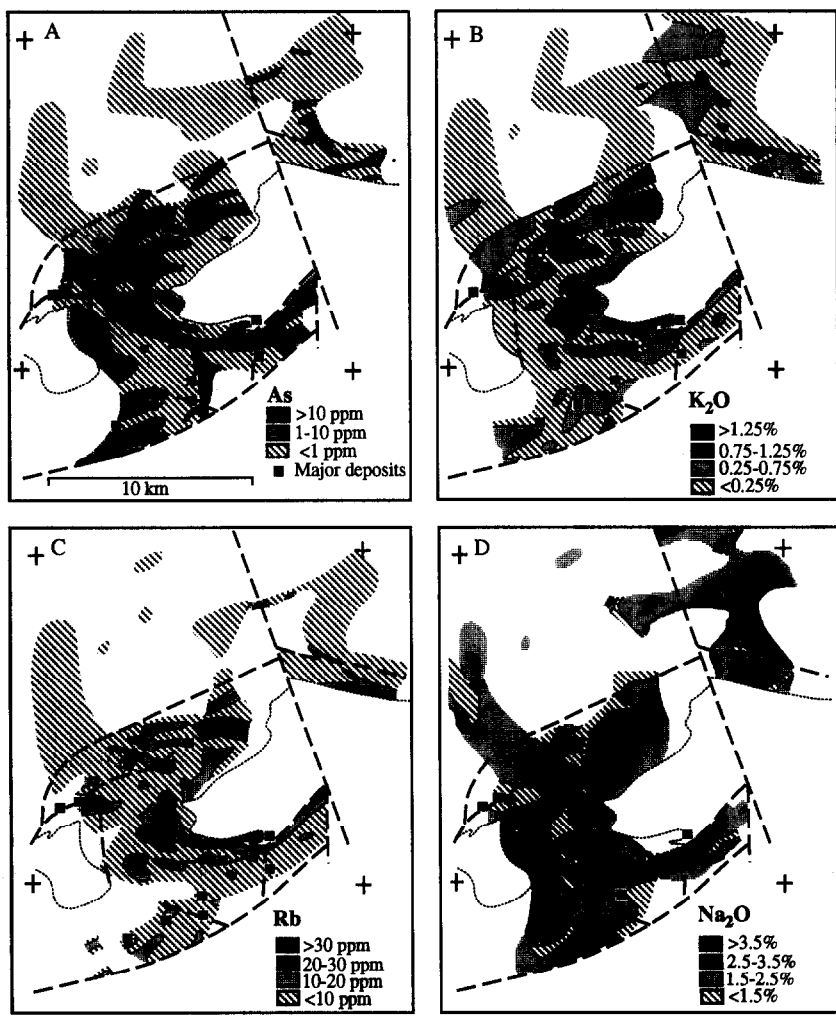
Notable exceptions to the isochemical behaviour do occur. In the Dome mine, Timmins, some veins and altered ultramafic schists show depletion and fractionation of HREE relative to the MREE. Rocks with a similar alteration mineralogy at the Hollinger deposit however, are characterized by no REE mobility (Kerrich and Fryer, 1979; Kerrich, 1986). At Taylor Township and Val d'Or, Abitibi subprovince there is extensive Zr, Hf, Y, P, and HREE metasomatic enrichment manifested as fluorapatite in the former and hydrothermal zircon, baddeleyite, monazite, and xenotime in the latter (Kerrich and King, 1993). These rare occurrences of REE and HFSE mobility were attributed to a local alkali magmatic fluid component. Pan and Fleet (1995) and Fleet et al. (1997) report REE-enriched minerals in calc-silicate assemblages from the Hemlo deposit, where higher fluid salinities may have contributed to REE complexing and transport, local fractionation of LREE from HREE, and Ti and Zr mobility.

### 6.3. Mass balance

Comparison of mass-balance studies between deposits formed at lower temperature greenschist facies conditions, vs. high temperature amphibolite and granulite facies conditions, illustrate that most deposits are characterized by enrichments of associated rare elements ( $\pm$  As, Sb, Se, Te, Bi, W, B) discussed above; large ion lithophile elements (LILE), K, Rb, Ba, Li, Cs, Tl; and volatiles ( $\text{H}_2\text{O}$ ,  $\text{CO}_2$ ,  $\text{CH}_4$ ,  $\text{H}_2\text{S}$ ). Other major elements (Fe, Mg, Ca, Na) are variably added or depleted depending on the bulk composition of the host lithology (Kerrich, 1983;

Kishida and Kerrich, 1987; Clark et al., 1989; Mikucki et al., 1990). The scale of alteration around deposits varies from several kilometers in the Timmins camp to narrow metre width selvedges in the Kirkland Lake camp (Figs. 12 and 13; Kerrich and Watson, 1984). Kishida and Kerrich (1987), showed that gold grade is highest at the crossover of the carbonate and alkali-metal saturation indices, consistent with the offset of the  $K_2O$  maxima from deposits in Fig. 13.

Within similar basalt lithologies in the Kambalda Domain, Western Australia, a change from K- to Na-metasomatism exists between deposits along the same major structure: the Hunt Mine metabasalts are characterized by K-metasomatism (Lesher et al., 1991); whereas the Victory Mine metabasalts are Na-metasomatised (Clark et al., 1989). High- $T$  deposits in metabasalts are characterized by substantial additions of Ca to inner alteration zones and depletion of Na (McCuaig, 1992, unpublished data). The



Contours of As,  $K_2O$ , Rb and  $Na_2O$  concentrations, Timmins district.

Fig. 12. Distributions of As,  $K_2O$ , Rb and  $Na_2O$  in relation to regional faults and major gold deposits of the Timmins mining camp, Ontario.  $K_2O$  and Rb maxima generally coincide, but are offset from both major faults and the deposits. Overall,  $Na_2O$  shows an antipathetic relationship to  $K_2O$  (modified from Davies et al., 1982).

reasons for these variations are unclear, but likely result from the progressive modification of the alkali and alkali earth metal to H activities of the fluid as it progressively reacted with rocks through which it advected. This in turn is controlled by the mineral assemblages stable in the  $P-T$  regimes the fluid encounters, such that Ca is fixed at high  $P-T$ , K at all  $P-T$ , and Na at low  $P-T$  conditions.

#### 6.4. LILE systematics

Potassium metasomatism is a characteristic feature of many lode gold deposits; accordingly, consid-

eration of LILE systematics may provide constraints on fluid sources, and hence the genetic origin of lode gold deposits (Perring and Barley, 1990; and references therein). Coherent behaviour of K, Rb, Ba, Cs and Tl is present over three orders of magnitude in K content, shown by K/Cs, K/Tl, K/Rb (130 to 430) and K/Ba (34 to 97) ratios that are in close compliance with the ratios of 'average crust' (K/Rb = 286, K/Ba = 37; Taylor and McLennan, 1985), and is independent of host lithology or K-bearing alteration phase (muscovite, K-feldspar, biotite) (Fig. 14). In deposits hosted by felsic intrusive rocks with high initial LILE contents, it may be difficult to discern whether the LILE ratios observed in alteration reflect those in the hydrothermal fluid. However, in deposits hosted by mafic-ultramafic volcanic rocks, with low initial LILE abundances, the enhanced measured levels of K, Rb and Ba must result from their co-enrichment by the hydrothermal ore-forming system (Kerrich, 1990a,b; Perring and Barley, 1990). LILE ratios in the deposits may reflect in part fluid–rock interaction along hydrothermal conduits, as well as ratios of the fluid source.

These LILE systematics in lode gold deposits contrast with those in fluids derived from magmatic,

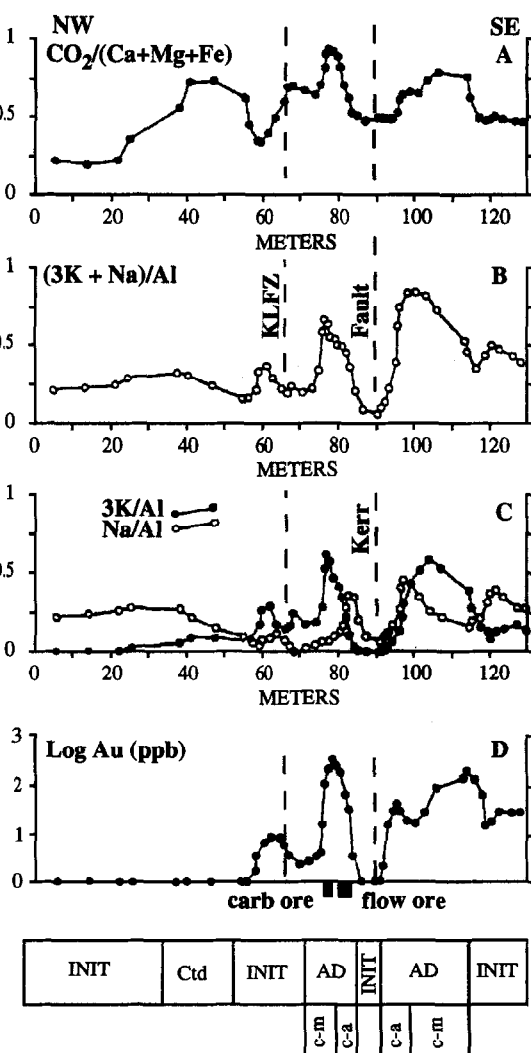


Fig. 13. (A, B, and C) Variations of alteration stages across the 3,850-ft level of the Kerr-Addison mine, relative to saturation indices of  $\text{CO}_2$  and alkali metals. Initial stage of alteration (INTT) is characterized by low  $\text{CO}_2 / (\text{Ca} + \text{Mg} + \text{Fe})$  and  $(3\text{K} + \text{Na})/\text{Al}$  indices. Advanced stage of alteration (AD) corresponds to areas of high  $\text{CO}_2 / (\text{Ca} + \text{Mg} + \text{Fe})$  and  $(3\text{K} + \text{Na})/\text{Al}$  indices. The broad  $\text{CO}_2 / (\text{Ca} + \text{Mg} + \text{Fe})$  peak north of the Kirkland Lake–Larder Lake fault zone has no associated  $(3\text{K} + \text{Na})/\text{Al}$  maxima, corresponding to an area of chloritoid alteration (CTD). Areas of the advanced stage of alteration (AD) can be subdivided into zones of carbonate–muscovite type (c-m) and carbonate–albite type (c-a) on the basis of high  $3\text{K}/\text{Al}$  or  $\text{Na}/\text{Al}$ , respectively. Note the symmetrical distribution of different saturation indices relative to the Kerr fault. All points correspond to the moving averages of five samples, projected on a N  $30^\circ$  W vertical plane (D). Distribution of moving averages of Au concentration across the 3850 = ft level of the Kerr-Addison mine, compared to the saturation indices of  $\text{CO}_2$  and alkali metals. Concentrations of Au are generally high south of the fault zone. Note that the gold maxima are slightly displaced relative to the maxima of the saturation indices. Peaks of Au correspond to points where  $3\text{K}/\text{Al}$  and  $\text{Na}/\text{Al}$  indices display similar values and are therefore in the transition zone between carbonate–muscovite and carbonate–albite alteration types (modified from Kishida and Kerrich, 1987).

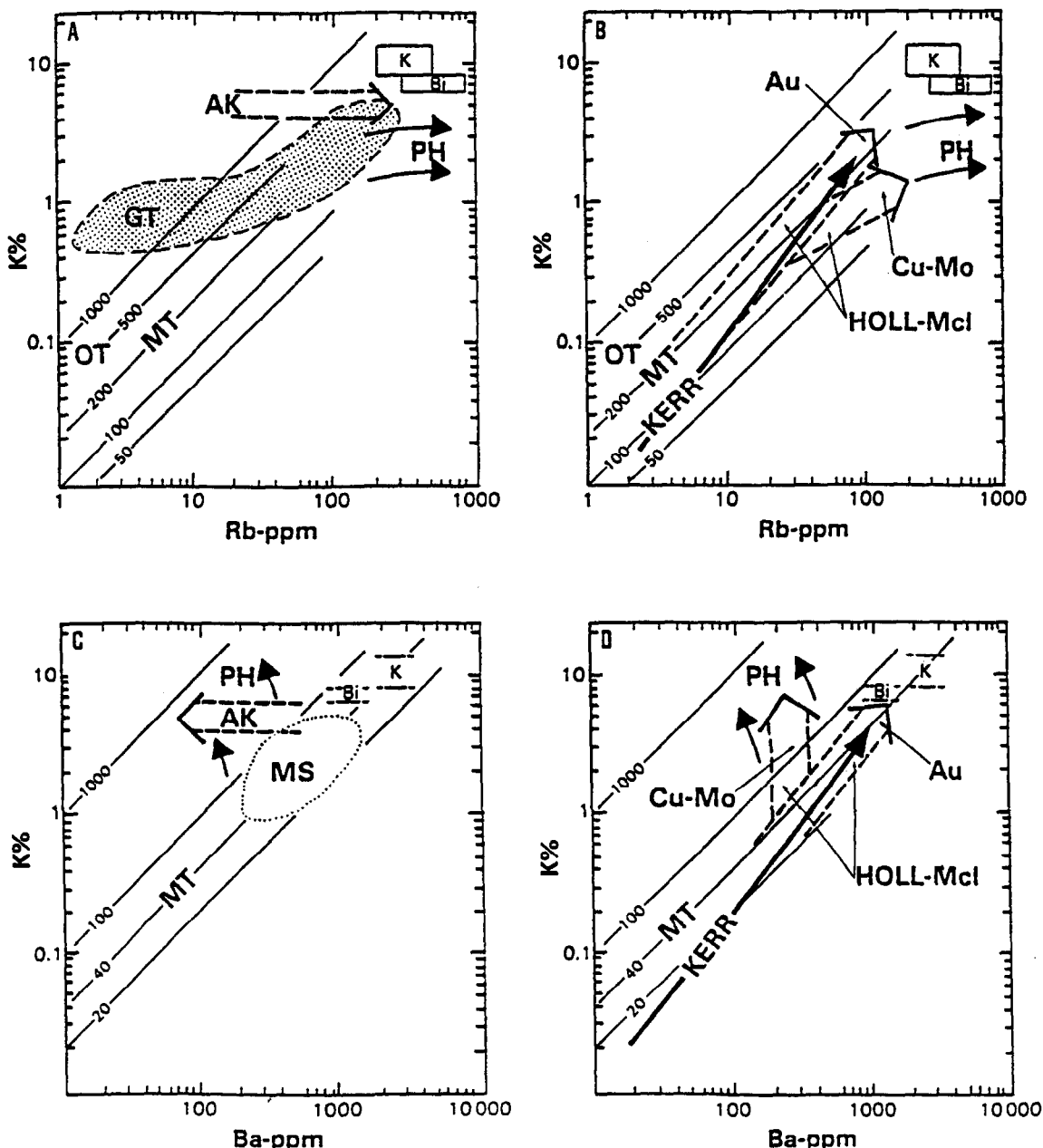


Fig. 14. K-Rb and K-Ba systematics. (A) MT—main trend of igneous rocks; OT—oceanic tholeiites; GT—granulite trend; PH—pegmatite-hydrothermal trend of magmatic fluids. AK—data for ortho-magmatic W, Mo greisens in the Ackley granite, Newfoundland; K, Bi-fields for igneous K-feldspar and biotite. (B) Data for the Kerr Addison (Kerr) and Hollinger-McIntyre lode gold and separately Cu-orebodies. (C,D) K-Ba data for the same rock units and in orebodies as in A,B. Note that both lode gold deposits plot close to the main trend, whereas the orthomagmatic orebodies follow the PH trend (from Kerrich, 1989c).

sea floor hydrothermal, or granulite formation processes. Deposits formed from dominantly magmatic ore fluids such as Cu-, and Mo-porphyry deposits,

Sn-W greisens, and certain pegmatites, display interelement trends between K, Rb, Ba, Cs and Tl that are in keeping with the characteristic partitioning

trends of late-stage magmatic systems. During progressive fractional crystallization of magmatic rocks K/Rb, K/Cs and K/Tl decrease, but K/Ba ratios increase (Fig. 14).

Many granulites, notably Archean granulite facies TTG's, are apparently depleted in LILE, leading some workers to postulate that the LILE enrichments characteristic of lode gold deposits may indicate ore fluids produced during granulitization processes in the lower crust (Cameron, 1988; Colvine et al., 1988). There are several problems with this model: (1) Weaver and Tarney (1993) have shown that the depletion of LILE in many Archean TTG is primary rather than a result of granulitization; (2) the K/Cs, K/Rb and K/Ba ratios of the deposits are not complementary to the ratios in granulites, and (3) much of the granulitization appears to predate gold mineralization. It is also problematic for this model that large volumes of LILE depleted TTG's are not evident in the Paleoproterozoic, Lower Palaeozoic, or Cordilleran lode gold provinces (for reviews see Kerrich, 1990a,b).

Experimental studies of basalt-fluid and peridotite-fluid exchange, and field studies of dehydration paths in subduction-accretion complexes may throw some light on the fluid-source for lode gold deposits. Both types of studies show that the soluble and highly incompatible elements Au, B, Cs, Rb, K, Ba, As, and Sb are enriched in fluids evolved at the greenschist-amphibolite facies transition relative to Th, REE, and base metals (Pearce and Peate, 1995; Bebout, 1996; Kogiso et al., 1997). Subduction-zone derived fluids generally flux the mantle wedge to generate arc magmas (Pearce and Peate, 1995, and references therein). Thus the association of many lode gold provinces with subduction-accretion complexes, the timing of lode gold mineralization after cessation of the main magmatic events, the solute composition of fluids of dehydration, and the element inventory of lode gold deposits, and the element inventory of structurally higher Au-Sb, Sb-Hg, and Hg deposits collectively (Section 13), may not be fortuitous.

## 7. Fluid inclusions

Fluid inclusions preserved in hydrothermal minerals provide the best constraints on several intensive

variables of the hydrothermal ore fluids, and are the only direct samples of the mineralizing fluid(s) (Crawford, 1992; Roedder and Bodnar, 1997). This section summarizes the data that has been obtained from fluid inclusions in lode gold deposits. Emphasis is placed on the limitations of the database, as multiple and often conflicting interpretations of similar data are presented in the literature.

Most of the data summarized below has been obtained from fluid inclusions in quartz. Other mineral phases, such as clinopyroxene and garnet in higher temperature lode deposits, and sphalerite, pyrite and even gold can preserve useful inclusions that have been analyzed in rare instances. Reconnaissance studies of fluid inclusions in such phases reveal fluids with broadly similar characteristics to those trapped within coexisting quartz, but to the authors' knowledge this correlation has yet to be confirmed by detailed analyses (van Hees and Kesler, 1990; Brown, 1993).

Problems involved in interpreting fluid inclusion data have been reviewed by various authors, but warrant listing here (Roedder, 1984; Ho et al., 1990a, 1992; Kesler, 1990; Crawford, 1992). These include: (1) the phase(s), usually quartz, hosting readily analyzed fluid inclusions are often difficult to relate to gold paragenetically, and thus the fluid studied may not be representative of the fluid from which gold was deposited; (2) many generations of fluid inclusions are often present in a single mineral phase so that it is important to identify what event the fluid studied actually represents; and (3) primary, and even pseudosecondary, fluid inclusions are difficult to preserve in a dynamically evolving quartz vein system, especially at high temperatures as outlined previously, so that the 'primary' inclusions analyzed rarely represent early stages of vein emplacement and hydrothermal alteration (Section 5).

In addition, the preservation potential of fluid inclusions in lode gold deposits when they are uplifted from their projected depths of formation is poorly understood (< 5 km to as deep as 25 km, Groves et al., 1992, 1998). Leakage, stretching, and diffusion may significantly affect the calculated  $P-T$  conditions and chemical and isotopic compositions of the inclusions. In addition, fluid pressure fluctuations from lithostatic to hydrostatic under isothermal conditions, results in a wide range of measured

homogenization temperatures (Roedder and Bodnar, 1980; Guha et al., 1991; Section 5). These and other potential problems require that fluid inclusions from lode gold deposits be carefully constrained paragenetically.

### 7.1. Greenschist facies deposits

#### 7.1.1. Volatiles and solutes

Fluid inclusion studies of lode gold deposits hosted in greenschist facies rocks are numerous and indicate uniform hydrothermal fluid conditions for these deposits regardless of age or geographic location. Examples include mid-Archean deposits in the Barberton greenstone belt (de Ronde et al., 1992); late Archean deposits of the Abitibi subprovince at Val d'Or and Timmins, and in the Yilgarn craton (Robert and Kelly, 1987; Spooner et al., 1989; Kesler, 1990; Guha et al., 1991; Ho et al., 1990a); Proterozoic deposits in the Trans Hudson Orogen of Northern Saskatchewan (Fedorowich et al., 1991); the Victorian gold province of south Australia; deposits in the Jurassic to Tertiary Cordillera (Weir and Kerrich, 1987; Goldfarb et al., 1989, 1997); and the Tertiary

Monte Rosa lodes of the Italian Alps (Diamond, 1990). Inclusions consist of  $H_2O-CO_2 \pm CH_4 \pm N_2 \pm H_2S$  fluids and generally occur in four broad categories: (1) two- or three-phase,  $H_2O-CO_2$  inclusions; (2)  $CO_2$ -rich inclusions with variable amounts of  $CH_4$  and small amounts of  $H_2O$ ; (3) 2-phase  $H_2O$  (liquid + vapour) inclusions; and (4) highly saline aqueous inclusions.

In the studies referred to above there is general agreement that fluids of inclusion types (2) and (3) represent trapping of immiscible phases exsolved from an original liquid represented by type (1) inclusions. These primary fluids possess  $X_{(CO_2+CH_4)}$  values ranging from 0.05 to 0.25 (10 to 45 wt.%), averaging 0.15.  $CO_2/CH_4$  ratios are variable, with high  $CH_4$  values attributed either to the interaction of the hydrothermal fluids with carbonaceous host rocks or to the initially lower oxidation state of the fluid (closer to the  $CO_2-CH_4$  buffer, see phase equilibria Section 8). The trapped fluids are generally < 6 wt.% NaCl equivalent, with  $Na > Ca \geq K \geq Mg$ , and daughter minerals are rare. The origin of the highly saline type (4) aqueous inclusions is controversial, and discussed at the end of this section.

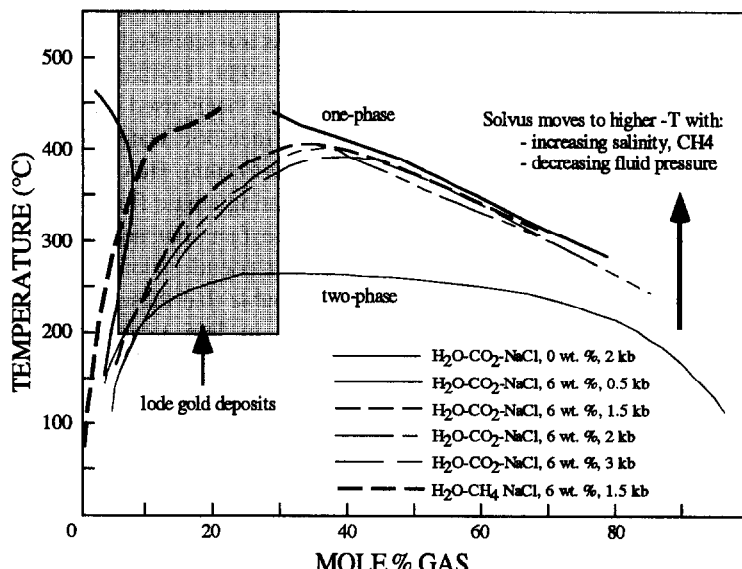


Fig. 15. Temperature vs. fluid composition phase diagram for the  $H_2O-CO_2-NaCl$  and  $H_2O-CH_4-NaCl$  systems, redrawn from Ho et al. (1992) and Naden and Shepherd (1989). Note that the solvus moves to higher temperatures with (1) increased salinity, (2) increased  $CH_4$  (or  $N_2$ ) content, and (3) decreasing fluid pressure. At higher temperatures, fluid immiscibility may be aided by shock nucleation processes during seismic events, in combination with large pressure drops within the fluid conduits.

### 7.1.2. Calculated P-T conditions

Homogenization temperatures ( $T_h$ ) for the primary types 1–3 inclusions range from 160° to 400°C, with most data clustering at  $300^\circ \pm 50^\circ\text{C}$  (Ho et al., 1992). Where fluid inclusions within a single sample population have similar ratios of volatile phases, these temperatures must be considered minimum estimates of trapping temperatures ( $T_t$ ). Where the range of phase proportions is wider, it is possible that phase immiscibility had occurred and that the inclusions were trapped at conditions close to the solvus curve of the  $\text{H}_2\text{O}-\text{CO}_2-\text{CH}_4-\text{NaCl}$  system, in which case  $T_h$  approximates  $T_t$  (Fig. 14; Roedder, 1984; Guha et al., 1991; Ho et al., 1992). In situations where phase immiscibility is inferred, or where  $T_t$  can be independently established by stable isotope mineral-pair fractionations or phase equilibria, trapping pressures can be estimated from fluid density data on  $\text{CO}_2$ -rich inclusions (Roedder, 1984). Pressures of 0.7 to 4.1 kbar have been calculated for deposits in greenschist facies rocks and are generally in the range of 1 to 3 kbar (Ho et al., 1992).

A range in  $T_h$  of  $> 200^\circ\text{C}$  is commonly obtained within individual deposits (Ho et al., 1990a; Kesler, 1990). This range in  $T_h$  may be due to post entrapment modification of fluid inclusions (volume changes, leakage), or to transient fluid pressure fluctuations during mineral deposition (Figs. 8B and 15). Evidence for fluid pressure fluctuations comes from careful documentation of phase ratios in primary or pseudosecondary fluid inclusion populations, interpreted as resulting from phase immiscibility triggered by rapid pressure drops during quartz deposition (Figs. 8B and 15; Robert and Kelly, 1987; Spooner et al., 1987; Kerrich, 1989a,b; Guha et al., 1991), and corroborates evidence from vein and fracture/shear zone morphologies and microstructures for sublithostatic to supralithostatic fluid pressure cycling (see Section 5).

Fluid pressure fluctuations during mineral deposition complicates interpretation of pressures and temperatures derived from fluid inclusion data. Given the isothermal conditions of alteration and vein emplacement implied by the lack of alteration zonation parallel to fluid conduits, and the uniform oxygen isotope compositions of quartz within individual deposits (see Section 9), the observed spread in  $T_h$  values is best interpreted as reflecting transient  $P_f$

fluctuations during hydraulic fracturing and subsequent mineral deposition under near isothermal conditions (Robert and Kelly, 1987; Guha et al., 1991; Wilkinson and Johnston, 1996). From a study of fluid inclusion planes in the Val d'Or lode deposits, Quebec, Bouillier and Robert (1992) found that successive cycles of opening and collapse in subhorizontal extension veins correlated with opening and slip on high-angle shear veins. They interpreted the observations as recording fluid pressure fluctuations in successive coseismic–interseismic cycles (Section 5).

### 7.1.3. Analyses of extracted fluids

Recent studies have extracted fluids by thermal (step) decrepitation of quartz, finely crushing quartz, or by laser microprobe in an attempt to analyze the chemical and isotopic compositions of the hydrothermal fluids responsible for alteration and mineralization (Pickthorn et al., 1987; Nesbitt et al., 1989; Böhlke and Irwin, 1990; van Hees and Kesler, 1990). Such studies confirmed the presence of C–O–H–N–S volatiles in fluid inclusions, as well as identifying solutes such as Na, Ca, Mg, K, Cl, Br, I, Ar, Kr and Xe. Where fluids from Cordilleran deposits were analyzed, the  $\delta\text{D}$  values,  $^{36}\text{Ar}$  and  $^{84}\text{Kr}/^{36}\text{Ar}$  compositions of the extracted fluids were found to be the same as air-saturated meteoric groundwaters (Nesbitt et al., 1989; Böhlke and Irwin, 1990, 1992). This data has been used to support a genetic model in which meteoric waters form a significant portion of the ore-forming fluid. However, given the difficulty in isolating single fluid inclusions for these analyses, and the fact that secondary inclusions greatly outnumber pseudosecondary and primary inclusions, it is probable that these analyses are sampling meteoric waters in late secondary fluid inclusions trapped during uplift of the terranes (Pickthorn et al., 1987; Goldfarb et al., 1989; Kerrich, 1990a; Kyser and Kerrich, 1990; Section 9). Meteoric water is explicitly ruled out as the ore-forming fluid for the Brusson deposit, NW Alps, based on the  $^{36}\text{Ar}/^{3}\text{He}$  systematics of fluid inclusion waters (Pettke and Diamond, 1997).

In a study of fluid inclusions from gold lodes in the Italian Alps, Yardley et al. (1993) determined that fluids were compositionally uniform, with 5% NaCl equivalent, dominated by NaCl, with lesser

$\text{CaCO}_3$  (aq),  $\text{KCl}$ , and  $\text{Na}_2\text{CO}_3$  (aq). There was substantial  $\text{H}_2\text{S}$  contents ( $> 10^{-3}$  molal), and minor  $\text{CH}_4$  ( $< 0.002$ – $0.003$  mole%). Trace element concentrations in ppm were as follows: Al (300–1000), Mg (10–135), Fe (20–170), B (100's), Li, Zn, and As (10's–100's), and Rb, Sr, Ba, 10's ppm. Bromine/Cl and I/Cl ratios are consistent with deeply circulating surface waters that underwent extensive exchange with crustal rocks, but there is an insufficient database or knowledge of halogen systematics to rule out metamorphic or other fluids.

### 7.2. Sub-greenschist, amphibolite and granulite facies deposits

Studies of fluid inclusions in sub-greenschist facies deposits such as Racetrack (Gebre-Mariam et al., 1991); Wiluna (Hagemann et al., 1993); and amphibolite–granulite facies deposits including three Mile Hill, Marvel Loch, and Griffin's Find (Hagemann and Ridley, 1993a,b) have established that the fluids responsible for hydrothermal alteration and mineralization had compositions similar to those for greenschist facies deposits, dominantly  $\text{H}_2\text{O}-\text{CO}_2$  with low to moderate salinities. However, some sub-greenschist facies deposits contain fluid inclusions with a wide range of salinity, from 0 to 22 wt.% NaCl equivalent (Hagemann and Ridley, 1993b).

Fluid inclusion data from high temperature deposits is difficult to interpret for several reasons: (1) the high recovery rates in quartz formed at these temperatures, and thus the difficulty in preserving 'primary' fluid inclusions; (2) the likelihood of post-modification of inclusions during cooling and uplift of these inclusions; and (3) the ubiquitous partial retrogression of the high-temperature assemblages in these deposits, indicating post-mineralization fluid movement through these rocks. Deposits in amphibolite and granulite facies rocks contain fluid inclusions with consistently higher  $\text{CH}_4/\text{CO}_2$  ratios than their greenschist facies counterparts, and may contain both primary and secondary high salinity aqueous inclusions (Hagemann and Ridley, 1993b). The high  $\text{CH}_4/\text{CO}_2$  ratios may be partially explained by  $\text{H}_2$  diffusion during post-entrapment modification accompanying uplift, driving reactions such as  $\text{CO}_2 + 4\text{H}_2 = 2\text{H}_2\text{O} + \text{CH}_4$  (Hagemann and Ridley, 1993b).

Pressure estimates obtained from subgreenschist facies deposits vary between hydrostatic and lithostatic, with extreme variations noted on the scale of individual deposits that is taken as reflecting extreme fluctuations in fluid pressure during quartz vein emplacement and mineralization (Fig. 8B; Hagemann and Ridley, 1993b). The pressure and temperature data obtained from fluid inclusions from higher- $T$  deposits is difficult to interpret due to the uncertainty in their post-formation  $P-T-t$  history (Hagemann and Ridley, 1993b; cf., Vitryk et al., 1994). Clockwise vs. anticlockwise  $P-T-t$  paths may produce significantly different measured  $T_h$  from inclusions that initially formed at a uniform temperature. Usually, pressure and temperature constraints from independent geothermometers and geobarometers must be employed in concert with textural observations. A potentially useful criterion for determining the sense of post-formation  $P-T$  paths for fluid inclusions has recently been proposed by Vitryk et al. (1994). In their study, natural fluid inclusions of various sizes and similar formation conditions subjected to external overpressuring simulating burial, or anticlockwise  $P-T$  paths, resulted in smaller inclusions reequilibrating before larger inclusions. In other cases, fluid inclusions subjected to internal overpressuring due to uplift, or clockwise  $P-T$  paths, result in larger inclusions reequilibrating before smaller inclusions. If valid, this criterion may prove useful in determining post-mineralization  $P-T$  paths for high-temperature lode gold deposits.

### 7.3. Saline fluid inclusions

Saline aqueous fluid inclusions (10 to 35 wt.% NaCl equivalent, daughter minerals common) are observed in many Archean lode gold deposits and their origin remains controversial (Guha and Kanwar, 1987; Robert and Kelly, 1987; Kesler, 1990; Ho et al., 1990a, 1992; Hagemann and Ridley, 1993b). In many cases they are incontrovertibly post mineralization, being transgranular in nature, cutting across planes of earlier fluid inclusions, often possessing irregular morphologies, and having homogenization temperatures averaging 50° to 100°C below those of inclusions associated with quartz vein emplacement and hydrothermal alteration.

These inclusions potentially represent samples of saline NaCl–CaCl<sub>2</sub> brines that have percolated down through the Precambrian shields through time (Guha and Kanwar, 1987), or deeply sourced fluids trapped post-peak metamorphism on a counter-clockwise  $P-T-t$  path (Hagemann and Ridley, 1993b). In some cases however, saline inclusions are documented as forming coeval with H<sub>2</sub>O–CO<sub>2</sub> inclusions (Robert and Kelly, 1987; Hagemann and Ridley, 1993b; Kerrich and King, 1993). In sub-greenschist facies deposits, combined stable isotope and fluid inclusion data suggest that the variably saline inclusions either represent the result of fractionation of salt into the H<sub>2</sub>O-rich liquid phase during phase separation (Robert and Kelly, 1987; S.G. Hagemann, pers. commun., 1994), or mixing of evolved saline formation brines with a primary H<sub>2</sub>O–CO<sub>2</sub> fluid advecting up through the metamorphic pile (Gebre-Mariam et al., 1991, 1993; Hagemann et al., 1993; Hagemann and Ridley, 1993b).

In deposits formed at greenschist to granulite facies conditions, stable isotope data does not support involvement of surface waters in the hydrothermal system. In these cases, the ‘primary’ saline fluid inclusions may have formed by large-scale fluid immiscibility, where solutes partitioned into the aqueous phase (e.g., Robert and Kelly, 1987; Johnson, 1991) or from a fluid that was immiscible with the primary H<sub>2</sub>O–CO<sub>2</sub> fluid at elevated temperatures and advected along the same structure (Hagemann and Ridley, 1993b; Kerrich and King, 1993). Pan and Fleet (1995) report a curvilinear correlation between salinity and  $T_h$  in fluid inclusions with negligible CO<sub>2</sub> contents from gold-related calc–silicate alteration at the Hemlo deposit, Ontario, which they interpret as evidence for mixing between a deeply sourced, hot, saline (magmatic?) fluid and lower-temperature surface waters.

## 8. Phase equilibria

The advent and continuous refinement of internally consistent thermodynamic databases for mineral phases and volatile species (Berman, 1988; Holland and Powell, 1990) has led to the widespread application of phase equilibria in studies of hydrothermal alteration associated with lode gold de-

posits (Weir and Kerrick, 1987; Böhlke, 1989; Clark et al., 1989; Ridley, 1990; Cassidy and Bennett, 1993; Mikucki and Ridley, 1993). Specifically, phase equilibria studies provide information on: (1) chemical reaction fronts associated with alteration envelopes; (2) variations in alteration mineralogy with temperature; (3) physico-chemical conditions of ore-forming fluids; and (4) possible genetic links between lode gold deposits formed at a variety of crustal levels.

Given the presence of steep chemical gradients away from the fluid conduits (Section 4), only veins formed by direct precipitation from the hydrothermal fluids, or fluid-buffered vein selvages, yield information about the  $P-T-X_{\text{fluid}}$  conditions at the time of deposition (Ridley, 1990; Mikucki and Ridley, 1993). Critical selvedge assemblages for lode gold deposits are listed in Table 1, and interdeposit comparisons of alteration mineralogy and fluid compositions can be made utilizing reactions between these phases (Ridley, 1990; Mikucki and Ridley, 1993).

Critical vein selvedge assemblages can be compared on  $T-X_{\text{CO}_2}$  plots given independent constraints on pressure and  $X_{\text{CO}_2}$  values from fluid inclusions, phase equilibria, and mineral geothermometers or barometers, (Fig. 16). Although  $X_{\text{CO}_2}$  conditions in amphibolite and granulite facies deposits are poorly constrained, in these cases the temperature of formation can be established by other techniques including stable isotope mineral-pair geothermometry (Kerrick; 1987; Norseman, T.C. McCuaig, unpublished data, 1993), or mineral chemistry geothermometers such as arsenopyrite geothermometry (Neumayer et al., 1993a,b). Alternatively, Weir and Kerrick (1987) used the coexistence of quartz and magnesite in the Mother Lode deposits, combined with an estimated temperature of 300°C and  $X_{\text{CO}_2} = 0.2$ , to infer a fluid pressure of 1.5 to 2 kbar.

The variance in vein selvedge assemblages between a number of Archean lode gold deposits, hosted in terranes at a variety of metamorphic grades, is consistent with their formation from a similar fluid, but at different pressures and temperatures (Figs. 16 and 17). This variation correlates with metamorphic grade of the host rocks (Fig. 3). Most lode gold deposits are characterized by alteration assemblages commensurate with the ambient metamorphic  $P-T$  conditions (Boyle, 1961; Clark et al.,

1986, 1989; Groves et al., 1989; Barnicoat et al., 1991; Witt, 1991; McCuaig et al., 1993). These observations provide compelling evidence that the ore-forming process operated close in time to metamorphism at syn- to post-peak thermal conditions.

Calculation of other ore fluid parameters such as pH,  $f(O_2)$ ,  $m_{\Sigma S}$ , and alkali cation ratios, require independent estimates of pressure and temperature, which can be supplied by fluid inclusion, stable isotope or thermodynamic means (Mikucki and Ridley, 1993). In greenschist facies deposits, pH is constrained by the stability of carbonates, sericite + albite, and rarely K-feldspar or paragonite, to a range of 5 to 6 (Fig. 17). The only pH calculation on amphibolite facies deposits has been performed by Mikucki and Ridley (1993), who estimate a pH range of 5 to 6 for these high temperature deposits (Fig. 17). Thus both low and high temperature deposits appear to have formed from fluids of approximately neutral pH.

Redox conditions of alteration assemblages indicate that most deposits formed from relatively reduced ore fluids, characterized by assemblages of pyrite  $\pm$  arsenopyrite  $\pm$  stibnite in the lowest temperature subgreenschist facies; pyrite  $\pm$  arsenopyrite  $\pm$  pyrrhotite at intermediate temperatures (greenschist to low-amphibolite facies); and löellingite + arsenopyrite  $\pm$  magnetite  $\pm$  ilmenite  $\pm$  pyrrhotite in high temperature conditions of amphibolite–granulite facies hosted deposits (Mikucki and Ridley, 1993; Fig. 3).

Some lode gold deposits formed from relatively oxidized fluids, however, and are characterized by assemblages containing magnetite or hematite at low to intermediate temperatures, and assemblages of pyrrhotite + pyrite  $\pm$  chalcopyrite  $\pm$  ilmenite  $\pm$  spinel at higher temperatures. The more oxidized assemblages may include barite and/or V-muscovite. Examples are some of the Kirkland Lake deposits and Hemlo (Kerrich, 1983; Pan and Fleet, 1995). There is some evidence that the more oxidized assemblages reflect fluid immiscibility by loss of reduced gas species from a primary reduced ore fluid, reflected in  $^{34}S$  depleted sulphides (Sections 9 and 11). In general, high-temperature deposits appear to have formed at higher values of  $f(O_2)$ . This observation is consistent with regulation of the redox conditions of ore-forming hydrothermal fluids at

all crustal levels by the hematite–magnetite,  $HSO_4^-/H_2S$  and  $CO_2/CH_4$  buffers (Fig. 18).

Collectively, the above observations are consistent with the formation of lode gold deposits, at all crustal levels, from similar ore fluids that maintained approximate thermal equilibrium with the rocks through which they advected. Redox conditions varied slightly with higher  $f(O_2)$  and S activity in the higher temperature deposits. Major cations activities where Ca metasomatism is dominant at high  $T$ , Na at low  $T$ , and K at all temperatures, suggest progressive modification of the fluids through fluid–wall

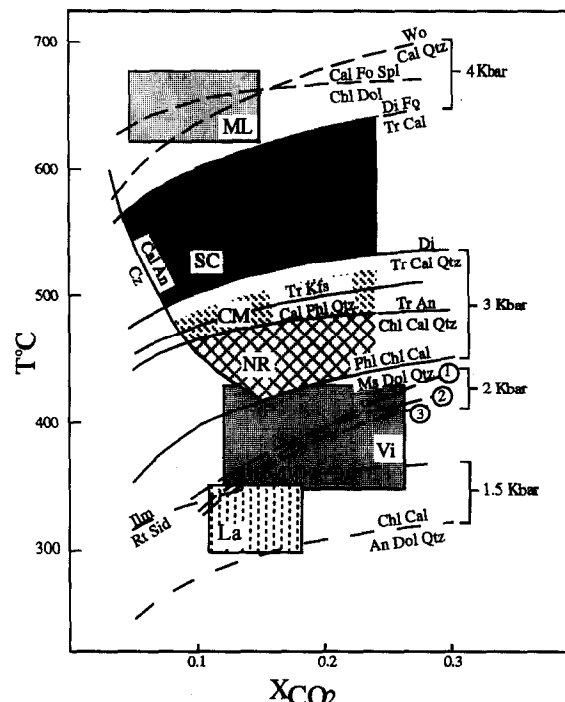


Fig. 16.  $T - X_{CO_2}$  phase diagram showing isobaric equilibrium curves for mineral assemblages at specific deposits of the Yilgarn Block, Western Australia. La = Lancefield, Hronsky and Ridley (1992); Vi = Victory, Clark et al. (1989); NR, CM and SC = North Royal, Crown–Mararoa and Scotia, respectively, McCuaig et al. (1993); ML = Marvel Loch, Mueller et al. (1991b). Reactions for the Victory mine are: (1)  $Ms + Dol = Bt + Chl + Cal$ ; (2)  $Bt + Chl + Dol = Act + Ms$ . Abbreviations: Act = actinolite; An = anorthite; Bt = biotite; Cal = calcite; Di = diopside; Fo = forsterite; Ilm = ilmenite; Kfs = K-feldspar; Phl = phlogopite; Rt = rutile; Sid = siderite; Spl = spinel; Tr = tremolite; Wo = wollastonite. Redrawn from McCuaig et al. (1993) and Mikucki and Ridley (1993), where complete data sources are listed.

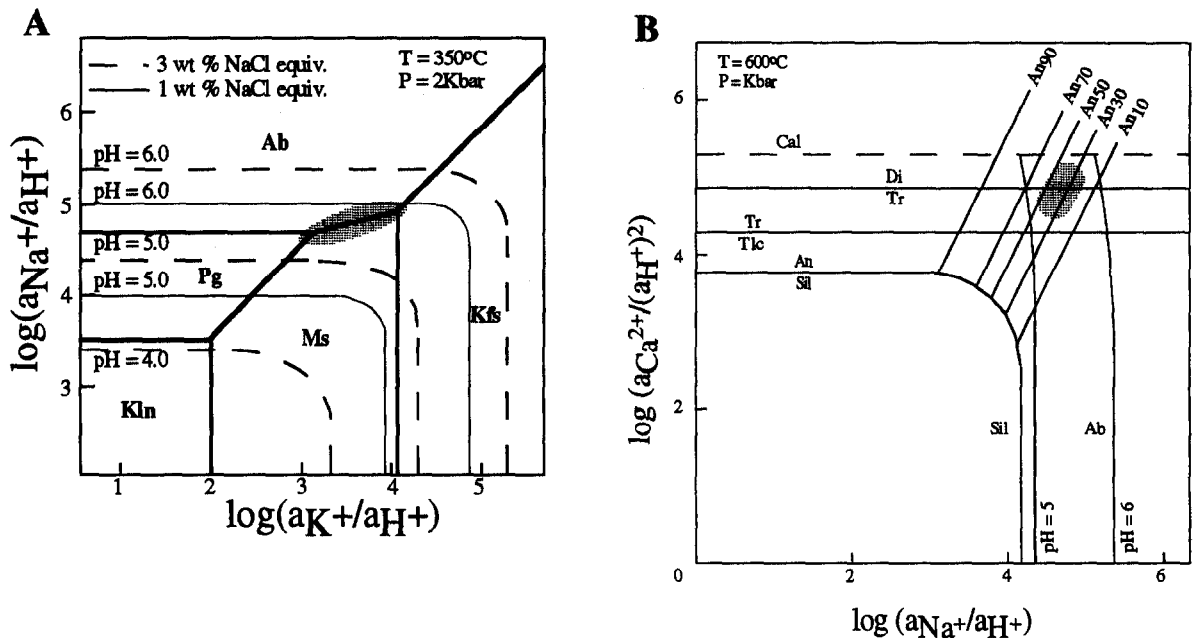


Fig. 17. (A) pH relationships in green schist facies deposits, determined from the stability relationships for Na-K aluminosilicates. Shaded area corresponds to the calculated fluid composition for most sub-amphibolite facies deposits. Ab = albite; Pg = paragonite; Kln = kaolinite; other abbreviations same as for Fig. 16. Redrawn from Mikucki and Ridley (1993), where original data sources are supplied. (B) pH relationships in amphibolite facies deposits determined from the stability relationships of Na-Ca aluminosilicates and Ca-Mg silicates. Shaded area shows likely fluid composition of typical amphibolite facies gold deposits, based on the coexistence of diopside, tremolite and plagioclase (An<sub>25–50</sub>). Redrawn from Mikucki and Ridley (1993).

rock interaction along conduits during their ascent (Mikucki and Ridley, 1993).

## 9. Stable isotope systematics

Hydrogen and oxygen isotope compositions of hydrothermal minerals can provide information on the temperature of mineralization, fluid/rock ratios, and the source of the ore-forming fluids (O'Neil, 1986; Kyser, 1987; Taylor, 1997). The stable isotope compositions of carbon and sulphur yield constraints on the source rocks from which these elements were derived, and potentially on the ambient  $f(O_2)$ , pH, and temperature conditions during mineralization (Ohmoto, 1986; Taylor, 1986; Kerrich, 1987; Ohmoto and Goldhaber, 1997).

### 9.1. Silicate oxygen and hydrogen isotopes

The most comprehensive database for silicates is from the Archean deposits of the Abitibi sub-

province, Canada. A prominent feature of lode gold deposits in this Abitibi subprovince is the uniformity in isotopic composition of quartz, which is the dominant vein mineral and resistant to retrograde exchange. The majority of measured  $\delta^{18}O$  values are in the restricted interval between 12.5‰ and 15.0‰. This uniform population of data embraces deposits distributed over 400 km, and variously hosted by ultramafic, mafic or felsic volcanic rocks, granitoids, and sedimentary rocks (Kerrick and Fryer, 1979; Kerrich, 1983). A similar uniformity of  $\delta^{18}O$  quartz values is present in the Norseman gold camp (Golding and Wilson, 1982). This tight clustering of  $\delta^{18}O$  quartz values within deposits is noted for many lode gold deposits of all ages and geographic locations, albeit with some interdeposit or intercamp variations (Kerrick, 1987; Weir and Kerrich, 1987; Golding et al., 1989; Kerrich, 1989b; Kontak et al., 1990; Fedorowich et al., 1991; Goldfarb et al., 1991b; de Ronde et al., 1992).

Quartz in mineralized selvedges of the bounding wall rock is isotopically similar to its vein counterpart, whereas quartz in contiguous rocks, external to the volume influenced by mineralization, constitutes distinct isotopic populations. The isotopic uniformity in vein quartz generally extends to other vein silicate phases such as chlorite, muscovite, biotite, amphibole, clinopyroxene, and garnet such that quartz-mineral fractionations remain approximately constant (Kerrich, 1987; Kerrich and Feng, 1992). These relationships imply a fluid dominated system along the hydrothermal conduit, uniform  $\delta^{18}\text{O}$  of the fluids, and essentially isothermal conditions during alteration and quartz vein emplacement. Systematic differences in  $\delta^{18}\text{O}$  between camps are apparent, and likely reflect differences in bulk  $\delta^{18}\text{O}$  values of the fluid source regions (Kerrich, 1989b; Kerrich and

Feng, 1992). Immiscible separation of  $\text{CO}_2$  is a consistent feature of most lode gold vein systems. However, oxygen isotope fractionation between ex-solved  $\text{CO}_2$  and residual  $\text{H}_2\text{O}$  is minimal and would be limited to  $< 3\text{\textperthousand}$ , consistent with the narrow observed range of quartz  $\delta^{18}\text{O}$  values within individual deposits (Kerrich, 1987, 1989b).

Calculated isotopic temperatures from coexisting quartz-muscovite-chlorite from deposits in the Superior Province of Canada are in the range 280° to 360°C, and are generally in agreement to within 40°C, but there are few examples of triple isotopic concordance (Kerrich, 1989b). Given textural evidence for their coprecipitation in each case, it is not clear as to whether this lack of equilibrium represents selective retrograde exchange of muscovite and/or chlorite, or alternatively is due to uncertainties in the mineral-water calibrations. Temperatures estimated from alteration phase equilibria tend to be equal to or greater than isotopic temperatures (Kerrich, 1989b; this review).

## 9.2. Oxygen and hydrogen isotope characteristics of the hydrothermal fluids

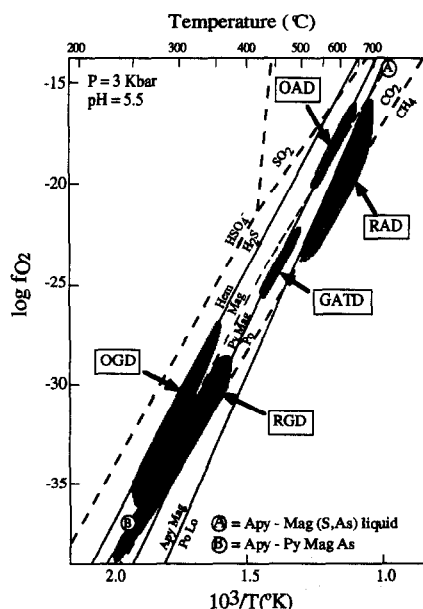


Fig. 18. Summary of oxidation state of ore forming fluids vs. temperature. Heavy solid lines = Fe-As-sulphide-oxide stability boundaries, heavy dashed lines = important redox buffers. OAD = oxidized amphibolite facies deposits; RAD = reduced amphibolite facies deposits; GATD = greenschist-amphibolite facies transition deposits; OGD = oxidized greenschist facies deposits; RGD = reduced greenschist facies deposits. Other abbreviations as in earlier figures. Higher temperature deposits are characterized by more oxidized fluids, and fluids appear to be regulated by the hematite-magnetite and  $\text{CO}_2-\text{CH}_4$  buffers at all crustal levels. Redrawn from Mikucki and Ridley (1993), where original data sources are listed.

The isotopic composition of hydrothermal fluids may be calculated from measured  $\delta\text{D}$  and  $\delta^{18}\text{O}$  values of minerals, by means of appropriate mineral-water fractionations, in conjunction with an estimate for the ambient temperature of mineralization (Taylor, 1974, 1986; Kyser, 1987).  $\delta\text{D}$  and  $\delta^{18}\text{O}$  values of hydrothermal fluids may also be measured directly on fluid inclusion water, provided that material dominated by primary inclusions is selected. Calculated hydrogen and oxygen isotope compositions of the hydrothermal ore-forming fluids for Archean and Proterozoic lode gold deposits plot in a relatively narrow field of  $-30$  to  $-80\text{\textperthousand}$   $\delta\text{D}$ , and  $+6$  to  $+11\text{\textperthousand}$   $\delta^{18}\text{O}$  (Fig. 19A, B). This field overlaps the magmatic and metamorphic field, but considering the database as a whole, values of greater than  $+8\text{\textperthousand}$  cannot be magmatic fluids alone. Some Phanerozoic deposits have  $\delta^{18}\text{O}$  values as high as  $+14\text{\textperthousand}$ , likely reflecting  $^{18}\text{O}$ -enriched metasedimentary rocks in the fluid source reservoir (Fig. 19; Böhlke and Kistler, 1986; Kerrich, 1987, 1989b; Kerrich and Feng, 1992).

Hydrogen isotope compositions of hydrothermal fluids calculated from mineral analyses have a relatively restricted range from  $-20$  to  $-80\text{\textperthousand}$ . In contrast, direct analyses of waters deprecipitated from fluid inclusions extend from  $-120\text{\textperthousand}$  to  $+5\text{\textperthousand}$  (Rye and Rye, 1974; Fyon et al., 1984; Nesbitt et al., 1986; Nesbitt and Muehlenbachs, 1989). The magnitude of the dispersion in  $\delta D_{\text{H}_2\text{O}}$  values cannot be attributed to mixing of depleted and enriched fluid reservoirs. Any such mixing would be reflected in shifts of both  $\delta D$  and  $\delta^{18}\text{O}$  fluid, but the uniformity of quartz  $\delta^{18}\text{O}$  values rules out this possibility.

Rather, the observed range in  $\delta D_{\text{H}_2\text{O}}$  may be due to: (1) the presence of  $\text{H}_2$  and/or  $\text{CH}_4$  in the aqueous fluid, coupled with immiscibility of the reduced gas species (Fyon et al., 1984); or (2) the inclusion populations analyzed are dominantly secondary and post-mineralization, likely meteoric fluids trapped as the host terrane was uplifted (see Kyser and Kerrich, 1990, 1991; Goldfarb et al., 1997).

Scenario (2) is supported by paragenetic, structural, and analytical evidence from Archean deposits for protracted fluid movements through the shield regions over geological time evidenced by deeper

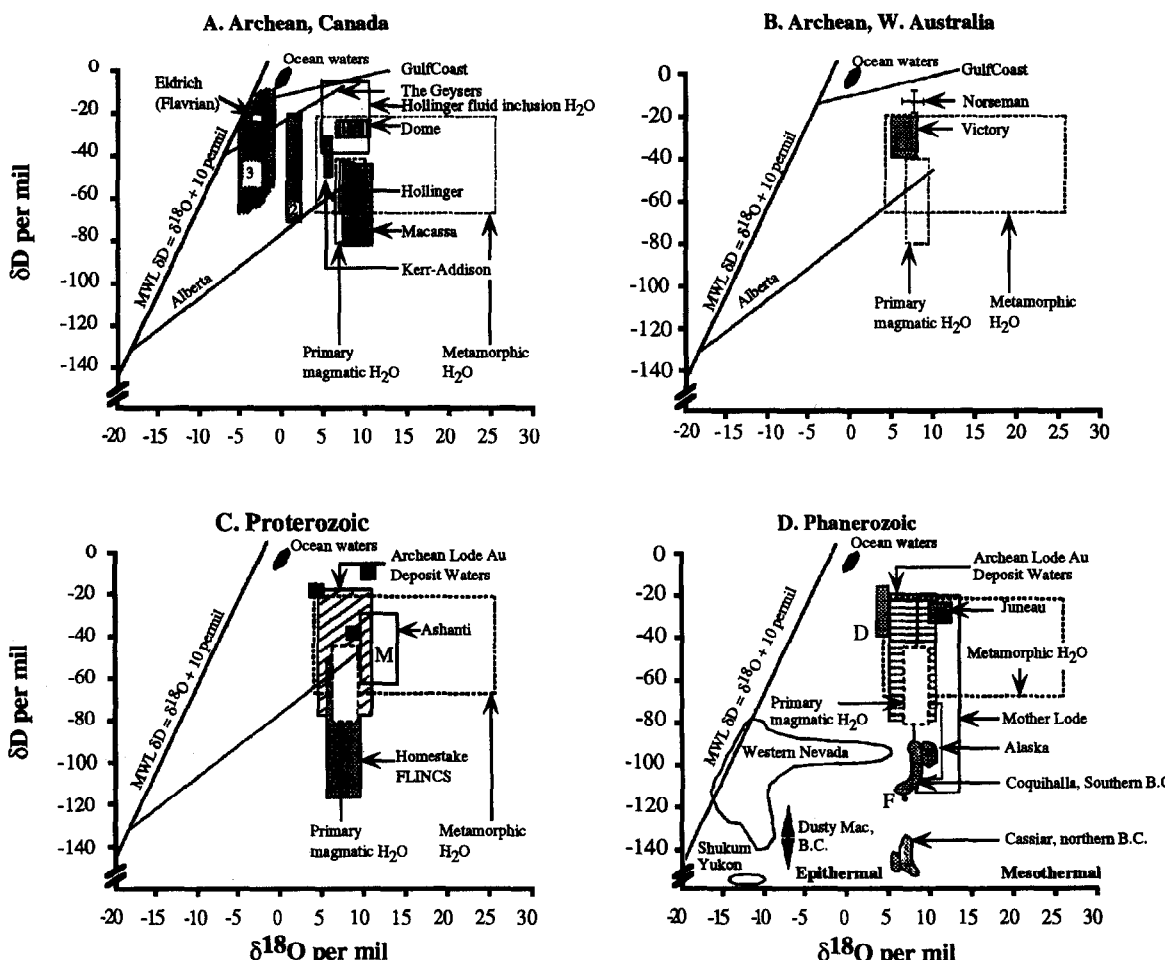


Fig. 19. Calculated isotopic compositions of ore-forming fluids associated with Archean (A,B), Proterozoic (C), and Phanerozoic (D) mesothermal gold deposits. Note that the  $\delta D$ -depleted trend from Homestake (C) and the Cordilleran mesothermal deposits, Juneau excepted (D) are exclusively based on bulk extraction of fluid inclusion waters (modified after Kerrich, 1989b, where complete sources are cited). Solid boxes in (C) are Trans Hudson deposits. F and OF (D) are the adjacent Fairview and Oro Fino deposits in southern British Columbia (after Zhang et al., 1989).

oxidation profiles along faults, hypersaline CaCl brines in vuggy cavities with remobilized gold, and  $^{18}\text{O}$ -shifted carbonates (Section 7). For example,  $\delta\text{D}$  analyses of fluid inclusion waters from the Homestake mine, South Dakota, and some of the Cordillera deposits (Rye and Rye, 1974), are much too depleted to be consistent with  $\delta^{18}\text{O}$  values of the host quartz and consequently may reflect in part secondary meteoric waters (Section 13). Based on hydrogen and oxygen data alone, it is not possible to discriminate between fluids of magmatic or metamorphic origin as the prime hydrothermal reservoir involved in the lode gold deposits. Collectively, however, the data extend to values above and below the magmatic water field.

Exceptions to these general characteristics occur in some subgreenschist facies deposits. Hydrogen and O-isotope data for the Archean Eldrich deposit, Noranda, signifies the involvement of some meteoric water (Fig. 19A; Kerrich, 1987). In some Yilgarn deposits calculated  $\delta D_{\text{H}_2\text{O}}$  values of  $-4.0\text{\textperthousand}$  to  $+5.0\text{\textperthousand}$ , combined with variably saline fluid inclusions (Section 7), have been interpreted as reflecting incursion of evolved surface waters into a dominantly deep-sourced hydrothermal system, or advection of a deep-sourced hydrothermal fluid into rocks that have partially equilibrated with surface-derived waters (Gebre-Mariam et al., 1991, 1993; Hagemann et al., 1993; Hagemann and Ridley, 1993b).

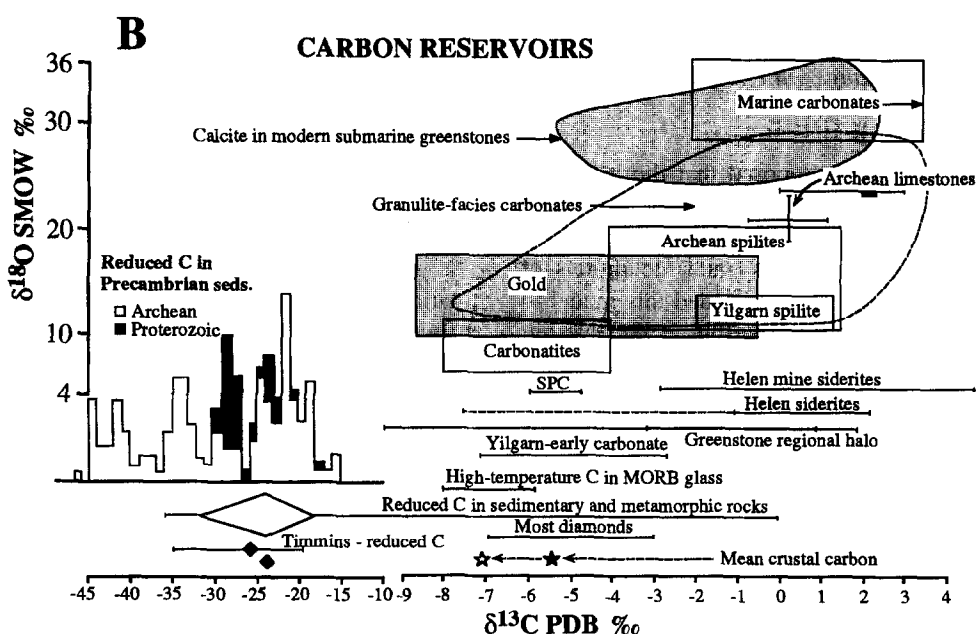
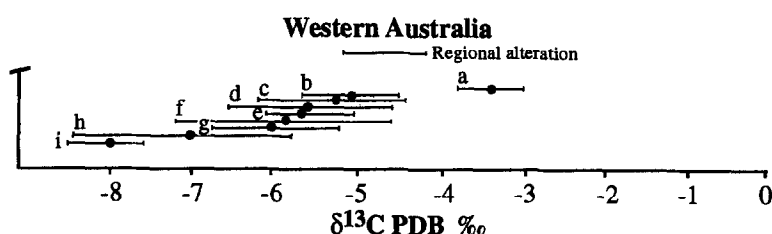
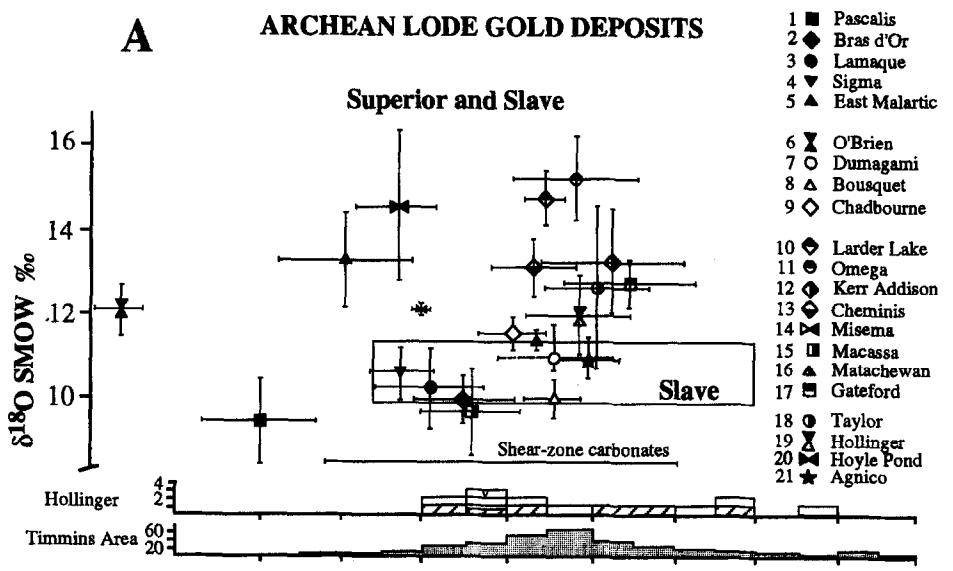
### 9.3. Retrograde exchange with surface meteoric waters

Nesbitt et al. (1986) proposed that the lode-gold (mesothermal) quartz vein systems in the Cordillera formed in response to deep circulation of meteoric water along transcurrent faults under conditions of low water/rock ratios. They extended this model to Archean lode gold deposits (Nesbitt, 1988; Nesbitt and Muehlenbachs, 1989). The meteoric water model stems from the observation that in Cordilleran lode Au deposits the  $\delta\text{D}$  values of  $\text{H}_2\text{O}$ , obtained by decrepitating fluid inclusions from some vein quartz were very depleted. Uniform  $\delta^{18}\text{O}$  quartz values at each deposit, but a spread of  $\delta\text{D}$  values, define a vertical band in  $\delta D_{\text{H}_2\text{O}}$  vs.  $\delta^{18}\text{O}_{\text{H}_2\text{O}}$  coordinates (Fig. 19D). On the other hand, for Cordilleran mesothermal deposits in Alaska, Pickthorn et al.

(1987) and Goldfarb et al. (1989, 1997) measured  $\delta\text{D}$  values of  $-75$  to  $-53\text{\textperthousand}$  on hydrothermal micas, giving calculated  $\delta\text{D}$  values for the hydrothermal fluids of  $-35$  to  $-20\text{\textperthousand}$ ; these are too enriched to be local meteoric water, and were interpreted to be metamorphic in origin. Data for the Proterozoic Homestake and Jurassic Mother Lode deposits also plot as vertical bands in  $\delta D_{\text{H}_2\text{O}}$  vs.  $\delta^{18}\text{O}_{\text{H}_2\text{O}}$  coordinates, defined by uniform  $\delta^{18}\text{O}$  quartz values, but a spread of  $\delta D_{\text{H}_2\text{O}}$  values from bulk extraction of fluid inclusions (Fig. 19C, B). For the Cordilleran deposits, there is a discrepancy between D-depleted values obtained from bulk extraction of fluid inclusion and the D-enriched values obtained from co-existing medium- to coarse-grained (0.1 to 2 mm) micas (e.g., Nesbitt et al., 1986; Zhang et al., 1989; Goldfarb et al., 1991b). Kyser and Kerrich (1991) interpreted vertical trends on  $\delta D_{\text{H}_2\text{O}}$  vs.  $\delta^{18}\text{O}_{\text{H}_2\text{O}}$  diagrams as selective secondary H-isotope exchange between hydroxy-silicates and low-temperature meteoric waters, in the absence of O-isotope exchange. The same vertical trends would arise from incorporation of meteoric waters into secondary fluid inclusions in quartz, where  $\delta\text{D}$  measurements were made on the secondary inclusions and  $\delta^{18}\text{O}$  on the quartz (see Section 13).

The  $\delta\text{D}$  results from bulk extraction of fluid inclusions may not reflect the primary ore-forming hydrothermal solutions, but rather secondary inclusions formed in the presence of surface meteoric waters infiltrating down the vein (Pickthorn et al., 1987). In detailed studies, Goldfarb et al. (1989, 1991b, 1997) showed that bulk extracted fluid inclusion waters from vein quartz of the Juneau mesothermal deposits exhibit a wide range of  $\delta\text{D}$  values from  $-48\text{\textperthousand}$  in relatively undeformed quartz to  $-110\text{\textperthousand}$ , in deformed counterparts. This span reflects decrepitation of variable proportions of two end-member fluids: primary ore fluids in primary inclusions and D-depleted meteoric water trapped in secondary inclusions along fractures. Significant spreads of  $\delta\text{D}$  values from bulk extraction of fluid inclusion waters are also evident in the data of Zhang et al. (1989) and Nesbitt and Muehlenbachs (1989) in deposits at similar latitudes.

Numerous lines of evidence indicate that late infiltration of meteoric water does indeed occur along such vein-hosting structures. Weir and Kerrich (1987)



showed that late vuggy vein quartz was precipitated from such meteoric waters in the Mother lode deposits, and O'Hanley et al. (1989) reported that the serpentine was shifted to low  $\delta D$  values along faults in the Cassiar mining district, British Columbia. In the Canadian Shield, the  $\delta^{18}\text{O}$  values of readily exchanged calcite and ferroan dolomite paragenetically associated with vein quartz were isotopically reset by exchange with later meteoric water, even though the quartz was not affected (Kerrich, 1990b). Isotopic evidence for meteoric water in secondary inclusions corroborates the fluid inclusion evidence that the rare gas isotope systematics on decrepitated inclusions may also be secondary (Section 7). Finally, the meteoric water model does not account for the observation that lode (mesothermal) vein systems are generally restricted to terrane boundary structures and their splays (Kerrich and Wyman, 1990; Barley and Groves, 1992; Sections 2 and 3). The model would predict mesothermal veins in any large transectural fault with the appropriate attributes of fluid infiltration, thermal structure and permeability; this does not seem to be the case (Kerrich, 1989a,b).

#### 9.4. Carbon isotope systematics

All lode gold deposits are characterized by hydrothermal carbonate providing compelling evidence that the fluid contained oxidized carbon compounds. The carbon isotope composition of carbonates may potentially act as a tracer for the source(s) of C (Ohmoto, 1986; Ohmoto and Goldhaber, 1997). Lode gold deposits of all ages encompass a large total spread of average  $\delta^{13}\text{C}$  values from approximately  $-23\text{\textperthousand}$  to  $+2\text{\textperthousand}$ , but individual deposits or camps

tend to have restricted ranges of  $\delta^{13}\text{C}$  values (Fig. 20; for reviews see Golding et al., 1989; Kerrich, 1987, 1989b, 1990b). Excluding the extremely negative values from the Meguma Terrane and Ashanti Belt that are accepted as reflecting a local biogenic source of carbon (Kontak et al., 1990; Oberthür et al., 1996; Kontak and Kerrich, 1997), the range is reduced to  $-11\text{\textperthousand}$  to  $+2\text{\textperthousand}$ .

For Archean lode gold deposits this spread of  $\delta^{13}\text{C}$  values has been interpreted in a number of different ways: (1) crustal C derived from metamorphic devolatilization of greenstone terranes (Kerrich and Fyfe, 1981; Groves and Phillips, 1987); (2) mixing of crustally derived C with  $\text{CO}_2$  of juvenile mantle origin (McNaughton et al., 1992); (3) mixing between  $\delta^{13}\text{C}$  depleted (reduced C) and  $\delta^{13}\text{C}$  enriched (oxidized C) reservoirs (Kerrich, 1987, 1990b); (4) a magmatic origin of the  $\text{CO}_2$  (in deposits where  $\delta^{13}\text{C} \approx -3\text{\textperthousand}$ ); or (5) a mantle origin for the  $\text{CO}_2$  ( $\delta^{13}\text{C}$  values of  $\approx -3\text{\textperthousand}$ ) [Fyon et al., 1984; Cameron, 1988; Colvine et al., 1988]. It is clear that  $\delta^{13}\text{C}$  values of  $-11\text{\textperthousand}$  to  $+2\text{\textperthousand}$  are not uniquely diagnostic of any one carbon source, but cannot reflect mantle C or magmatic C alone (Kerrich, 1989b, 1990b).

The minimal variation in  $\delta^{13}\text{C}$  values within individual deposits implies fluid dominated, isothermal conditions of alteration, corroborating oxygen isotope, fluid inclusion, phase equilibria and paragenetic evidence. Where intradeposit variations do occur they result from three dominant processes: (1) Rayleigh fractionation effects with progressive consumption of  $\text{CO}_2$  as the hydrothermal fluid infiltrates into the wall rock, causing carbonates in distal alteration zones to be isotopically depleted relative to

Fig. 20. Average carbon- and oxygen-isotope composition of hydrothermal ferroan dolomites and calcites from specified Au deposits (after Kerrich, 1989b and references therein). Bars represent 1 SD of the mean. Also shown for comparison are data for the Hollinger mine and Timmins camp deposits collectively (Burrows et al., 1986 and references therein) and shear-zone carbonates (Veizer et al., 1989a); Western Australian data from Groves et al. (1989). (B) Oxygen- and (or) carbon-isotope compositions of specified carbon reservoirs. Carbonatite-field and granulite-facies carbonates after Valley (1986a,b); reduced carbon in Superior Province rocks from Schoell and Wellmer (1981) and Strauss (1986); Timmins reduced C from Wilson and Rucklidge (1987); vesicle-filling calcite in Slave Province and Superior Province Archean spilites after Kerrich (1986); greenstone-belt regional halo carbonates from Veizer et al. (1989a) (most of the data are between  $+1$  and  $-3\text{\textperthousand}$ —heavy bar); high-temperature C in MORB glass after Taylor (1986); carbonate in modern submarine greenstones from Muehlenbachs (1986) and references therein; Archean limestones after Schidlowski et al. (1975) and Veizer et al. (1989b) (cross and bar respectively); SPC, Superior Province carbonates (Strauss, 1986); Helen mine after Thode and Goodwin (1983). Fields for marine carbonate, most diamonds, and reduced C in metamorphic and sedimentary rocks after Ohmoto and Rye (1979). Estimates of average crustal carbon after Hoefs (1987) and Ohmoto and Rye (1979).

vein carbonate; (2) Reaction with carbonaceous wall rocks. Positive shifts in  $\delta^{13}\text{C}_{\text{carbonate}}$  occur due to buffering of the fluid to lower  $f(\text{O}_2)$  by reaction with C-rich rocks, whereas negative shifts in  $\delta^{13}\text{C}_{\text{carbonate}}$  will occur if the fluid equilibrates with depleted aqueous hydrothermal species before precipitating carbonate; or (3) Immiscibility of  $\text{CH}_4$  and  $\text{CO}_2$ : immiscibility will have a negligible effect on

the isotopic composition of carbonates, as fractionations between  $\text{CO}_2$  and  $\text{HCO}_3^-$  are minimal. However,  $\text{CO}_2-\text{CH}_4$  fractionation is approximately 25 per mil at 300°C and can significantly shift the  $\delta^{13}\text{C}$  values of residual oxidized aqueous carbon species, and hence the  $\delta^{13}\text{C}$  of carbonate that subsequently precipitates (Ohmoto, 1986; Kerrich, 1990b; Ohmoto and Goldhaber, 1997).

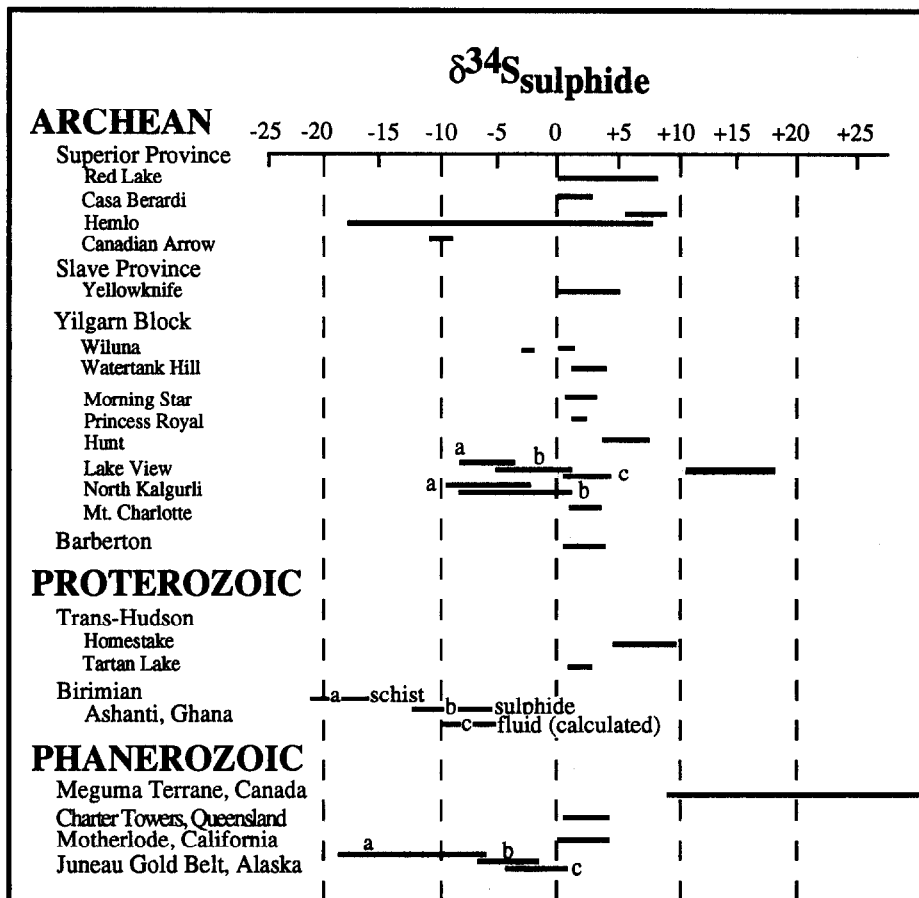


Fig. 21. Compilation of  $\delta^{34}\text{S}$  values from sulphides (thin bars) and rare barite (heavy bars) from lode gold deposits. Data sources: Superior and Slave Provinces and Mother Lode district, Kerrich (1987, 1989b, and primary references therein); Wiluna, Hagemann et al. (1993); remainder of Western Australian deposits, Golding et al. (1990, and primary references therein); Barberton, de Ronde et al. (1992); Homestake, Rye and Ohmoto (1974); Ashanti, Oberthür et al. (1996); Tartan Lake, Fedorowich et al. (1991); Meguma Terrane, Kontak et al. (1990); Charter's Towers, Peters and Golding (1989); Juneau district, Goldfarb et al. (1991b). Labels a, b and c for the Juneau deposits denote the sulphur isotope compositions of sulphides in graphitic phyllite, greywacke, and igneous rocks, respectively. North Kalgoorlie: a = main and steep lodes, b = flat lodes. Lakeview: a, b, and c represent compositions of sulphides from lodes in the Golden Mile Dolerite, Paringa basalt, and interflow sedimentary units, respectively. Ashanti belt: a-unmineralized schist; b-sulphides in ore; c-calculated fluid composition.

### 9.5. Sulphur isotopes

Sulphur isotope compositions of hydrothermal S-bearing minerals are controlled by the total S isotope composition of the fluids, and by the temperature,  $f(O_2)$ , and pH at the site of mineralization (Ohmoto, 1986; Ohmoto and Goldhaber, 1997). The first parameter can be regarded as a source characteristic whereas the latter three relate to the environment of deposition. Accordingly, interpretation of the distribution of  $\delta^{34}S$  values relies on a knowledge of the  $\delta^{34}S$  values characteristic of the various possible S reservoirs, and of mineral paragenesis that constrains the ambient temperature, Eh and pH.

A compilation of sulphur isotope compositions of sulphides and rare sulphates from lode gold deposits is presented in Fig. 21. The bulk of the  $\delta^{34}S$  values are restricted to the interval 0 to +9‰: this relatively tight clustering can be interpreted to indicate that the fluid redox state was below the  $SO_2/H_2S$  boundary, and that the sulphur source was isotopically uniform, and bracketed by -1 to 8‰. Sulphur of this composition could be derived either directly from magmas or indirectly by dissolution and/or desulphidation of primary magmatic sulphide minerals or average crustal sulphur (Lambert et al., 1984; Kerrich, 1987, 1989b; Golding et al., 1990; Ho et al., 1992).

A few deposits are systematically depleted or enriched relative to the main population of data. Turbidite-hosted deposits of the Palaeozoic Meguma Terrane contain sulphides with  $\delta^{34}S$  values ranging from +9 to +24, indicating that most sulphur was derived from the host sediments (Kontak et al., 1990). A similar model is proposed by Goldfarb et al. (1991b), who demonstrate that the  $\delta^{34}S$  of sulphides from Juneau gold belt deposits correspond to the  $\delta^{34}S$  values of hosting sediments (Fig. 21).

Negative  $\delta^{34}S$  obtained for the Wiluna, Lake View, North Kalgoorlie, Canadian Arrow and Hemlo deposits have been attributed to significant oxidation of the fluids (Lambert et al., 1984; Cameron and Hattori, 1987; McNeil and Kerrich, 1986; Phillips et al., 1986; Hagemann et al., 1993). Three mechanisms have been proposed to account for the fluid oxidation in these deposits: (1) extensive interaction of hydrothermal fluids with  $Fe^{2+}$ -bearing silicates in wall rocks, where fluid oxidation is linked to con-

sumption of reduced aqueous S in the formation of pyrite (Lambert et al., 1984); (2) intrinsically oxidizing magmatic fluids (Cameron and Hattori, 1987); or (3) fluid oxidation accompanying immiscible separation of reduced gases such as  $CH_4$ ,  $H_2S$  and  $H_2$  (Drummond and Ohmoto, 1985). If significant phase immiscibility occurs, then  $H_2S$  will partition into the vapour phase, leaving the residual fluid relatively oxidized. The fluid will respond by the reduction of aqueous  $SO_4^{2-}$  to  $H_2S$ , leaving the aqueous  $H_2S$  depleted in  $^{34}S$ , such that sulphides precipitating in the orebodies from aqueous  $H_2S$  will have negative  $\delta^{34}S$  values relative to those deposited from the primary homogeneous fluid. Mechanism (1) is unlikely to be quantitatively significant because of fluid/rock redox mass balance, and the rarity of negative  $\delta^{34}S$  values for deposits in Fe-rich lithologies. Mechanism (2) is also improbable given that the ore fluids are likely not magmatic, the paragenesis in many deposits signifies reducing conditions, and mineralization postdates the host intrusions. Mechanism (3) is supported by fluid inclusion evidence for local immiscibility, and the presence of sulphates in some deposits with  $^{34}S$ -depleted sulphides. Sulphates may coexist with  $^{34}S$  depleted sulphides if the ion activity product of  $SO_4^{2-}$  and aqueous bivalent metal cations exceeds saturation; for example  $CaSO_4$  at Kalgoorlie and Kirkland Lake, or  $BaSO_4$  at Hemlo.

### 9.6. Summary of stable isotopes

The overall uniformity of  $\delta^{18}O$ ,  $\delta^{13}C$ , and  $\delta^{34}S$  values of the ore-forming fluid within individual mining camps, but provinciality between camps, signifies very large and uniform fluid and rock source volumes, and approximately isothermal conditions of alteration and mineralization within mining camps, albeit with lateral variations at a 100 km scale. It is important to emphasize that the ore fluid, S, and C may, or may not, all come from the same source. For example, the fluid could be generated by metamorphic reactions at depth and acquire C and S from the source rocks, or alternatively acquire additional S or C from rocks along the fluid conduit 'en route' to the deposit, or at the site of gold deposition. The Meguma

deposits are a case in point where the fluids are derived from external to the turbidite terrane, but the S is locally derived. Exceptions from these general features may occur due to processes operating within the deposit, or in very high-level, low-temperature subgreenschist facies deposits, where there is some evidence for the incursion of surface waters into the hydrothermal systems, or exchange with rocks that have equilibrated with surface-derived waters.

## 10. Radiogenic isotopes

Radiogenic isotope studies of mineral deposits can provide three types of information: (1) tracing the source of ore and gangue constituents; (2) constraining the primary age of mineralization; and (3) establishing the time or times of secondary disturbance. This section synthesizes the information that Sr and Pb isotope studies have provided on the source of these elements in the lode deposits. For

reviews of the application of radiogenic isotopes to ore deposits see Doe and Zartman (1979), Faure (1986), Kerrich (1991), and Farmer and DePaolo (1997).

Isotope tracer studies are subject to the following caveats: (1) for the element in question, there has been an absolute mass increase from, or exchange with, the primary mineralizing fluids; (2) the isotopic composition of the ore fluid reflects that of the principal source reservoir; and (3) there was no secondary isotopic disturbance. Gold cannot be used as an isotopic tracer given its monoisotopic character ( $^{197}\text{Au}$ ). Consequently, any information on gold source rocks is by inference from Sr or Pb isotopes, or stable isotopes as summarized in Section 9.6.

### 10.1. Strontium isotope systematics

Strontium-isotope analyses of whole rocks and mineral separates have been reported for a number of

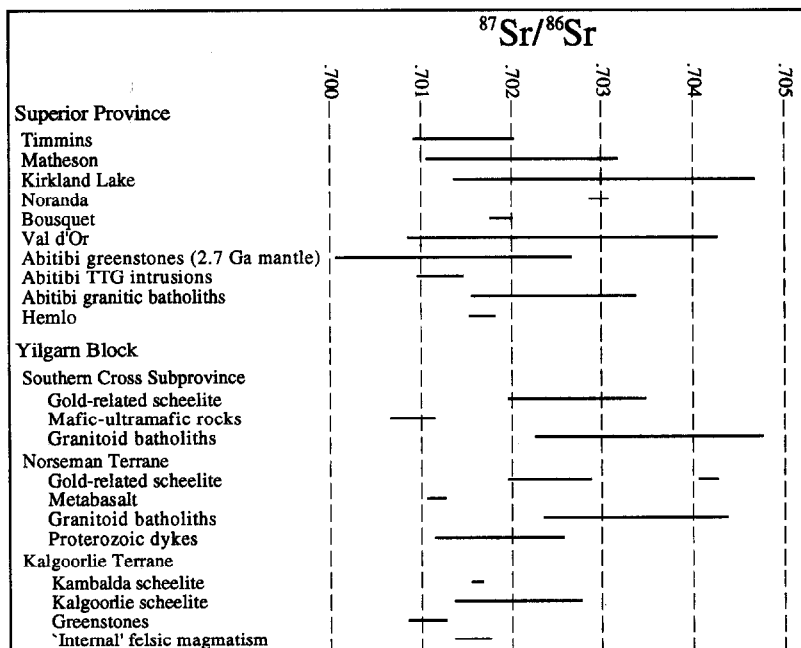


Fig. 22. Compilation of initial  $^{87}\text{Sr}/^{86}\text{Sr}$  ratios of strontium-rich minerals from some Archean lode gold deposits. Data sources: Superior Province, Kerrich (1989b, and primary references therein); Yilgarn Block, Mueller et al. (1991a). Note that in many deposits, alteration minerals possess initial  $^{87}\text{Sr}/^{86}\text{Sr}$  ratios that are more radiogenic than those of contemporaneous mantle or host lithologies. Therefore, the fluid  $^{87}\text{Sr}/^{86}\text{Sr}$  composition in these cases must be derived from sources external to the greenstone belts (i.e., older crust), indicating a crustal-scale plumbing system with fluid input from deep crustal levels.

Archean lode gold deposits of the Abitibi sub-province, Canada, and the Southern Cross and Norseman–Wiluna greenstone belts of Western Australia (Fig. 22). Rb–Sr whole-rock isochrons on alteration domains in the Abitibi deposits yield linear arrays, but with ages systematically 200 to 260 Ma younger than the mineralization, based on independent age criteria. Accordingly, the initial  $^{87}\text{Sr}/^{86}\text{Sr}$  ratios calculated from these isochrons are meaningless in terms of characterizing the ore-forming fluids, because the Sr-rich carbonates are not robust, and have exchanged  $^{87}\text{Sr}/^{86}\text{Sr}$  with late fluids (Kerrich, 1991).

For these reasons, Sr isotope tracer studies have relied on retentive, Sr-rich minerals such as tourmaline, scheelite, piedmontite, and actinolite, which are paragenetically associated with gold. Five basic results have emerged from the Sr isotope data (Kerrich, 1989b): (1) In the Abitibi belt, different Sr-rich minerals from a given deposit are concordant with respect to  $^{87}\text{Sr}/^{86}\text{Sr}$ , confirming closed system behaviour post-mineralization; (2) initial  $^{87}\text{Sr}/^{86}\text{Sr}$  ratios of individual deposits or districts are generally uniform; (3) initial ratios are generally decoupled from that of the wall rocks; (4) there are geographical variations of  $^{87}\text{Sr}/^{86}\text{Sr}$ , and (5) most initial ratios are variably more radiogenic than the contemporaneous mantle, and the prevalent mafic to ultramafic volcanic rocks and granitoids of the greenstone terranes (Fig. 22).

Contemporaneous initial ratios of major lithological units in Archean supracrustal sequences are established within reasonable limits. Information on the unexposed basement to greenstone belts is restricted to indirect estimates, which reveal a variably more radiogenic character with provinciality of Sr (and other) radiogenic isotope systems (Fig. 22; Mueller et al., 1991a). If the estimated  $^{87}\text{Sr}/^{86}\text{Sr}_i$  of the minerals correspond to the isotope composition of the ore-forming fluids, and in turn to the source reservoir(s) sampled by the hydrothermal fluids, then decoupling of initial ratios in deposits from contiguous host rocks, rules out local remobilization of Sr alone. Complex and laterally variable source regions, including old radiogenic basement, are indicated (Kerrich, 1989b, 1991; Mueller et al., 1991a), corroborating independent evidence for a crustal-scale plumbing system (Groves et al., 1992).

Lode gold deposits of the Meguma Terrane, Nova Scotia, have Sr-isotope compositions ranging from 0.70018 to 0.72284. Collectively, the data rule out derivation of Sr predominantly from the Meguma Group turbidite host rocks. Given radiogenic Pb-isotope compositions for the deposits, both the Sr and Pb were likely derived from the older underlying radiogenic Liscombe gneisses, but the fluids exchanged some Sr and Pb as they advected through the turbidite host rocks (Kontak and Kerrich, 1997). In the Mesozoic Mother Lode gold province, California, Böhlke and Kistler (1986) demonstrated geographical variations of  $^{87}\text{Sr}/^{86}\text{Sr}_i$  from 0.7039 to 0.7183. Sr-isotope compositions within individual mines or districts are uniform, even though fluids traverse a variety of wall rocks of different age, composition and metamorphic grade, with differing contemporaneous  $^{87}\text{Sr}/^{86}\text{Sr}$  ratios. Consequently, the Sr budget of the fluid reflects a large, external, isotopically homogeneous reservoir. Variations in the  $^{87}\text{Sr}/^{86}\text{Sr}_i$  of mineralization between different districts was attributed to the regional distribution of lithologies, with the strong east–west gradient of initial ratios likely due to progressively larger contributions of continental detritus, from a distal to in-board setting, in the source regions. The population of initial ratios includes values both less and more radiogenic than broadly contemporaneous Mesozoic plutonic rocks of the Sierra Nevada batholith ( $^{87}\text{Sr}/^{86}\text{Sr} \leq 0.704$ ). Initial Sr-isotope ratios and calculated  $\delta^{18}\text{O}_{\text{H}_2\text{O}}$  values covary. From Sr-isotope data Pettke and Diamond showed that the source of Sr was in calc schists located 10 km below the gold-quartz vein deposit at Brusson, NW Alps.

Initial Sr-isotope ratios of scheelites (Bell et al., 1989) and tourmalines (King and Kerrich, 1989b) from the Timmins district have similar distributions, although the secondary scheelite is considered to be ~250 Ma younger than the gold-related primary tourmaline (Kerrich, 1991; Section 4.1). The ore deposits represent a low Rb/Sr environment, especially where there is abundant carbonate, and relatively little  $^{87}\text{Sr}$  would have evolved between 2.67 and 2.4 Ga. This effect is also seen in the relatively primitive initial ratios of isochrons from ore deposits, reset at 2.5 to 2.4 Ga. The anomalously young apparent age of scheelites at  $2403 \pm 47$  Ma is close in time to the giant Matachewan diabase swarm

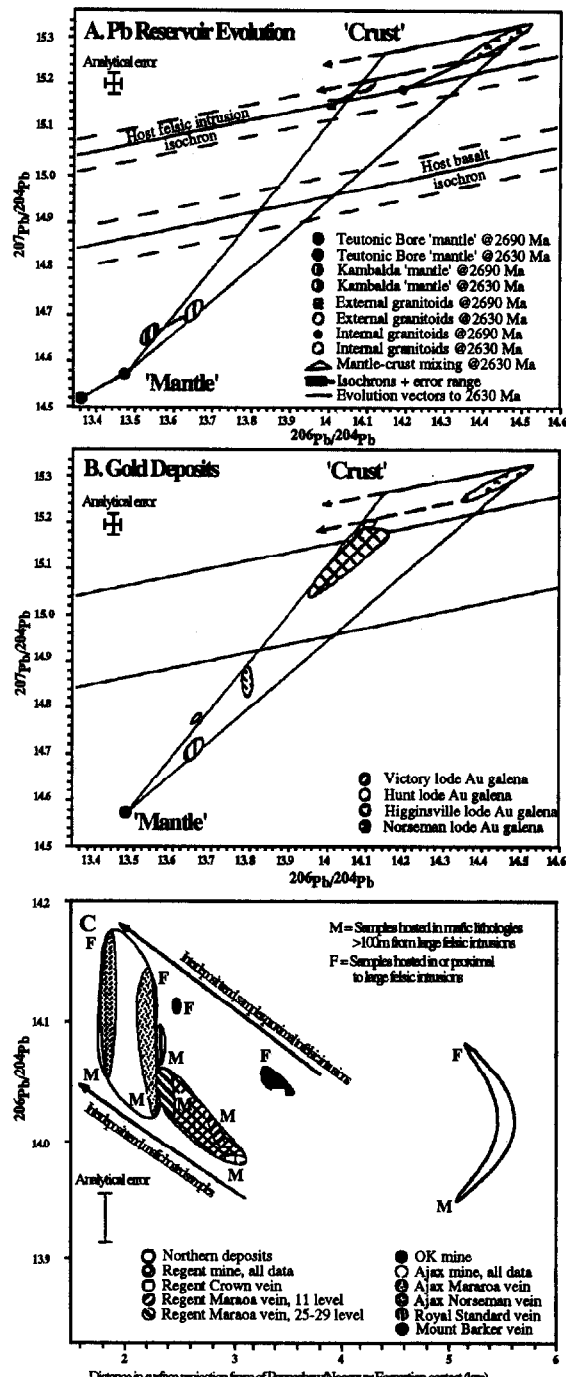
at 2400 Ma, that likely remobilized Ca, Sr, and W, to precipitate the secondary scheelites.

### 10.2. Lead isotope systematics

In the Superior Province lode gold deposits are characterized by common Pb in pyrites and galena that is variably more radiogenic, and has a higher  $\mu$  value, than Pb in contemporaneous volcanogenic massive sulphide deposits which is close to mantle values. Data for many of the gold deposits plot on secondary isochrons which are subject to a number of possible interpretations, including later disturbance at  $\sim 2200$  Ma in the Superior Province, (Franklin et al., 1983; Kerrich, 1991); or  $\sim 2000$  Ma at Norseman, Western Australia (Perring and McNaughton, 1990). In the Norseman–Wiluna belt,

McNaughton et al. (1992, 1993) demonstrated a regional variation in initial Pb isotope compositions with the more radiogenic Pb compositions correlat-

Fig. 23. (A) Composition and evolution of possible Pb reservoirs for the Norseman Terrane, and Western Australia (B) early galena and altaite data from the Norseman and Higginsville lode gold deposits in  $^{207}\text{Pb}/^{204}\text{Pb}$  vs.  $^{206}\text{Pb}/^{204}\text{Pb}$  space, and comparison to data from other lode gold deposits of the southern Kalgoorlie Terrane, 'mantle' and host rocks at the time of mineralization (ca. 2630 Ma). Lode gold galena and altaite data reflect mixing of Pb from two reservoirs: mantle or mantle-derived greenstones, and older crust or felsic intrusions derived from older crust. Data sources: Teutonic Bore 'mantle' @ 2690 Ma (pyrite in VMS ore) from McNaughton et al. (1990); Kambalda 'mantle' @ 2700 Ma (pyrite in Cu–Ni ores) from Browning et al. (1987); Victory and Hunt lode gold galena, and internal granitoids initial ratios @ 2690 Ma (crossed circle), isochron and evolution to 2630 Ma from Perring et al. (1990) and Perring and McNaughton (1992); External granitoids initial ratios (crossed square), isochron and evolution to 2630 Ma calculated using data of Oversby (1975) and a U/Pb<sub>zircon</sub> age of 2690 Ma (Campbell and Hill, 1988). Mantle compositions were evolved from syngenetic sulphide ore formation to 2630 Ma using a mantle  $^{238}\text{U}/^{204}\text{Pb}$  range of 7.5–8.0 (Moorbath and Taylor, 1981). Woolyeeenyer basalt isochron from Perring and McNaughton (1992) and a U/Pb<sub>boulderyite</sub> age of 2715 Ma (Hill et al., 1992). (C) Variation of  $^{206}\text{Pb}/^{204}\text{Pb}$  compositions of early galena and altaite from Norseman lode gold deposits with distance from the Penneshaw Formation/Noganyer Formation (basement) contact, illustrating the controls of proximity to felsic intrusions vs. increasing proximity to the basement contact on galena and altaite compositions. Samples are subdivided by mine and vein system, and classed according to proximity to felsic intrusions. On the terrane scale, galena+altaite compositions become more radiogenic with increasing proximity to older crust. Within deposits, compositions become more radiogenic with proximity to felsic intrusives, and with depth [McCuaig, 1996 (unpublished)].



ing with increasing proximity of the deposits to regional granitoid–gneiss domes (Fig. 23; Ho et al., 1992; McNaughton et al., 1992, 1993).

Lead isotope data from galena in gold-bearing veins of the Proterozoic Homestake deposit, South Dakota, plot on an array interpreted by Rye et al. (1974) to yield a 1.6 Ga formation age, and a 2.5 Ga source of Pb. Consequently, syndepositional formation, or a Tertiary age of mineralization can be ruled out. Field relations and Pb and stable isotope data indicate that the Homestake deposit is another example of a lode gold deposit formed synkinematically, post-peak metamorphism, with externally derived metals, and a large-scale plumbing system tapping the basement. For the Alpine Monte Rosa vein deposits, Curti (1987) showed that the Pb isotope ratios were consistent with a source in Caledonian metapelites, with a possible contribution from Hercynian granites, and that a source in proximal ophiolite greenstones and associated stratiform sulphides could be ruled out.

### *10.3. Synthesis of Sr and Pb isotopes*

In summary, the radiogenic isotope systematics of lode gold deposits signify that Sr and Pb were not entirely locally derived from the deposit-hosting supracrustal sequences, but that deeper, variably more radiogenic sources are required. As for stable isotopes, the Sr and Pb (and Au) may have been derived from the same large-scale reservoir; alternatively, their isotope systematics may be perturbed by exchange with lithologies ‘en route’ to the deposit. In either case, the radiogenic isotope data rule out models for lode gold genesis that invoke an ore forming system that is solely indigenous to, and confined within, the greenstone belts.

An empirical observation for lode deposits of both the Canadian and Australian Archean cratons is that gold mineralization is contemporaneous with late accretion of tectonostratigraphic terranes, or delamination, and closely follows the termination of granitic magmatism (Section 2; Kerrich and Cassidy, 1994; Kent et al., 1996). This is also true for the Meguma deposits, Victoria gold province, and also lode deposits of the Cordillera (Section 12.1). This fact may

signify that the thermal structure of the lithosphere cooled below the temperature for generating felsic melts. The implications are that the source of the ore-forming fluids was dehydration of hydrated oceanic crust and sediments subcreted beneath the terrane bounding fault (Kerrich and Wyman, 1990, 1993; Elder and Cashman, 1992). Such fluids would be relatively un-radiogenic, and rich in Sr but with low Pb contents. Advecting up the terrane boundary fault the fluids would first exchange with radiogenic crust, having relatively low Sr but high Pb contents, then enter the greenstone sequence and further exchange with non-radiogenic supracrustal rocks possessing high Sr but low Pb concentrations. This lithological complexity in the source-plumbing conduit–sink system would explain the complexity of the isotope systematics, as well as inter-camp variations, and trends with respect to greenstone–granite contacts (Kerrich, 1989b; Ho et al., 1992; McNaughton et al., 1992; McCuaig, 1996; Pettke and Diamond, 1997).

## **11. Transport and deposition mechanisms for gold**

### *11.1. Transport of gold in solution*

The mechanisms of gold sourcing, transport, and deposition are extremely complex and have been reviewed by various workers (Seward, 1973, 1991; Cathles, 1986; Romberger, 1986, 1990; Fyfe and Kerrich, 1984; Kerrich and Fyfe, 1988a,b; Shenberger and Barnes, 1989; Letnikov and Vilor, 1990; Mikucki and Groves, 1990; Hayashi and Ohmoto, 1991). Thermodynamic data on gold-complexing ligands is only available for a narrow range of possible ligands, and narrow ranges of *P* and *T* (generally < 1 kbar, < 300°C), and lacking for the *P*–*T* conditions of lode-gold forming hydrothermal systems. However, this limited database suggests that gold is transported as a thiosulphide complex under greenschist and subgreenschist facies conditions as  $\text{Au}(\text{HS})_2^-$ , and under amphibolite facies conditions potentially as  $\text{AuHS}^0$  (Seward, 1973, 1991; Shenberger and Barnes, 1989; Mikucki and Groves, 1990). Thioarsenide complexes (Romberger, 1986)

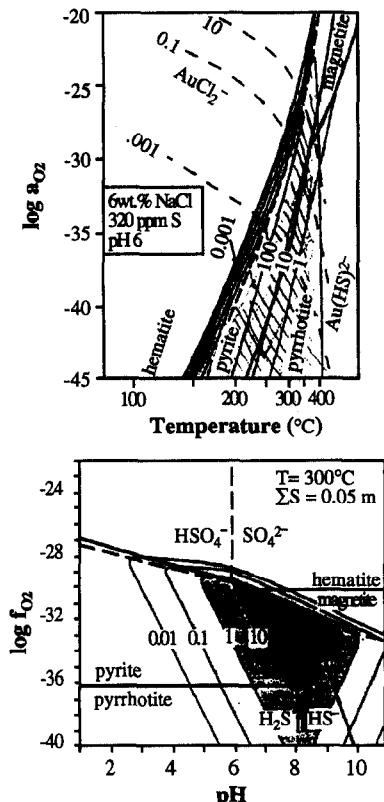


Fig. 24. Aqueous solubility of gold as a function of temperature and oxygen activity, from Romberger (1990). Heavy solid lines are for bisulphide complexes ( $\text{Au}(\text{HS})_2^-$  only), dashed lines are for chloride complexes, thin solid lines denote stability fields of Fe-oxides and -sulphides, thin dot-dash line represents boundary between aqueous sulphate and sulphide fields. Shaded area is the field in which gold-bisulphide complexes dominate. Note that consideration of  $\text{AuHS}^0$  complexes would push the field of gold-sulphide dominance to higher temperatures (cf. Mikucki and Groves, 1990). (Lower panel) Calculated gold solubilities in the form of  $(\text{Au}(\text{HS})_2^-)$  as a function of pH and  $\log f_{\text{O}_2}$ . Solubility contours (thin solid lines) are in ppm. Heavy solid lines separate stability fields of Fe-sulphides and oxides, dashed lines separate stability fields of aqueous species. From Roberts (1988).

and carbonyl, carbonyl-chloride or carbonyl-sulphide complexes may also be significant carriers of gold (Kerrich and Fyfe, 1981; Fyfe and Kerrich, 1984). Gold-chloride complexes are probably insignificant contributors to gold solubility at temperatures less than  $400^\circ\text{C}$ , but may be important at higher temperatures (Fig. 24A; Mikucki and Groves, 1990; Romberger, 1990), although the characteristically low abundances of base metals, which readily form solu-

ble complexes with chloride, in lode gold deposits would require gold to be deposited without affecting the stability of base metal-chloride complexes (Fyfe and Kerrich, 1984; Section 6).

### 11.2. Deposition of gold from solution

Regardless of the actual concentration of gold in lode gold-forming fluids, in order to form an economic orebody it is necessary to induce a change in the fluid chemistry that will efficiently remove gold from solution by destabilizing gold complexes. Based on available data summarized above, destabilization could be accomplished by a number of processes: (1) cooling the fluid; (2) oxidation of the fluid; (3) reduction of the fluid; (4) increasing pH of the fluid, especially for chloride complexes, or; (5) lowering  $\Sigma S$  in the fluid, specifically for thiosulphate complexes (Fig. 24A, B). This modification of fluid chemistry can be achieved by one or more of the following methods: (1) large-scale pressure and temperature gradients along the fluid plumbing system; (2) reaction of the fluid with the wall rocks surrounding the fluid conduit; (3) transient pressure fluctuations inducing phase immiscibility in the fluid; (4) fluid mixing; or (5) chemisorption.

#### 11.2.1. Broad pressure and temperature gradients as a depositional mechanism for gold

Broad pressure and temperature gradients, such as those found in geothermal and epithermal systems, are unlikely to exist in lode gold environments on the scale of a single deposit, based on the multiple lines of evidence for near isothermal conditions of alteration and vein emplacement summarized previously. However, such  $P-T$  gradients may be important on the terrane scale, such that gold deposition is favoured in a certain  $P-T$  ‘window’ (Phillips and Powell, 1993). If  $P-T$  gradients are a dominant control on gold deposition on a terrane scale, then deposits should correlate with metamorphic isograds as at Red Lake, Ontario (Andrews et al., 1986); and on the Alpine Fault, New Zealand, (Craw and Koons, 1989). Such depositional controls may explain the location of the majority of giant lode gold deposits in greenschist facies environments.

Alternatively, the location of giant deposits in greenschist facies terranes may reflect a rheological control, as rocks of this  $P-T$  range are within the brittle–ductile transition, where fluid pressure transients to supralithostatic fluid pressure generate hydraulic fractures, inducing high permeability, and enhanced fluid flow. These processes may aid both in preparing structural sites for orebodies, and in generating chemical changes necessary for gold precipitation to occur via phase immiscibility (Kerrich, 1989a,b).

#### *11.2.2. Fluid-wall rock reaction as a depositional mechanism for gold*

Gold sited dominantly in alteration haloes surrounding quartz veins or in replacement bodies within select lithologies, was likely deposited as a direct result of metasomatic fluid-rock interaction. There are many possible mechanisms by which this can occur. Sulphidation of the wall rocks has been demonstrated as an efficient gold deposition mechanism in lode deposits (Neall and Phillips, 1987) and is commonly invoked as the dominant depositional mechanism for many large replacement orebodies including Kambalda (Clark et al., 1986, 1989; Neall and Phillips, 1987), and BIF-hosted deposits (Neumayer et al., 1993a,b). In this process,  $H_2S$  and S in Au–S complexes from the fluid are consumed by the reaction of Fe-silicates or Fe-oxides to Fe-sulphides in the wall rocks of the fluid conduit. The loss of sulphur (decrease in  $\Sigma S$ ) from the fluid destabilizes the gold–sulphur complexes causing gold to precipitate by reactions involving  $Au(HS)_2^- + FeO_{(silicate, oxides)} \rightarrow Au + FeS_2$  (unbalanced). If this process is dominant, the gold grades in resultant orebodies should correlate with the total sulphide content of the adjacent wall rocks. If Fe-sulphides form by this process in veins, iron from wall rock phases is consumed in the reaction, leaving ferromagnesian silicates and/or carbonates in the wall rocks surrounding orebodies more magnesium-rich than those external to the orebody.

Intense K and  $CO_2$  metasomatism can also cause gold deposition (Fyfe and Kerrich, 1984; Kishida and Kerrich, 1987). These metasomatic processes release  $H_2$  into the hydrothermal fluid, thus decreasing the pH of the fluid and potentially causing gold

to precipitate. If K and/or  $CO_2$  metasomatism contributes to the deposition of gold in an orebody, significant gold grades should occur in the wall rocks adjacent to the quartz veins and gold grades should correlate with the dynamic alteration fronts, as in the Kerr–Addison deposit, Ontario (Kishida and Kerrich, 1987), and Allegheny District, CA (Böhlke, 1989).

Reaction of primary ore fluid with graphitic wall rocks produces significant quantities of methane through reactions such as  $2C + 2H_2O \rightarrow CH_4 + CO_2$ . Cox et al. (1991) developed a model for the Victoria Gold fields of southern Australia in which residual fluids from a pulse of hydrothermal ore fluids penetrated and reacted with carbonaceous wall rock to generate  $CH_4$ . During the following hydrothermal pulse the ore fluid was reduced by residual fluids, promoting gold precipitation. As summarized earlier, C isotope compositions of vein carbonates may indicate if this process was operative (Kerrich, 1990b).

#### *11.2.3. Phase immiscibility as a depositional mechanism for gold*

As summarized earlier, phase separation in ore fluids may arise from transient pressure drops during seismic events. This process generally results in an increase in the pH of the ore fluid, as the acid volatile species  $H_2S$ ,  $CO_2$ , and  $SO_2$  partition into the vapour phase. An increase in the oxygen fugacity of the fluid also occurs, because the reduced volatile species  $CH_4$ ,  $H_2S$ , and  $H_2$  partition into the vapour phase more readily than their oxidized counterparts  $CO_2$ ,  $SO_2$ , and  $H_2O$  (Drummond and Ohmoto, 1985; Naden and Shepherd, 1989; Mikucki and Groves, 1990; Bowers, 1991). Examination of Fig. 24B reveals that increasing pH and oxygen fugacity may have competing effects on gold solubility and can actually increase the solubility of gold in the ore fluid. Whether or not gold will precipitate depends on the initial redox and pH conditions of the fluid and the relative magnitude of the  $f(O_2)$  and pH increases.

The total sulphur content of the fluid decreases as  $H_2S$  is exsolved into the vapour phase during phase immiscibility (Mikucki and Groves, 1990). This process can lead to gold precipitation through reactions

such as  $\text{Au}(\text{HS})_2^- + 1/2\text{H}_2 = \text{Au} + \text{H}_2\text{S} + \text{HS}^-$ . Whether or not gold actually precipitates depends on the relative magnitude of sulphur loss vs. pH and  $f(\text{O}_2)$  increases. Fluid pressure cycling leading to sudden pressure drops during quartz vein formation are common in lode gold systems, hence phase immiscibility provides a gold depositional mechanism, controlled by processes operating strictly within the fluid conduit, that can explain orebodies where gold is sited dominantly within veins (Section 5; Sibson et al., 1988; Kerrich, 1989b; Guha et al., 1991; Bouillier and Robert, 1992; Wilkinson and Johnston, 1996; Fig. 8B).

It was commonly believed that at temperatures and pressures above the greenschist–amphibolite transition, phase separation was rare; however, addition of solutes (Ho et al., 1992) or volatiles such as  $\text{CH}_4$  or  $\text{N}_2$  (Naden and Shepherd, 1989) drives the solvus to higher  $P$ – $T$  conditions (Fig. 15). Recent experimental data suggest that phase immiscibility may be common in moderate-salinity fluids under high-T, moderate-P conditions (Johnson, 1991). Shock nucleation processes during seismic events may aid phase immiscibility where a one-phase fluid would be metastable under ambient conditions (Kerrich, 1989a).

#### *11.2.4. Fluid mixing as a depositional mechanism for gold*

Mixing of two distinct fluid reservoirs is unlikely in the majority of lode gold systems due to the uniformity between calculated ore fluid compositions from lode gold deposits of all ages and geographic location, and uniform  $\delta^{18}\text{O}_{\text{mineral}}$  values at individual deposits (Kerrich, 1989b; Phillips and Powell, 1993). However, recent studies have demonstrated that fluid mixing does occur on two distinct scales.

(1) Mixing of two externally derived fluids. Potential examples of this process include mixing of deeply sourced fluids with surface waters in some sub-greenschist facies environments, or mixing of metamorphic and deeper magmatic or mantle-derived fluids in some higher temperature deposits.

(2) Mixing of internally derived end member fluids, as in the model of Cox et al. (1991) [See Section 11.2.2]. This mechanism can also explain the location of large gold concentrations sited within quartz veins with negligible gold in surrounding wall

rock alteration selvedges. Fluid inclusions and stable and radiogenic isotope data are potential monitors as to whether these processes have operated (Sections 7 and 9).

#### *11.2.5. Chemisorption of gold*

Chemisorption processes may also be operative within the wall rocks or fluid conduit, whereby gold precipitates on the surface of coevally or previously precipitated sulphide minerals, by half-cell reactions of the form  $\text{Au}(\text{HS})_2^- + e \rightarrow \text{Au}^0 + 2\text{HS}^-$  (Jean and Bancroft, 1985; Starling et al., 1989). Morphological studies of gold in high grade oreshoots with abundant native gold suggests that this may be a significant gold precipitation mechanism in many deposits (see below). Details of this process are outlined by Knipe et al. (1994).

#### *11.3. Siting of gold versus introduction of gold*

In many deposits the majority of the gold, if not all, appears paragenetically late, as native metal or, more rarely, tellurides or sulphosalts occupying fractures in sulphides, quartz veins, and silicate and carbonate gangue (Robert and Brown, 1986b; Hamilton and Hodgson, 1986; Fedorowich et al., 1991; de Ronde et al., 1992; Cassidy and Bennett, 1993; McCuaig et al., 1993), leading some workers to speculate on late introduction of gold (~40 to 100 Ma post-peak metamorphism, or even post-vein emplacement and alteration (see Section 12).

There are, however, abundant examples of deposits where gold is associated with primary vein-forming minerals. Examples include: (1) gold in sulphide lattice structures (Cathelineau et al., 1989; Neumayer et al., 1993a); (2) gold as inclusions in sulphides (e.g., Andrews et al., 1986; Barnicoat et al., 1991; Caddey et al., 1991; Fedorowich et al., 1991; Gebre-Mariam et al., 1991; Goldfarb et al., 1991a,b; de Ronde et al., 1992; Hagemann et al., 1993; McCuaig et al., 1993); (3) gold in silicate and carbonate gangue (Caddey et al., 1991; Cassidy, 1992); (4) and gold in textural equilibrium with sulphides or silicates (Andrews et al., 1986; Robert and Brown, 1986b; Peters and Golding, 1989; Caddey et al., 1991; Fedorowich et al., 1991; Gebre-Mariam et al., 1991; de Ronde et al., 1992; Cassidy and Bennett, 1993; Hagemann et al., 1993; McCuaig et al., 1993). In these examples, at least part of the gold

must have been introduced and deposited coevally with hydrothermal alteration and quartz vein emplacement.

The study of Neumayer et al. (1993a) demonstrates that gold sited at löellingite–arsenopyrite boundaries, a common texture observed in higher-temperature deposits, was initially introduced as lattice-bound gold with löellingite, then locally exsolved during retrogression of löellingite to arsenopyrite. Similarly, other studies have demonstrated that gold mineralization was likely continuous throughout protracted and episodic histories of quartz vein emplacement and hydrothermal alteration (Peters and Golding, 1989; Cox et al., 1991; de Ronde et al., 1992; McCuaig et al., 1993). Remobilization during recrystallization or deformation, for example  $\text{Fe}(\text{Au})\text{S}_2 = \text{FeS}_2 + \text{Au}$  may also produce texturally late gold from gold that was introduced with earlier stages of alteration (Romberger, 1986). Gold also may be locally mobilized and redeposited on the surface of pre-existing sulphides by chemisorption processes (Jean and Bancroft, 1985; Knipe et al., 1994). Such ore modification processes may explain the common presence of ‘apparently late’ gold on fractures in, or as rims on, sulphides.

Guha and Kanwar (1987) have documented commanding evidence for Proterozoic remobilization of gold by late hypersaline brines into a secondary paragenesis within Archean deposits of the Chibougamu district, Quebec. Similarly, Boyle (1979) reported gold as veins in permafrost, remobilized by subglacial groundwaters from an Archean shear zone in the Yellowknife district. Collectively, these observations demonstrate that the final siting of gold need not equate with the initial mode or timing of gold introduction and deposition, and corroborates evidence from reset isotopic systems which indicate numerous post-fluid events in Precambrian terranes (Section 12; Kerrich and Cassidy, 1994; Kent and McCuaig, 1997).

## 12. Radiogenic ages: primary mineralization and resetting events

Constraining the age of mineralization is a critical aspect of the larger  $P$ – $T$ – $t$ – $d$ – $f$  history of the host

terrane, as both primary and secondary fluid events are encoded in hydrothermal alteration assemblages associated with lode gold deposits. Precise age controls are also vital for assessing the secular relationship of mineralization and alteration to regional magmatism, metamorphism, and deformation, and for screening out secondary reset ages in the deposits. For example, based on precise age constraints, Goldfarb et al. (1997) have been able to relate lode gold deposits of Alaska to collision events among the Kula, Farallon, and North American plates.

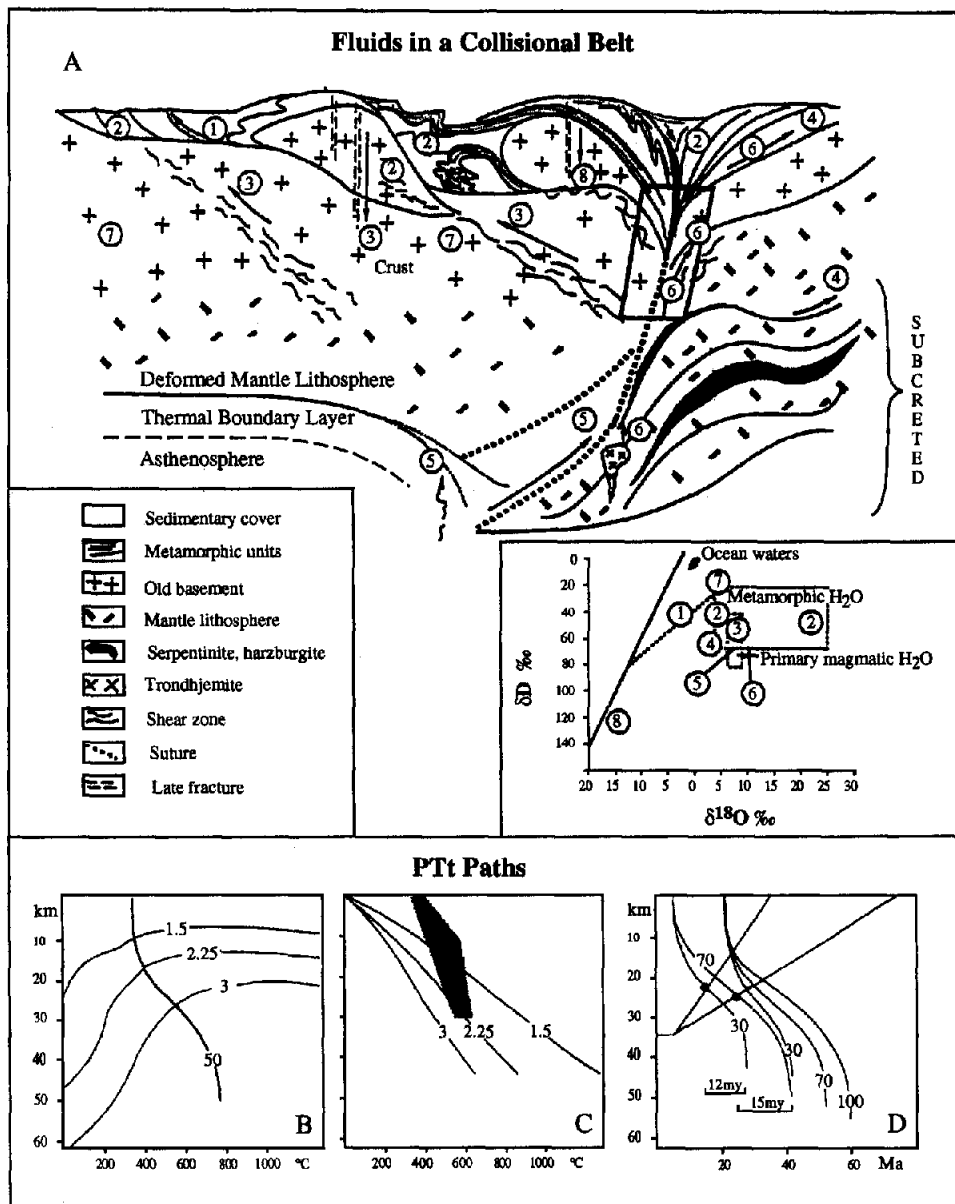
### 12.1. Synkinematic, symmetamorphic mineralization

Temporal relationships between (1) gold mineralization and (2) magmatism, deformation, and metamorphism appear to be straightforward in the majority of lode gold metallogenic provinces of all ages. Primary gold concentration into vein and replacement orebodies is coeval with uplift following transpressional collision of allochthonous terranes, and post-dates syncollisional peak-metamorphism by a few m.y., to at most 40–50 m.y. (Fig. 25; Table 4; Wyman and Kerrich, 1988; Kerrich and Wyman, 1990, 1993; Goldfarb et al., 1993, 1997; Kerrich and Cassidy, 1994; Miller et al., 1994; Kent et al., 1996; Ford and Snee, 1996). For terranes without regional faults controlling the distribution of gold deposits, such as the Slave Province, N.W.T., Canada and Victorian gold province of South Australia, outboard accretion may lead to inboard delamination of the lithospheric mantle or thermal boundary layer, with input of asthenospheric heat leading in turn to crustal heating (Scrimgeour and Sandiford, 1993). The essential process of generating metamorphic ore fluids by dehydration of crustal rocks is the same in both cases.

This progression of events is exemplified by age relationships in many post-Archean lode gold deposits. In the Paleoproterozoic Trans Hudson orogen, gold introduction at the Tartan Lake deposit at  $\approx$  1790 Ma was  $\approx$  30 to 40 m.y. later than peak metamorphism over  $\approx$  1840–1820 Ma (Fedorowich et al., 1991). Similarly, mesothermal deposits of the Palaeozoic Meguma terrane were emplaced within a few m.y. of magmatism and peak metamorphism ( $\approx$  370 Ma; Kontak et al., 1990). The timing of Mesozoic–Cenozoic deposits of the North American Cordillera are also well constrained. In the Mother

Lode gold province, gold mineralization is bracketed between the early (152–136 Ma) and main (115–104 Ma) phases of the Sierra Nevada batholith, and the maximum duration of ore formation was 14–35 m.y. (Landefeld, 1988). Elder and Cashman (1992) conclude that changes in the Farallon–North American

plate convergence at 150 to 133 Ma was coeval with, and the cause of, regional tectonic activity and gold mineralization in the Klamath mountains of northern California. In the Juneau district of Alaska, Goldfarb et al. (1991a, 1997) have constrained mineralization over a 200 km sector of the Coast Range Megalinea-



ment to within a 1 m.y. interval, specifically during a change in plate vectors, in the waning stages of regional metamorphism. In the Southern Alps, New Zealand, gold mineralization is interpreted to be a result of continental collision (McKeag and Craw, 1989; Koons and Craw, 1991; Smith et al., 1996; Koons et al., 1998), and in the Cenozoic Monte Rosa lodes of the European Alps, gold mineralization is constrained to 4–8 m.y. post-peak Alpine metamorphism (Curti, 1987).

In the Archean Superior Province, gold deposits formed concurrently with accretion of allochthonous terranes that was generally diachronous from north to south, and is constrained by crosscutting relationships with precisely dated igneous rocks (Wyman and Kerrich, 1988; Kerrich and Wyman, 1993; Kerrich and Cassidy, 1994). Similarly, for the majority of late-Archean lode gold deposits in the Yilgarn Craton, mineralization closely follows peak metamorphism and accretionary development (Groves et al., 1989; Kent et al., 1996). Precise age determinations of gold mineralization derived from U–Pb studies of zircon and monazite from cross-cutting intrusions or U–Pb rutile, and Pb–Pb mineral isochrons using titanite and coexisting silicates and/or sulfides, show remarkable synchronicity across the Yilgarn Craton at ca. 2630 to 2640 Ma (Kerrich and Cassidy, 1994; Kent and McDougall, 1995).

Recently, it has been suggested that some gold deposits in the Superior Province are premetamorphic. Rarely, there are small zones of aluminous alteration. At the Campbell Mine of the Red lake camp, Northwestern Ontario, aluminous assemblages in basalts trend from quartz, andalusite, sericite, chlorotoid, margarite, cordierite, to flanking quartz, chloritoid, chlorite, garnet, cummingtonite (Penczak and Mason, 1997). Margarite- and kyanite-bearing assemblages are present in the Bousquet cold camp, Abitibi belt. There is general consensus that the aluminous zones represent metamorphosed epithermal hydrothermal alteration zones. It is not clear however, as argued by Penczak and Mason (1997), that the Au–As–Sb–Zn (Hg) vein-related mineralization is also epithermal, and pre-metamorphic, as the majority of gold deposits in the Red lake camp formed in ductile shear zones, where the tectonic fabric is syn- or post-metamorphic (Andrews et al., 1986). On the basis of a 2685 Ma dyke cross-cutting gold ore are at the Kiena deposit, Quebec, and an estimate of 2677 to 2643 Ma for regional metamorphism, Morasse et al. (1995) argue for a premetamorphic age for gold mineralization. Yet 15 km away near Val d'Or peak metamorphism has been constrained at 2690 Ma. The simple arguments of Morasse et al. (1995) ignore the fact that in high-T, low-P type metamorphic terranes heat may be ad-

Fig. 25. (A) Schematic diagram illustrating possible fluid reservoirs involved in a collisional and/or transpressive geodynamic regime. (1) Formation waters tectonically expelled from cover thrust units, advect along thrust faults. (2) Syntectonic veins buffered by low-, or high- $\delta^{18}\text{O}$  lithologies. (3) Metamorphic fluids from old basement. (4) **Metamorphic fluids from dehydration of subcreted oceanic lithosphere: these are the principal hydrothermal ore fluid for lode gold deposits.** (5) Mantle volatiles from late decompression advect up suture. (6) Magmatic fluids from trondjemites generated by melting base of subcreted lithosphere. (7) Formation brines that penetrated basement during extensional phase. (8) Low- $\delta^{18}\text{O}$  meteoric water from high-altitude mountain range. (B,C,D) Timing relationships between metamorphism at shallow and deep crustal levels modelled for *deep-later* type metamorphic terranes. Piezothermal arrays calculated with the model and method of England and Thompson (1984). (B) A piezotherm for an erosion rate of 35 km per 50 m.y. and onset of erosion at 20 m.y. after initial thickening (thick line). Thin lines represent the 400°C isotherm for heat source distribution II of England and Thompson (1984) and contoured for different thermal conductivities. (C) The changes of metamorphic peak temperature with depth. Contours are for differing conductivities of (a). The light-shaded field indicates the area in which crustal melting is likely to occur and the dark-shaded field is that of likely fluid production. (D) Piezothermal arrays for two different times of erosion onset at 5 and 20 m.y. after initial homogeneous crustal thickening to double thickness crust and for characteristic erosion times of 30, 70 and 100 m.y. Superimposed straight lines are particle trajectories of rocks now preserved at the surface. Times and depth of metamorphic peak for these rocks is shown by the dots and time intervals between metamorphism at these levels and at the bottom of the crust are labelled with the brackets. (From Stüwe et al., 1993a,b) [modified from Kerrich and Cassidy, 1994].

Table 4  
Synthesis of geodynamic settings and metamorphic, tectonic, and geochronological relations in some lode gold metallogenic provinces (modified from Kerrich and Wyman, 1990)

Setting (tectonostratigraphic terrane)	Lithological ages (Ma)	Accretion/ deformation (Ma)	Regional metamorphism (Ma)	Magmaism (Ma)	Uplift (Ma)	Mineralization (Ma)	Comments	Source
<i>Cenozoic lode gold provinces</i>								
Monte Rosa nappes terrace, Italian Alps	Mesozoic Paleozoic	Tertiary	38 ± 2	Calc-alkaline post-peak metamorphism; post-kinetic	Post-peak metamorphism	(1) 29.9; 33.4 K-micas (2) 20 to < 20 unrelated	Mineralization is post-peak metamorphism	Curti (1987)
<i>Mesozoic–Cenozoic Cordilleran lode gold provinces</i>								
Valdez Group, Chugach terrane, AK	Late-Cretaceous	Late-Cretaceous to Early Tertiary (< 65)	Coeval with accretion (< 65)	(1) Calc-alkaline: 53–50 (2) Mafic-felsic: 37–34	Post-peak metamorphism	(1) HopeSunrise and Port Valdez: 53–52 (2) Port Wells: < 34	Mineralization is post-peak metamorphism	Goldfarb et al. (1986)
Juneau gold belt, AK	70–50	70–55	(1) Monzodioritic: 105 (2) Tonalite: 68–61 (3) Calc-alkaline 54–48	Post-peak metamorphism (60–65)	56.1–55.0	Mineralization is post-peak metamorphism	Goldfarb et al. (1988, 1991a,b)	
Mother Lode and Foothills Metamorphic Belt, CA	Late Triassic (≤ 150)	Paleozoic Jurassic (160–140)	Multiple pre-ore events	Sierra Nevada batholith (1) 152–136 (2) 115–104 (3) 92–80	Post-orogenic post-peak metamorphism (ca. 140)	Grass-Valley: – 140 Allegheny- Mother Lode: 116–110	Mineralization is post-peak metamorphism and likely unrelated to magmatism	Böhme and Kistler (1986), Landefeld (1988)

<i>Paleozoic lode gold provinces</i>											
Meguma terrane, Appalachians	Cambrian– Ordovician	Acadian (Early to Mid. Devonian)	Mid-Devonian (400 ± 10)	Late-Devonian (ca. 370–360)	Post-peak metamorphism (ca. 370)	ca. 380–362	Mineralization is post-peak metamorphism synchronous	Kontak et al. (1990)			
Lachlan fold belt— Stawell Zone	Cambrian– Ordovician	(1) Benambran (445–425) (2) Tabberabberan (390–360)	Late Ordovician To Early Silurian	Browning (~408–383)	ca. 390–370	Mineralization post-dates cleavage development	Sandiford and Keays (1986), Cox et al. (1991), Phillips (1993)				
Bendigo–Ballart Zone	Cambrian– Ordovician	West: Browning (415–390) East: Tabberabberan (390–360)	Early to Mid. Devonian	West Browning (~408–383) East Tabberabberan (390–360)	ca. 390–370	Mineralization post-dates cleavage development					
<i>Late Archean lode gold provinces<sup>a</sup></i>											
Yilgarn Craton– Kalgoorlie Terrane	2800–2600	2700–2650	ca. 2660	(1) 2800 (2) 2690 and 2670–2650	2650–2600	Mineralization is late- to post-kinematic	McNaughton et al. (1990), Barley and Groves (1992)				
Yellowdine and Southwest	> 3000 to 2600	2700–2650	ca. 2640	(1) ca. 3000–2800 (2) 2700–2600	2650–2630	Mineralization is late- to post-kinematic	McNaughton et al. (1990), Barnicoat et al. (1991)				
Superior Province— Red Lake belt, Uchi Subprovince	Archean	2709	2750–2700	2720–2715	~2720	Mineralization synchronous with late plutonism and metamorphism	Andrews et al. (1986), Corfu and Andrews (1987)				
Southern Abitibi Subprovince	Archean	< 2703–2675	< 2698–2670	(1) TTG; (2) calke-alkaline; 2690–2680 (3) alkaline; 2676–2670	(1) 2680–2670 or (2) 2630–2400	Mineralization is post-peak metamorphism; late kinematic	Claoué-Long et al. (1990), Corfu (1993), Zweng et al. (1993)				

vected in a series of magmatic pulses, and there is not necessarily a single peak of metamorphism (Stüwe et al., 1993a,b).

## 12.2. Aberrantly young 'ages' for mineralization

Superficially, the timing of gold mineralization in the Archean Abitibi belt, Canada, eastern Yilgarn Block, Western Australia, and some deposits in the Proterozoic La Ronge Domain, Saskatchewan, appear to be exceptions to the global temporal patterns described above, where alteration minerals yield radiogenic ages as late as 270 m.y. post-peak metamorphism, as summarized in Kerrich and Cassidy (1994). Two classes of explanation have been advanced to account for the unusually young ages: (1) the dates reflect isotopic resetting during post-mineralization reactivation of structures, and the primary gold event was late kinematic and broadly coeval with peak metamorphism (Kerrich and Cassidy, 1994); or (2) the young ages date gold mineralization (Bell et al., 1989; Jemielita et al., 1990; Hanes et al., 1992; Fayek and Kyser, 1995). A difficulty in the Abitibi subprovince, eastern Yilgarn Block and La Ronge Domain is the paucity of igneous rocks cross-cutting gold deposits on which precise U-Pb ages can be determined.

Mounting evidence for isotopic resetting of alteration minerals is detailed in Kerrich and Cassidy (1994) and includes: (1) field evidence indicating reactivation of Archean structures in Proterozoic time (Kamineni et al., 1990); (2) exchange of H isotopes in hydrous minerals with late surface waters (Kyser and Kerrich, 1991); (3) O isotope disequilibrium between carbonates and paragenetically associated gold-bearing quartz, resulting from selective retrograde exchange of the carbonates with late, low-temperature hypersaline brines (Kerrich, 1987, 1990a,b); (4) Proterozoic Pb isotope disturbance of some Archean gold deposits (Franklin et al., 1983; Perring and McNaughton, 1990; McCuaig and McNaughton, submitted); (5) Proterozoic remobilization of gold and other elements in Archean gold deposits (Guha and Kanwar, 1987; Perring and McNaughton, 1990), (6) reversed blocking temperature sequences in some

deposits, such that typically more robust systems such as Sm–Nd and U–Pb yield younger ages than more sensitive systems such as Rb–Sr or  $^{40}\text{Ar}/^{39}\text{Ar}$  (Kerrich and Cassidy, 1994; Kent and McCuaig, 1997), and (7) Ages of  $\sim 2685$  Ma from concordant U–Pb ages of hydrothermal zircons (containing fluids inclusions, and inclusions of gold, pyrite, scheelite) associated with gold mineralization, versus ages of 2630 to 2670 Ma on the same vein systems at Val d'Or Canada, based on different reset isotopic systems and minerals (Kerrich and King, 1993; Kerrich and Cassidy, 1994).

These results appear to obviate thermal events as the cause of scattered ages and endorse selective resetting of isotopic systems by hydrothermal overprinting and/or remobilization. Models for young (late gold) mineralization are also inconsistent with the fundamental field relationships whereby the deposits form in gross rheological and thermal equilibrium with their host terranes, not 50–270 m.y. later (Sections 3–5, 7 and 8). Variable resetting in the gold deposits is mirrored in volcanic massive sulphides that are incontrovertibly synvolcanic. At the giant Kidd Creek Cu–Zn VMS, the U–Pb<sub>zircon</sub> age of the host felsic rocks is  $2717 \pm 2$  Ma, whereas younger ages are recorded by U–Pb<sub>monazite</sub> ( $2659 \pm 3$  Ma), U–Pb<sub>rutile</sub> ( $2664 \pm 25$  Ma;  $2624 \pm 64$  Ma),  $^{40}\text{Ar}/^{39}\text{Ar}_{\text{muscovite}}$  ( $2618 \pm 8$  Ma), Sm–Nd<sub>whole-rock isochron</sub> ( $2674 \pm 40$  Ma), and Rb–Sr<sub>whole-rock isochron</sub> ( $2576 \pm 26$  Ma) [Kerrich and Cassidy, 1994, and references therein].

In summary, well documented studies all demonstrate a late kinematic timing of gold mineralization for the majority of deposits, shortly post-peak metamorphism. The Archean structures were repeatedly reactivated, stable and radiogenic isotope systems selectively reset, reversed blocking sequences locked in, and many elements, including gold, were remobilized to varied extends by post-mineralization fluid events. The fact that some gold deposits clearly post-date peak metamorphic fabrics does not invalidate temporal association between mineralization, given that metamorphism is of deep later  $P-T$  type, where peak metamorphism may be 20 Ma to 60 Ma younger at deeper than at shallower levels (Sandiford and Keays, 1986; Sandiford and Powell, 1991; Stüwe et al., 1993a,b).

### 13. Unresolved questions

Notwithstanding the large analytical databases and body of observations that have been established for lode gold deposits, as summarized above, there remain a number of outstanding questions.

#### 13.1. Korean gold deposits

Gold deposits in Korea, described as mesothermal in character, are spatially and temporally associated with Jurassic granites. They are distinct from higher level epithermal counterparts. The lode (mesothermal) deposits share many characteristics in common with Archean and younger lode gold deposits: they are structurally hosted massive quartz vein systems, with high Au/Ag (5:1 to 8:1) ratios, and relatively low sulphide content. The ore fluids are dilute aqueous,  $\text{CO}_2 + \text{CH}_4$ -bearing, having low salinities of ~4 equivalent wt.% NaCl. Gold was deposited between 400 and 290°C, during fluid unmixing, at pressures of 1.2 to 1.5 kbar. In deposits of the Jungwang area fluids had  $\delta^{18}\text{O}$  +5 to +7.7‰, and  $\delta\text{D}$  –78 to –113‰. Given estimates of –143 to –81‰ for the  $\delta\text{D}$  of palaeometeoric water, Shelton et al. (1988, 1990) argued that the ore fluids were highly evolved meteoric water. For the Samhwanghak mine of the Yangdong area, So and Yun (1997) found a similar low salinity aqueous carbonic fluid, but with  $\delta^{18}\text{O}$  6 to 8‰ and  $\delta\text{D}$  –62 to –72‰. Based on the ore fluids  $\delta^{18}\text{O}$  and  $\delta\text{D}$  values, and temperature–oxygen fugacity relationships, So and Yun (1997) interpreted the ore fluids to be magmatic, derived from a nearby S-type granitoid. According to Shelton et al. (1988, 1990) and So and Yun (1997) the Korean mesothermal gold deposits are directly analogous to Archean and Cordilleran counterparts. However, could these two Korean deposits with such similar characteristics have been formed from two wholly distinct ore fluids, or is there an alternative explanation for the  $\delta D_{\text{H}_2\text{O}}$  values, and how does a meteoric model fit most Archean lode deposits, where there is no compelling evidence for meteoric ore fluids?

There is a common problem with the meteoric water model for the Korean and Cordilleran deposits, as discussed by Goldfarb et al. (1989) and Kerrich (1989b). Given palaeometeoric water with  $\delta\text{D}$

–140‰,  $\delta^{18}\text{O}$  would have been –19‰. Consequently, the ore fluid would have shifted in  $\delta^{18}\text{O}$  by +27‰, from –19‰ to the estimated value of about +8‰ by fluid/rock interaction at low water/rock ratios. During such interaction fluids evolve along J-shaped trajectories on  $\delta D_{\text{H}_2\text{O}}$  vs.  $\delta^{18}\text{O}_{\text{H}_2\text{O}}$  diagrams, from the meteoric water line to the magmatic/metamorphic fields, and hence would of necessity lose the initial D-depleted meteoric water signature. In all the studies of Korean and Cordilleran lode gold deposits  $\delta D_{\text{H}_2\text{O}}$  was measured by decrepitating fluid inclusions in quartz or calcite. As demonstrated by Goldfarb et al. (1991b, 1997), decrepitation may also release fluid inclusions that contain low- $\delta\text{D}$  meteoric water, masking the primary ore fluid. Alternatively, or in addition, deep sourced non-meteoric, ore fluids may react with  $\delta\text{D}$ -depleted organic matter to acquire a low  $\delta\text{D}$  signature that mimics meteoric water (Goldfarb et al., 1989; see discussion between Nesbitt and Muehlenbachs, 1991, and Peters et al., 1991). Hence, low  $\delta\text{D}$  values obtained by decrepitating fluid inclusions are not necessarily diagnostic of deeply circulated meteoric waters.

In summary, the structural style, Au/Ag ratios, paragenesis and ore fluid characteristics of the Korean lode (mesothermal) deposits are remarkably similar to those of lode gold metallogenic provinces of all ages. The *single* feature of variably low  $\delta\text{D}$  values in *some* Korean and Cordilleran deposits is insufficient to constrain the ore fluids as meteoric water, nor to infer that all lode deposits formed from meteoric water. Finally, we note that shallow-level Archean deposits where there is evidence for involvement of meteoric water, like the Eldrich deposit Noranda (Kerrich, 1987; Fig. 19), and Wiluna and Racetrack deposits, Yilgarn block (Hagemann et al., 1994) have conspicuously different mineral parageneses, structural style and ore minerals than deeper level equivalents. Consequently, there are no facts to endorse the deeper level ore deposits as having formed from meteoric waters; rather the deeper-level lode deposits formed from a deep-sourced fluid, and the shallower-level lode deposits from the same ore-forming fluid that mixed with shallow surface fluids.

It is possible that the spatial and temporal association of the Samhwanghak deposit with an S-type granite translates into a genetic orthomagmatic rela-

tionship. However, it is unlikely that this has general applicability to lode gold deposits. In the Abitibi belt, where lode deposits are associated with granitoids these are slab-derived TTG's or wedge-derived lamprophyres (Wyman and Kerrich, 1988); in the Yilgarn block tonalite-granitoids are dominantly intracrustal melts (Cassidy, 1992); the Meguma deposits are associated with in space and time with peraluminous, A-type granites (Kontak et al., 1990); and the Mother lode deposits formed between the early and main phases of the calc-alkaline Sierra Nevada batholith (Landefeld, 1988).

### 13.2. Vertical zonation, Au–Hg

There is an Au–Sb association in several lode gold deposits of Archean to Phanerozoic age. Based on this and other lines of evidence Nesbitt et al. (1989) proposed that the Au–Sb deposits were part of an overall vertical zonation from Au–Sb–Hg deposits. The ore-forming fluids for Au–Sb deposits are remarkably similar to those in lode gold deposits, albeit at lower temperatures and pressures, endorsing the vertical zonation. For example, at the Snowbird property, British Columbia, the ore fluids were dilute aqueous,  $\text{CO}_2 \pm \text{CH}_4$ -bearing solutions, with 1.8 to 3.6 equivalent wt.% NaCl, where  $X_{\text{CO}_2} \sim 0.1$  and pressure  $> 800$  bar (Madu et al., 1990).

Goldfarb et al. (1990) described high-level Hg–Sb mineralization from southwestern Alaska. The mineralization was attributed to low grade metamorphism of the Kuskokwim sedimentary rocks. Low  $\delta D$  values for ore fluids was attributed to breakdown of D-depleted organic matter. Mercury mineralization at Almaden, Spain, is arguable the largest geochemical anomaly globally, with 30% of world Hg production. Recent geochemical studies have constrained the timing of mineralization to be coeval with regional metamorphism (Hall et al., 1997). Around the Pacific Rim, ore fluids of Recent Hg deposits, and thermal springs actively depositing Hg, have many properties in common with those of the Hg–Sb, Au–Sb, and Au–Ag lode deposits. In summary, there is compelling evidence for an overall vertical zonation from Au–Ag, Au–Sb, to Sb–Hg, and Hg deposits, all formed from similar dilute, aqueous, carbonic fluids. However, it is unlikely that

all higher-level deposits have deeper-level counterparts, or vice versa.

Nesbitt and coworkers have suggested that there is a gold deposit continuum, in which one fundamental processes, the convective circulation of meteoric water, is responsible for several types of gold deposits. The types of deposits are 'broken out' based on geodynamic setting and pressure estimates: epithermal Ag–Au deposits in magmatic arcs formed at 0 to 200 bar; Carlin-type deposits in regions of intra-continental extension formed between 500 and 1000 bar; and mesothermal (lode) Au–Ag deposits that are generated in vertically extensive strike-slip or normal faults at 8000 bar (Nesbitt et al., 1986; Nesbitt, 1988).

The pros and cons of evolved meteoric water as an ore-forming fluid for lode (mesothermal) deposits has been discussed above. Here we simply note that the J-shaped trajectories in  $\delta D_{\text{H}_2\text{O}}$  vs.  $\delta^{18}\text{O}_{\text{H}_2\text{O}}$  expected for meteoric water–rock interaction are present in epithermal and Carlin-type deposits (Taylor, 1997, and references therein). In the deeper-level lode (mesothermal) deposits, where 'apparent' meteoric water–rock interaction would occur under lower water/rock ratios and higher temperature, given deeper crustal depth and lower permeabilities, more pronounced J-shaped trajectories would be expected (Nesbitt, 1988, 1995; Nesbitt et al., 1989; Zhang et al., 1989), but this is not the case. Peters et al. (1991) demonstrated that the Hodgkinson gold deposit, Queensland, has significantly more D-depleted ore fluids than other lode gold deposits in the Hodgkinson province. These results are consistent with D-depleted organic matter contributing to D-depleted ore fluids (Peters et al., 1991), but are inconsistent with a latitudinal control expected for the  $\delta D$  of meteoric water. Exchange of an ore fluid with D-depleted organic matter does not necessarily imply that  $^{13}\text{C}$  depleted carbonates would be present in the deposit, as H-isotope exchange may occur in the absence of C-isotope exchange.

In the Canadian Cordillera, there is almost as much difference between two lode Au deposits in southern British Columbia, as between the less depleted deposit and a deposit in northern British Columbia (Zhang et al., 1989). These results are contrary to the anticipated latitudinal control of meteoric water  $\delta D$ . Peters et al. (1991) argued that

many of the  $\delta D_{H_2O}$  results of Nesbitt and coworkers are more readily explained by variable contributions from, or exchange with, D-depleted organic material.

### 13.3. Real time analogs

Black smokers at mid ocean ridges and in back arc basins have provided a real-time analog for many of the processes thought to be involved in the formation of volcanogenic massive base metal sulphide (VMS) deposits. Are there also real-time analogs, as surface discharge, or active hydrothermal systems on terrane boundaries, that are a high level expression of deeper fluid advection along structures forming lode gold deposits now?

Although waters of meteoric origin are the dominant near-surface geothermal systems, some hot spring fluids are apparently derived from dehydration reactions. A series of distinctive hot, or warm springs aligned on major crustal structures occur in the circum-Pacific belt. When compared to meteoric water dominated hot spring systems, the structurally controlled variety are distinctive in terms of: (1) discharge at ridges rather than in depressions, signifying a geopressurized fluid; (2) abundant CO<sub>2</sub>; (3) low salinity; (4) relatively enhanced solute concentrations of As, Sb, B, Li, Rb (etc); (5) low abundances of base metals; and (6) an association with mercury and/or sulphur deposits. Isotopically, the CO<sub>2</sub> springs are consistent with fluids of metamorphic origin, with little or no involvement of local meteoric water. In California, the CO<sub>2</sub>-hot springs have been interpreted as the surface expression of active metamorphism in the underlying Franciscan complex (Barnes, 1970).

All of the hot or warm springs discussed above involve advective flow of thermal waters, likely of metamorphic origin, along major crustal structures. The structures formed in collisional or transpressive regimes, representing the termination of subduction, and are associated with clockwise 'deep later' metamorphism, as deduced for lode gold deposits in this review. Barnes (1970) specifically identified situations where young sequences undergoing dehydration had been thrust beneath crystalline basement, a scenario also present in some of the lode gold deposits (Section 12). Measured isotopic compositions of thermal waters at Wilbur Spring and Sulphur

Banks in California are consistent with isotopic equilibration of water with a Franciscan-type sedimentary sequence at temperatures of 200–350°C. Other thermal waters in the region fall along mixing lines between end member isotopic compositions, and consequently consist of mixtures of meteoric water with other fluid reservoirs. Tritium analyses indicate a minor component of recent (post 1954) meteoric water in all of the hot springs. Hot springs of this type are also known along major fault zones in the Himalayas.

In the Southern Alps, New Zealand, Craw and Koons (1989) describe dilute aqueous, CO<sub>2</sub>-bearing fluids generated by metamorphic dehydration being released up structures during rapid uplift. Gold is precipitated from these fluids either by cooling, or mixing with dilute low-salinity meteoric fluids. Craw and Koons (1989) suggest that these may be analogs of mesothermal gold systems. Another line of evidence on the source of hydrothermal fluids for lode gold deposits comes from deeply subducted rocks that have been exhumed. In the Catalina schist of California, lawsonite–albite grade metasedimentary rocks have been metasomatized by metamorphic fluids derived from amphibolite-grade counterparts. The former are enriched in B, As, Sb, Cs, K, Rb, and Ba, the exact element budget characteristically enriched in lode gold deposits (Kerrich, 1983; Bebout, 1996).

## 14. Summary and conclusions

### 14.1. Fluid conditions

*P-T-t-X* conditions of the ore fluids associated with lode gold deposits, calculated from the various techniques detailed above, are summarized in Table 3. The sum of microstructural, macrostructural and metamorphic observations signify that the alteration associated with lode gold deposits of all ages formed synkinematically, and close to peak metamorphic conditions, in gross rheological and thermal equilibrium with the host terrane. Fluid infiltration was episodic in nature, driven by fault–valve mechanisms involving transient sublithostatic to supralithostatic fluid pressure cycling within the fluid conduits.

Fluid inclusion, stable and radiogenic isotope, whole-rock geochemistry, and thermodynamic stud-

ies allow reconstruction of the composition of the fluid responsible for gold mineralization and local and regional hydrothermal alteration. Application of these techniques indicate a similar fluid composition for deposits of all crustal levels and age, comprising H–O–C–N–S volatile species ( $X_{CO} \approx 0.05\text{--}0.3$ ), solutes Na  $\gg$  K  $\geq$  Ca  $\geq$  Mg, low to moderate salinities (generally  $< 6$  wt.% NaCl equivalent), at near neutral pH and reduced to slightly oxidized conditions. Isothermal conditions appear to have prevailed within individual deposits, but temperature variations are noted on the terrane scale. Variations in redox conditions [higher  $f(O_2)$  and S at high  $T$ ] and major cation activities (Ca metasomatism dominant at high- $T$ , Na at low- $T$ , K at all- $T$ ) suggest progressive modification of the fluids through fluid–wall rock interactions along conduits during their ascent. Significantly, Sr and Pb isotope studies reveal that the fluids have equilibrated with older crust that underlies some supracrustal belts. The marked similarity in fluid compositions, timing of alteration and mineralization to deformation and metamorphism, and the observed correlation of structural style and alteration mineralogy with metamorphic grade, point to a crustal continuum of gold deposition with deposits at different crustal levels related by the same overarching genetic processes in similar geodynamic settings.

#### *14.2. Fluid sources and timing of fluid release in a P–T–t framework*

The greatest volume of fluid available to form the large hydrothermal systems associated with lode gold metallogenic provinces results from metamorphic devolatilization of subcreted supracrustal sequences at  $P$ – $T$  conditions corresponding to the greenschist–amphibolite transition in convergent margin settings. Reactions involving the breakdown of talc, magnesite, and chrysotile (ultramafic rocks), muscovite, chlorite, epidote (mafic rocks), and biotite and chlorite (pelitic rocks) release large quantities of structurally bound water with compositions consistent with those summarized above, and calculated from inverse modelling of hydrothermal alteration (Table 2; Fig. 25; Kerrich, 1983; Kerrich and Wyman, 1990; Powell et al., 1991; Phillips and Powell, 1993;

Stüwe et al., 1993a,b; Hanson, 1997). These reactions occur in a  $P$ – $T$  ‘window’ which, when allied with models for terrane evolution, predict definite  $P$ – $T$ – $t$  paths of fluid release. The short time lag of  $\approx 10$  to 40 m.y. between peak metamorphism in the host rocks and gold mineralization has been accounted for by thermal rebound in a tectonically thickened crust (Sandiford and Keays, 1986; Kerrich, 1989b). During collision, isotherms are disturbed such that peak temperatures are attained at progressively later times at increasing crustal depths during thermal re-equilibration (England and Richardson, 1977; England and Thompson, 1984; Platt and England, 1993). For convergent deformation of the lithosphere, Scrimgeour and Sandiford (1993) calculated that if crustal thickening was accompanied by thinning of mantle lithosphere (delamination), then advection of asthenospheric heat could cause more than 50% dehydration of the lower crust. They applied this model to the Proterozoic ‘Granites’ gold deposit, Northern Territory, Australia.

While these models provide considerable insight into the timing of fluid flow, hydrothermal alteration and gold deposition observed in sub-amphibolite facies host rocks, they do not apparently account for alteration and gold deposition at higher metamorphic grades, nor for the deep crustal fluid components indicated by radiogenic isotope studies of alteration minerals. To explain these situations, various fluid sources may be invoked including devolatilization of subcreted material, magmatic fluids or mantle degassing up translithospheric structures, which would then mix at mid-crustal levels with fluids produced by metamorphic devolatilization of greenstones. In structures of transcrustal extent with which the lode gold mineralization is associated, some contributions of juvenile or magmatic fluids are expected and evidence is mounting for their involvement in the formation of higher temperature deposits, but the dominantly low salinity, moderate  $CO_2$  contents, and range of calculated  $\delta D$ ,  $\delta^{13}C$ ,  $\delta^{18}O$  and  $\delta^{34}S$  compositions are not consistent with these sources forming the principal ore fluid reservoir. Surface waters may be involved in lode gold deposits formed at very high crustal levels, but are unlikely to have contributed to primary alteration and mineralization processes in deposits formed at greater than greenschist facies conditions.

### 14.3. Geodynamic setting of lode gold deposits

Globally, giant lode gold metallogenic provinces appear at four distinct times in Earth history: the late-Archean (~2.7 Ga), the Paleoproterozoic, the lower Palaeozoic, and in Mesozoic rocks of the North American Cordillera. Each of these times corresponds to major accretionary processes; part of the supercontinental cycle. The specific geodynamic setting is of transpressive accretion of allochthonous terranes to one another, or a pre-existing continental margin, typified by Cordilleran tectonics. This tectonic regime is distinct from continent–continent collision, such as the Alpine–Himalayan Orogen. The former is sometimes referred to as an external and the latter an internal orogen (Barley and Groves, 1992).

Within the accretionary regime, lode gold deposits and shoshonitic lamprophyres are associated in space and time, both being hosted by translithospheric structures representing terrane boundaries between distinct tectonostratigraphic terranes (Wyman and Kerrich, 1988; Kerrich and Wyman, 1990; Rock et al., 1989). The geodynamic setting of transpressive accretion appears particularly favourable for the generation of both shoshonitic lamprophyres and lode gold deposits. The lode gold–lamprophyre association reflects a common geodynamic setting of transpressive accretion involving a number of distinct processes in the post-collision phase. Thus the gold deposits and shoshonites are not part of the geological evolution of the allochthonous terranes, but rather formed at their boundaries following collision (Fig. 25). The spatial and temporal association assists in ruling out alternative models for gold that invoke earlier or much later time frames relative to the narrow window of accretion (Kerrich and Wyman, 1993). Based on structural style in the southern Superior Province, and the ubiquitous metamorphosed nature of terranes hosting lode-gold deposits, Polat and Kerrich (1997) suggested that the terranes are high-*T*, low-*P* type subduction accretion complex's, where subduction–accretion, metamorphism, magmatism, and gold mineralization are closely associated in space and time.

Internal orogens, such as the Proterozoic Trans Hudson, Appalachian, and Alpine orogenic belts do not feature large lode gold provinces (with the ex-

ception of the Homestake Mine, SD), but rather small deposits, albeit with structural, mineralogical, and geochemical similarities to giant Archean and Phanerozoic counterparts and similar post-peak metamorphic temporal relations; shoshonitic lamprophyres are sparse. These relationships may stem from the presence of deep plumbing systems that develop in the terrane boundaries of transpressive external orogens, in contrast to smaller, shallower, and less connected structural networks in internal orogens.

### Acknowledgements

The authors accept responsibility for any errors of fact, or misrepresentation in this paper. It is a pleasure to acknowledge the critical judgement of this overview by K.F. Cassidy, whose insightful suggestions here have greatly improved the text. S. Hagemann graciously supplied unpublished fluid inclusion and stable isotope data on subgreenschist facies and amphibolite–granulite facies deposits, without which this synthesis would have been incomplete. We are indebted to B. Jansen for reviewing an early draft of the manuscript, and two journal reviewers, Jonathon G. Price and Stephen Peters, whose critiques greatly improved the final version. We thank J. Fan, Y. Jia and A. Polat for assistance with computer drafting and word processing. T.C. McCuaig acknowledges receipt of NSERC and University of Saskatchewan postgraduate scholarships. R. Kerrich acknowledges the George McLeod endowment to the Department of Geological Sciences, University of Saskatchewan.

### References

- Abraham, A.P.G., Spooner, E.T.C., 1995. Late Archean regional deformation and structural controls on gold–quartz vein mineralization in the northwestern Slave Province, N.W.T. Can. J. Earth Sci. 8, 1132–1154.
- Andrews, A.J., Hugon, H., Durocher, M., Corfu, F., Lavigne, M.J., 1986. the anatomy of a gold bearing greenstone belt: Red Lake, Northwestern Ontario, Canada. In: MacDonald, A.J. (Ed.), Gold '86, An International Symposium on the Geology of Gold. Toronto, pp. 3–22.

- Bain, G.W., 1933. Wall rock mineralization along Ontario gold deposits. *Econ. Geol.* 28, 705–745.
- Barley, M.E., Groves, D.I., 1992. Supercontinental cycles and the distribution of metal deposits through time. *Geology* 20, 291–294.
- Barnes, I., 1970. Metamorphic waters from the Pacific tectonic belt of the west coast of the United States. *Science* 168, 973–975.
- Barnicoat, A.C., Fare, R.J., Groves, D.I., McNaughton, N.J., 1991. Synmetamorphic lode-gold deposits in high-grade Archean settings. *Geology* 19, 921–924.
- Bau, M., 1991. Rare-earth mobility during hydrothermal and metamorphic fluid–rock interaction and the significance of the oxidation state of europium. *Chem. Geol.* 93, 219–230.
- Bebout, G.E., 1996. Volatile transfer and recycling at convergent margins: Mass-balance and insights from high  $P/T$  metamorphic rocks. In: Bebout, G.E., Scholl, D.W., Kirby, S.H., Platt, J.P. (Eds.), *Subduction Top to Bottom*. Geophys. Monograph 9b, 179–193.
- Bell, K., Anglin, C.D., Franklin, J.M., 1989. Sm–Nd and Rb–Sr systematics of scheelites: possible implications for the age and genesis of vein hosted gold deposits. *Geology* 17, 500–504.
- Berger, B.R., Bagby, W.C., 1991. The geology and origin of Carlin-type gold deposits. In: Foster, R.P. (Ed.), *Gold Metallogeny and Exploration*. Blackie, pp. 210–248.
- Berman, R.G., 1988. Internally consistent thermodynamic data for minerals in the system  $\text{Na}_2\text{O}-\text{K}_2\text{O}-\text{CaO}-\text{MgO}-\text{FeO}-\text{Fe}_2\text{O}_3-\text{Al}_2\text{O}_3-\text{SiO}_2\text{TiO}_2-\text{H}_2\text{O}-\text{CO}_2$ . *J. Petrol.* 29, 445–522.
- Böhlke, J.K., 1989. Comparison of metasomatic reactions between a common  $\text{CO}_2$ -rich vein fluid and diverse wall rocks: intensive variables, mass transfers, and Au mineralization at Alleghany, California. *Econ. Geol.* 84, 291–327.
- Böhlke, J.K., Irwin, J.J., 1990. Noble gases and halides in gold quartz veins as indicators of fluid sources, salinity sources, mixing, and unmixing. In: Robert, F., Sheahan, P.A., Green, S.B. (Eds.), *Greenstone Gold and Crustal Evolution*. NUNA Conference Volume: 134.
- Böhlke, J.K., Irwin, J.J., 1992. Laser microprobe analysis of Cl, Br, I and K in fluid inclusions: implications for sources of salinity in some ancient hydrothermal fluids. *Geochim. Cosmochim. Acta* 56, 203–226.
- Böhlke, J.K., Kistler, R.W., 1986. Rb–Sr, K–Ar and stable isotope evidence for the ages and sources of fluid components of gold bearing quartz veins in the northern Sierra Nevada Foothills Metamorphic Belt, California. *Econ. Geol.* 81, 296–322.
- Bonham Jr., H.F., 1989. Bulk mineable gold deposits of the Western United States. In: Keays, R.R., Ramsay, W.R.H., Groves, D.I. (Eds.), *The Geology of Gold Deposits: The Perspective in 1988*. Econ. Geol. Monogr. 6, 193–207.
- Bouillier, A.-M., Robert, F., 1992. Palaeoseismic events recorded in Abitibi gold–quartz vein networks, Val d'Or, Abitibi, Quebec, Canada. *J. Struct. Geol.*, 161–179.
- Bowers, T.S., 1991. The deposition of gold and other metals; pressure-induced fluid immiscibility and associated stable isotope signatures. *Geochim. Cosmochim. Acta* 55, 2417–2434.
- Boyle, R.W., 1961. The geology, geochemistry and origin of the gold deposits of the Yellowknife District. *Geol. Surv. Can. Mem.* 310, 193 p.
- Boyle, R.W., 1979. The geochemistry of gold and its deposits. *Geol. Surv. Bull. Can.* 280, 584.
- Brown, P.E., 1993. Ore fluids and Archean lode-gold – fluid inclusion evidence. *Geol. Soc. Am. Abstr. Prog.* 25, A-111.
- Browning, P., Groves, D.I., Blockley, J.G., Rosman, K.J.R., 1987. Lead isotope constraints on the age and source of gold mineralization in the Archean Yilgarn Block, Western Australia. *Econ. Geol.* 82, 971–986.
- Burrows, D.R., Wood, P.C., Spooner, E.T.C., 1986. Carbon isotope evidence for a magmatic origin for Archean gold–quartz vein ore deposits. *Nature* 321, 851–854.
- Caddey, S.W., Bachman, R.L., Campbell, T.J., Reid, Rolland, R.R., Roben, P.O., 1991. The Homestake gold mine, an early Proterozoic iron-formation hosted gold deposit, Lawrence County, South Dakota. *U.S. Geol. Surv. Bull.* 1857–J, 67.
- Cameron, E.M., 1988. Archean gold: Relation to granulite formation and redox zoning in the crust. *Geology* 16, 109–112.
- Cameron, E.M., Hattori, K., 1987. Archean gold mineralization and oxidized hydrothermal fluids. *Econ. Geol.* 82, 1177–1191.
- Campbell, I.H., Hill, R.I., 1988. A two-stage model for the formation of the granite–greenstone terrains of the Kalgoorlie–Norseman area, Western Australia. *Earth Planet. Sci. Lett.* 90, 11–25.
- Campbell, I.H., Lesher, C.M., Coad, P., Franklin, J.M., Gorton, M.P., Thurston, P.C., 1984. Rare-earth element mobility in alteration pipes below massive Cu–Zn sulphide deposits. *Chem. Geol.* 45, 181–202.
- Cassidy, K.F., Bennett, J.M., 1993. Gold mineralisation at the Lady Bountiful mine, Western Australia: an example of a granitoid hosted Archean lode gold deposit. *Min. Deposita* 28, 388–408.
- Cassidy, K.F., 1992. Archean granitoid-hosted gold deposits in greenschist to amphibolite facies terrains: a high  $P-T$  to low  $P-T$  depositional continuum equivalent to greenstone-hosted deposits. Ph.D. thesis, The University of Western Australia, Nedlands (unpublished), 296 pp.
- Cathelineau, M., Boiron, M.-C., Holliger, P., Marion, Denis, M., 1989. Gold in arsenopyrites: crystal chemistry, location and state, physical and chemical conditions of deposition. In: Keays, R.R., Ramsay, W.R.H., Groves, D.I. (Eds.), *The Geology of Gold Deposits: The Perspective in 1988*. Econ. Geol. Mono. 6, 328–341.
- Cathles, L.M., 1986. The geologic solubility of gold from 200–350 °C, and its implications for gold-base metal ratios in vein and stratiform deposits. In: Clark, L.A. (Ed.), *Gold in the Western Shield*. Canadian Inst. Min. Metall. Spec. Vol. No. 38, pp. 187–210.
- Claoué-Long, J.C., King, R.W., Kerrich, R.W., 1990. Archean hydrothermal zircons in the Abitibi greenstone belt: Constraints on the timing of gold mineralization. *Earth Planet. Sci. Lett.* 198, 109–128.
- Clark, M.E., Archibald, N.I., Hodgson, C.J., 1986. Structural and metamorphic setting of the Victory gold mine, Kambalda, Western Australia. In: MacDonald, A.J. (Ed.), *Proceedings of*

- Gold '86, An International Symposium on the Geology of Gold. Toronto, pp. 243–254.
- Clark, M.E., Carmichael, D.M., Hodgson, C.J., Fu, M., 1989. Wall-rock alteration, Victory gold mine, Kambalda, Western Australia: processes and  $P-T-X_{CO_2}$  conditions of magmatism. In: Keays, R.R., Ramsay, W.R.H., Groves, D.I. (Eds.), *The Geology of Gold Deposits: the Perspective in 1988*. Econ. Geol. Monogr. 6, 445–459.
- Colvine, A.C., 1989. An empirical model for the formation of Archean gold deposits: products of final cratonization of the Superior Province, Canada. In: Keays, R.R., Ramsay, W.R.J., Groves, D.I. (Eds.), *The Geology of Gold Deposits: the Perspective in 1988*. Econ. Geol. Monogr. 6, 37–53.
- Colvine, A.C., Fyon, J.A., Heather, K.B., Marmont, S., Smith, P.M., Troop, D.G., 1988. Archean Lode Gold Deposits in Ontario. Ont. Geol. Surv. Misc. Paper 139, 136 p.
- Connolly, J.A.D., 1997. Devolatilization-generated fluid pressure and deformation-propagated fluid flow during prograde regional metamorphism. *J. Geophys. Res.* 102, 149–173.
- Corfu, F., 1993. The evolution of the southern Abitibi greenstone belt in light of precise U-Pb geochronology. *Econ. Geol.* 88, 1323–1340.
- Corfu, F., Andrews, A.J., 1987. Geochronological constraints on the timing of magmatism, deformation, and gold mineralization in the Red Lake greenstone belt, northwestern Ontario. *Can. J. Earth Sci.* 24, 1302–1320.
- Couture, J.F., Pilote, P., Machado, N., Desrochers, J.P., 1994. Timing of gold mineralization in the Val-d'Or District, southern Abitibi Belt; evidence for two distinct mineralizing events. *Econ. Geol.* 89, 1542–1551.
- Cox, S.F., Etheridge, M.A., Wall, V.J., 1990. Fluid pressure regimes and fluid dynamics during deformation of low-grade metamorphic terranes: implications for the genesis of mesothermal gold deposits. In: Robert, F., Sheahan, P.A., Green, S.B. (Eds.), *Greenstone Gold and Crustal Evolution*. NUNA Conference Volume, pp. 46–53.
- Cox, S.F., Wall, V.I., Etheridge, M.A., Potter, T.F., 1991. Deformational and metamorphic processes in the formation of mesothermal vein-hosted gold deposits—examples from the Lachlan Fold Belt in central Victoria. *Ore Geol. Rev.* 6, 391–423.
- Craw, D., Koons, P.O., 1989. Tectonically-induced hydrothermal activity and gold mineralization adjacent to major fault zones. In: Keays, R.R., Ramsay, W.R.H., Groves, D.I. (Eds.), *The Geology of Gold Deposits: the Perspective in 1988*. Econ. Geol. Monogr. 6, 463–470.
- Crawford, M.L., 1992. Fluid inclusions—what can we learn?. *Earth-Sci. Rev.* 32, 137–139.
- Curti, E., 1987. Lead and oxygen isotope evidence for the origin of the Monte Rosa gold lode deposits (Western Alps, Italy): a comparison with Archean lode deposits. *Econ. Geol.* 87, 7115–7140.
- Davies, I.F., Whitehead, R.E.S., Cameron, R.A., Duff, D., 1982. Regional and local patterns of  $CO_2-K-Rb-As$  alteration: A guide to gold in the Timmins area. In: Hodder, R.W., Petruk, W. (Eds.), *Geology of Canadian Gold Deposits*. Can. Inst. Min. Metall., Spec. Vol. 24, 130–143.
- de Ronde, C.E.J., Spooner, E.T.C., de Wit, M.J., Bray, C.J., 1992. Shear zone-related, Au quartz vein deposits in the Barberton greenstone belt, South Africa: field and petrographic characteristics, fluid properties, and light stable isotope geochemistry. *Econ. Geol.* 87, 366–402.
- Diamond, L., 1990. Fluid inclusion evidence for  $P-V-T-X$  evolution of hydrothermal solutions in Late-Alpine gold-quartz veins at Brusson, Val-D'Ayas, Northwest Italian Alps. *Am. J. Sci.* 290, 912–958.
- Doe, B.R., Zartman, R.E., 1979. Plumbotectonics: 1. the Phanerozoic. In: Barnes, H.L. (Ed.), *Geochemistry of Hydrothermal Ore Deposits*, 2nd edn. Holt, Reinhart and Winston, New York, pp. 450–479.
- Drew, L.J., Berger, B.R., Kurbanov, N.K., 1996. Geology and structural evolution of the Muruntau gold deposit, Kyzylkum Desert, Uzbekistan. *Ore Geol. Rev.* 11, 175–196.
- Drummond, S.E., Ohmoto, H., 1985. Chemical evolution and mineral deposition in boiling hydrothermal systems. *Econ. Geol.* 80, 126–147.
- Drury, M.R., Urai, J.L., 1990. Deformation-related recrystallization processes. *Tectonophysics* 172, 235–253.
- Eisenlohr, B.N., Groves, D.I., Partington, G.A., 1989. Crustal-scale shear zones and their significance to Archean gold mineralization in Western Australia. *Mineral. Deposita* 24, 1–8.
- Elder, D., Cashman, S.M., 1992. Tectonic control and fluid evolution in the Quartz Hill, California, lode gold deposits. *Econ. Geol.* 87, 1795–1812.
- Eliopoulos, D.G., 1982. Geochemistry and origin of the Du-magami pyritic gold deposit, Bousquet Township, Quebec. M.Sc. Thesis, University of Western Ontario, unpubl.
- England, P.C., Richardson, S.W., 1977. The influence of erosion upon the mineral facies of rocks from different metamorphic environments. *J. Geol. Soc. London* 134, 201–213.
- England, P.C., Thompson, A.B., 1984. Pressure-temperature-time path of regional metamorphism: I. Heat transfer during the evolution of regions of thickened continental crust. *J. Petrol.* 25, 894–928.
- Farmer, G.L., DePaolo, D.J., 1997. Source of hydrothermal compositions: Heavy isotopes. In: Barnes, H.L. (Ed.), *Geochemistry of Hydrothermal Ore Deposits*, 3rd edn. Wiley, New York, pp. 31–62.
- Faure, G., 1986. *Principles of Isotope Geology*, 2nd edn. Wiley, New York, 589 p.
- Fayek, M., Kyser, T.K., 1995. Characteristics of auriferous and barren fluids associated with the Proterozoic Contact Lake lode gold deposit, Saskatchewan, Canada. *Econ. Geol.* 90, 385–406.
- Fedorowich, J., Stauffer, M., Kerrich, R., 1991. Structural setting and fluid characteristics of the Proterozoic Tartan Lake gold deposit, Trans-Hudson orogen, northern Manitoba. *Econ. Geol.* 86, 1434–1467.
- Fleet, M.E., Seller, M.H., Pan, Y., 1997. Rare earth elements, protoliths, and alteration at the Hemlo gold deposits, Ontario, Canada, and comparison with argillic and sericitic alteration in the Highland Valley Porphyry District, British Columbia, Canada. *Econ. Geol.* 92, 551–568.
- Ford, R.C., Duke, N.A., 1993. Concentration of gold during retrograde metamorphism of Archean banded iron formations, Slave Province, Canada. *Can. J. Earth Sci.* 30, 1566–1581.

- Ford, R.C., Snee, L.W., 1996.  $^{40}\text{Ar}/^{39}\text{Ar}$  thermochronology of white mica from the Nome District, Alaska; the first ages of lode sources to placer gold deposits in the Seward Peninsula. *Econ. Geol.* 91, 213–220.
- Foster, R.P., Piper, D.P., 1993. Archaean lode gold deposits in Africa: crustal setting, metallogenesis and cratonization. *Ore Geol. Rev.* 8, 303–347.
- Franklin, J.M., Roscoe, S.M., Loveridge, W.D., Sangster, D.F., 1983. Lead isotope studies in Superior and Southern Provinces. *Geol. Surv. Can. Bull.* 351, 60.
- Fryer, B.J., Kerrich, R., Hutchinson, R.W., Peirce, M.G., Rogers, D.S., 1979. Archean precious metal hydrothermal systems, Dome mine, Abitibi greenstone belt: I. Patterns of alteration and metal distribution. *Can. J. Earth Sci.* 16, 421–439.
- Fyfe, W.S., Kerrich, R., 1984. Gold: natural concentration processes. In: Foster, R.P. (Ed.), *Gold '82*. Geol. Soc. Zimbabwe, Spec. Publ. 1, 99–127.
- Fyfe, W.S., Price, N.J., Thompson, A.B., 1978. Fluids in the Earth's Crust. Elsevier, Amsterdam, 383 p.
- Fyon, J.A., Crocket, J.H., Schwarcz, H.P., 1984. The Carshaw and Malga iron-formation-hosted gold deposits of the Timmins area. In: Colvine, A.C. (Ed.), *The Geology of Gold in Ontario*. Ont. Geol. Surv. Misc. Paper 110, 98–110.
- Gebre-Mariam, M., Groves, D.I., Ho, S.E., McNaughton, N.J., Vearncombe, J.R., 1991. The Archaean lode-gold deposit at Racetrack, near Kalgoorlie, Western Australia: a transitional mesothermal–epithermal hydrothermal system. In: Pagel, M., Leroy, J.L. (Eds.), *Source, Transport and Deposition of Metals*. Balkema, Rotterdam, pp. 661–664.
- Gebre-Mariam, M., Groves, D.I., McNaughton, N.J., Mikucki, E.J., 1993. Multiple fluid sources and depositional mechanisms at the Archean mesozonal–epizonal Golden-Kilometre gold mine, Western Australia. In: Hach-Ali, F., Torres-Ruiz, J., Gerville, F. (Eds.), *Current Research in Geology Applied to Ore Deposits*, pp. 453–456.
- Goldfarb, R., Leach, D.L., Miller, M.L., Pickthorn, W.J., 1986. Geology, metamorphic setting and genetic constraints of epigenetic lode-gold mineralization within the Cretaceous Valdez Group, south-central Alaska. In: Keppie, J.D., Boyle, R.W., Hanes, S.J. (Eds.), *Turbidite-hosted Gold Deposits*. Geol. Assoc. Can. Spec. Pap. 32, 87–105.
- Goldfarb, R.J., Leach, D.L., Pickthorn, W.J., Paterson, C.J., 1988. Origin of lode gold deposits of the Juneau gold belt, southeastern Alaska. *Geology* 16, 440–443.
- Goldfarb, R.J., Leach, D.L., Rose, S.C., Landis, G.P., 1989. Fluid inclusion geochemistry of gold-bearing quartz veins of the Juneau Gold belt, southeastern Alaska: implications for ore genesis. In: Keays, R.R., Ramsay, W.R.H., Groves, D.I. (Eds.), *The Geology of Gold Deposits: The Perspective in 1988*. Econ. Geol. Monogr. 6, 363–375.
- Goldfarb, R.J., Gray, J.E., Pickthorn, W.J., Gent, C.A., Cieutat, B.A., 1990. Stable isotope systematics of epithermal mercury–antimony mineralization, southwestern Alaska. In: Goldfarb, R.J., Nash, J.T., Stoeser, J.W. (Eds.), *Geochemical studies in Alaska by the U.S. Geological Survey, 1989*. U.S. Geol. Surv. Bull., E1–E9.
- Goldfarb, R.J., Snee, L.W., Miller, L.D., Newberry, R.J., 1991a. Rapid dewatering of the crust deduced from ages of mesothermal gold deposits. *Nature* 354, 296–298.
- Goldfarb, R.J., Newberry, R.J., Pickthorn, W.J., Gent, C.A., 1991b. Oxygen, hydrogen, and sulphur isotope studies in the Juneau gold belt, southeastern Alaska: constraints on the origin of hydrothermal fluids. *Econ. Geol.* 86, 66–80.
- Goldfarb, R.J., Snee, L.W., Pickthorn, W.J., 1993. Orogenesis, high-T thermal events, and gold vein formation within metamorphic rocks of the Alaskan Cordillera. *Min. Mag.* 57, 375–394.
- Goldfarb, R.J., Miller, L.D., Leach, D.L., Snee, L.W., 1997. Gold deposits in metamorphic rocks of Alaska. *Mineral Deposits of Alaska*. Econ. Geol. Monogr. 9, 151–190.
- Golding, S.D., Wilson, A.F., 1982. Geochemical and stable isotope studies of the Crown and Mararoa Reefs, Norseman, Western Australia. *Rev. Bras. Geosci.* 12, 445–456.
- Golding, S.D., McNaughton, N.J., Barley, M.E., Groves, D.I., Ho, S.E., Rock, N.M.S., Turner, J.V., 1989. Archean carbon and oxygen reservoirs: their significance for fluid sources and circulation paths for Archean mesothermal gold deposits of the Norseman–Wiluna belt, Western Australia. In: Keays, R.R., Ramsay, W.R.H., Groves, D.I. (Eds.), *The Geology of Gold Deposits: The Perspective in 1988*. Econ. Geol. Monogr. 6, 376–388.
- Golding, S.D., Clark, M.E., Keele, R.A., Wilson, A.F., Keays, R.R., 1990. Geochemistry of Archean epigenetic gold deposits in the Eastern Goldfields Province, Western Australia. *Geol. Depart. Univ. Extension, Univ. West. Aust. Publ.* 23, pp. 141–176.
- Groves, D.I., 1993. The crustal continuum model for late Archean lode gold deposits of the Yilgarn Block, Western Australia. *Mineral. Deposita* 28, 366–374.
- Groves, D.I., Foster, R.P., 1991. Archaean lode gold deposits. In: Foster, R.P. (Ed.), *Gold Metallogeny and Exploration*. Blackie, 63–103.
- Groves, D.I., Phillips, G.N., 1987. The genesis and tectonic controls on Archaean lode gold deposits of the Western Australian shield: a metamorphic-replacement model. *Ore Geol. Rev.* 2, 287–322.
- Groves, D.I., Barley, M.E., Ho, S.E., 1989. Nature, genesis, and tectonic setting of mesothermal gold mineralization in the Yilgarn Block, Western Australia. In: Keays, R.R., Ramsay, W.R.H., Groves, D.I. (Eds.), *The Geology of Gold Deposits: The Perspective in 1988*. Econ. Geol. Monogr. 6, 71–85.
- Groves, D.I., Barley, M.E., Barnicoat, A.C., Cassidy, K.F., Fare, R.J., Hagemann, S.G., Ho, S.E., Hronsky, J.M.A., Mikucki, E.J., Mueller, A.G., McNaughton, N.J., Perring, C.S., Ridley, J.R., Vearncombe, J.R., 1992. Sub-greenschist- to granulite-hosted Archaean lode gold deposits of the Yilgarn Craton: a depositional continuum from deep-sourced hydrothermal fluids in crustal-scale plumbing systems. In: Glover, J.E., Ho, S.E. (Eds.), *The Archaean: Terrains Processes and Metallogeny*. Geol. Dep. Univ. Extension, Univ. West. Aust. Publ. No. 22, pp. 325–337.
- Groves, D.I., Ridley, J.R., Bloem, E.M.J., Gebre-Mariam, M., Hagemann, S.G., Hronsky, J.M.A., Knight, J.T., McNaughton, N.J., Ojala, J., Viebrecher, R.M., McCuaig, T.C., Holyland,

- P.W., 1995. Lode gold deposits of the Yilgarn Block: products of late-Archean crustal-scale overpressured hydrothermal systems. In: Coward, M.P., Ries, A.C. (Eds.), Early Precambrian Processes. Geol. Soc. London Spec. Publ. 95, 155–172.
- Groves, D.I., Goldfarb, R.J., Gebre-Marian, M., Hagemann, S.G., Robert, F., 1998. Orogenic gold deposits: A proposed classification in the context of their crustal distribution and relationship to other gold deposit types. Miner. Deposita, in press.
- Guha, J., Kanwar, R., 1987. Vug brines—fluid inclusions: A key to understanding of secondary gold enrichment processes and the evolution of deep brines in the Canadian Shield. In: Fritz, P., Frantz, S.K. (Eds.), Saline water and gases in the crystalline rocks. Geol. Assoc. Can. Spec. Pap. 33, 95–101.
- Guha, J., Lu, H.Z., Dubé, B., 1991. Fluid characteristics of vein and altered wall rock in Archean mesothermal gold deposits. Econ. Geol. 86, 667–684.
- Hagemann, S.G., Ridley, J.R., 1993a. Meriwa-report on fluid inclusion analyses in the Griffins Find, Marvel Loch (Savage lode) and Three Mile Hill gold deposits. In: Ridley, J.R., Groves, D.I. (Eds.) Meriwa Project M 154: Exploration and Deposit Models for Gold Deposits in Amphibolite–Granulite Facies Terrains, Western Australia, in press.
- Hagemann, S.G., Ridley, J.R., 1993b. Hydrothermal fluids in epizone and katabatic crustal levels in the Archean: implications for  $P-T-X-t$  evolution of lode-gold mineralisation. In: Williams, P.R., Haldane, J.A. (compilers), Kalgoorlie '93: an international conference on crustal evolution, metallogenesis and exploration of the Eastern Goldfields. Aust. Geol. Surv. Organ., Record 1993/54: pp. 123–130.
- Hagemann, S.G., Groves, D.I., Ridley, J.R., 1993. The Wiluna lode-gold deposits, Western Australia: an example of a high crustal-level Archean lode-gold system. In: Hach-Ali, F., Torres-Ruiz, J., Gervilla, F. (Eds.), Current Research in Geology Applied to Ore Deposits, pp. 469–472.
- Hagemann, S.G., Gebre, M.M., Groves, D.I., 1994. Surface-water influx in shallow-level Archean lode-gold deposits in Western Australia. Geology 22, 1067–1070.
- Hall, C.M., Higueras, P.L., Kesler, S.E., Lunar, R., Dong, H., Halliday, A.N., 1997. Dating of alteration episodes related to mercury mineralization in the Almaden District, Spain. Earth Planet. Sci. Lett. 148, 287–298.
- Hamilton, J.V., Hodgson, C.J., 1986. Mineralization and structure of the Kolar gold field, India. In: MacDonald, A.J. (Ed.), Proceedings of Gold '86, An International Symposium on the Geology of Gold, Toronto 1986, pp. 270–283.
- Hanes, J.A., Archibald, D.A., Hodgson, C.J., Robert, F., 1992. Dating of Archean auriferous quartz vein deposits in the Abitibi greenstone belt, Canada.  $^{40}\text{Ar}/^{39}\text{Ar}$  evidence for a 70- to 100-m.y. time gap between plutonism–metamorphism and mineralization. Econ. Geol. 87, 1849–1861.
- Hanes, J.A., Archibald, D.A., Queen, M., Farrar, E., 1994. Constraints from (super 40) Ar/(super 39) Ar geochronology on the tectonothermal history of the Kapuskasing Uplift in the Canadian Superior Province. Can. J. Earth Sci. 31, 1146–1171.
- Hanson, R.B., 1997. Hydrodynamics of regional metamorphism due to continental collision. Econ. Geol. 92, 880–891.
- Hayashi, K.-I., Ohmoto, H., 1991. Solubility of gold in NaCl- and  $\text{H}_2\text{S}$ -bearing aqueous solutions at 250–350°C. Geochim. Cosmochim. Acta 55, 2111–2126.
- Henley, R.W., 1991. Epithermal gold deposits in volcanic terranes. In: Foster, R.P. (Ed.), Gold Metallogeny and Exploration. Blackie, pp. 133–164.
- Hill, R.I., Campbell, I.H., Chappell, B.W., 1992. Crustal growth, crustal reworking, and granite genesis in the southeastern Yilgarn Block, Western Australia. Geol. Dep. Univ. Extension, Univ. Western Australia Publ. 22, pp. 203–212.
- Ho, S.E., Bennett, J.M., Cassidy, K.F., Hronsky, J.M.A., Mikucki, E.J., Sang, J.H., 1990. Fluid inclusion studies. In: Ho, S.E., Groves, D.I., Bennett, J.M. (Eds.), Gold deposits of the Archean Yilgarn Block, Western Australia: Nature, Genesis and Exploration Guides. Geol. Dep. Univ. Extension, Univ. Western Australia Publ. 20, pp. 198–211.
- Ho, S.E., Groves, D.I., BeMett, J.M. (Eds.), 1990b. Gold deposits of the Archean Yilgarn Block, Western Australia: Nature, Genesis and Exploration Guides. Geol. Dep. Univ. Extension, Univ. Western Australia Publ. 20, 407 p.
- Ho, S.E., Groves, D.I., McNaughton, N.J., Mikucki, E.J., 1992. The source of ore fluids and solutes in Archean lode gold deposits of Western Australia. J. Volcanol. Geotherm. Res. 50, 173–196.
- Hodgson, C.J., 1982. A review of the geological characteristics of 'gold only' deposits in the Superior Province of the Canadian Shield. Geology of Canadian Gold Deposits. Can. Inst. Min. Metall. Spec. Vol. 24, 211–229.
- Hodgson, C.J., 1989. The structure of shear-related, vein type gold deposits: a review. Ore Geol. Rev. 4, 231–273.
- Hodgson, C.J., 1993. Mesothermal lode-gold deposits. In: Kirkham, R.V., Sinclair, W.D., Thorpe, R.I., Duke, J.M. (Eds.), Mineral Deposit Modelling. Geol. Assoc. Can. Spec. Pap. 40, 635–678.
- Hoefs, J., 1987. Stable Isotope Geochemistry, 3rd edn. Springer-Verlag, Berlin, 241 pp.
- Holland, T.J.B., Powell, R., 1990. An enlarged and updated internally consistent dataset with uncertainties and correlations: the system  $\text{K}_2\text{O}-\text{Na}_2\text{O}-\text{CaO}-\text{MgO}-\text{FeO}-\text{Fe}_2\text{O}_3-\text{Al}_2\text{O}_3-\text{TiO}_2-\text{SiO}_2-\text{C}-\text{H}_2-\text{O}_2$ . J. Meta. Geol. 8, 89–124.
- Hronsky, J.M.A., Cassidy, K.F., Grigson, M.W., Groves, D.I., Hagemann, S.G., Mueller, A.G., Ridley, J.R., Skwarnecki, M.S., Vearncombe, J.R., 1990. Deposit- and mine-scale structure. In: Ho, S.E., Groves, D.I., Bennett, J.M. (Eds.), Gold deposits of the Archean Yilgarn Block, Western Australia: Nature, Genesis and Exploration Guides. Geol. Dep. Univ. Extension, Univ. Western Australia Publ. 20, pp. 38–59.
- Hronsky, J.M.A., Ridley, J.R., 1992. The relationship between structure, fluid flow patterns and ore shoots in a mesothermal shear zone hosted gold deposit. 11th Aust. Geol. Conv. Abstr., 74–75.
- Humphries, S.E., 1984. The mobility of the rare earth elements in the crust. In: Henderson, P. (Ed.), Rare Earth Element Geochemistry. Elsevier, Amsterdam, pp. 317–342.
- Hurst, M.E., 1935. Vein formation at Porcupine, Ontario. Econ. Geol. 30, 103–127.

- Jackson, S.L., Cruden, A.R., White, D., Milkereit, B., 1995. A seismic-reflection-based regional cross section of the southern Abitibi greenstone belt. *Can. J. Earth Sci.* 32, 135–148.
- Jean, G.E., Bancroft, G.M., 1985. An XPS and SEM study of gold deposition at low temperature on sulphide mineral surfaces: concentration of gold by adsorption/reduction. *Geochim. Cosmochim. Acta* 49, 979–987.
- Jemielita, R.A., Davis, D.W., Krogh, T.K., 1990. U–Pb evidence for Abitibi gold mineralization postdating greenstone magmatism and metamorphism. *Nature* 346, 831–834.
- Johnson, E.L., 1991. Experimentally determined limits for H<sub>2</sub>O–CO<sub>2</sub>–NaCl immiscibility in granulites. *Geology* 19, 925–928.
- Kaminiemi, D.C., Stone, D., Peterman, Z.E., 1990. Early Proterozoic deformation in the Western Superior Province, Canadian Shield. *Geol. Soc. Am. Bull.* 102, 1623–1634.
- Kent, A.J.R., McCuaig, T.C., 1997. Disturbed <sup>40</sup>Ar–<sup>39</sup>Ar systematics in hydrothermal biotite and hornblende at the Scotia gold mine, Western Australia: evidence for argon loss associated with post-mineralisation fluid movement. *Geochim. Cosmochim. Acta* 61, 4655–4669.
- Kent, A.J.R., McDougall, I., 1995. <sup>40</sup>Ar–<sup>39</sup>Ar and U–Pb age constraints on the timing of gold mineralization in the Kalgoorlie gold field, Western Australia. *Econ. Geol.* 90, 845–859.
- Kent, A.J.R., Cassidy, K.F., Fanning, C.M., 1996. Archean gold mineralization synchronous with the final stages of cratonization, Yilgarn Craton, Western Australia. *Geology* 24, 879–882.
- Kerrich, R., 1983. Geochemistry of gold deposits in the Abitibi greenstone belt. *Can. Inst. Min. Metall., Spec. Paper* 27, 75 p.
- Kerrich, R., 1986. Fluid infiltration into fault zones: chemical, isotopic and mechanical effects. *J. Pure Appl. Geophys.* 124, 225–268.
- Kerrich, R., 1987. The stable isotope geochemistry of Au–Ag vein deposits in metamorphic rocks. In: Kyser, T.K. (Ed.), *Min. Assoc. Can. Short Course* 13, pp. 287–336.
- Kerrich, R., 1989a. Geodynamic setting and hydraulic regimes: Shear zone hosted mesothermal gold deposits. In: Bursnall, J.T. (Ed.), *Mineralization and Shear Zones*. *Geol. Assoc. Can. Short Course Notes* 6, pp. 89–128.
- Kerrich, R., 1989b. Geochemical evidence on the sources of fluids and solutes for shear zone hosted mesothermal Au deposits. In: Bursnall, J.T. (Ed.), *Mineralization and Shear Zones*. *Geol. Assoc. Can. Short Course Notes* 6, pp. 129–197.
- Kerrich, R., 1989c. Source processes for Archean Au–Ag vein deposits: evidence for lithophile-element systematics of the Hollinger–McIntyre and Buffalo Ankerite deposits, Timmins. *Can. J. Earth Sci.* 26, 755–781.
- Kerrich, R., 1990a. Mesothermal gold deposits: A critique of genetic hypothesis. In: Robert, F., Sheahan, P.A., Green, S.B. (Eds.), *Greenstone Gold and Crustal Evolution*. NUNA Conference Volume, pp. 13–31.
- Kerrich, R., 1990b. Carbon isotope systematics of Archean Au–Ag vein deposits in the Superior Province. *Can. J. Earth Sci.* 27, 40–56.
- Kerrich, R., 1991. Radiogenic isotope systems applied to mineral deposits. In: Heaman, L., Ludden, J.N. (Eds.), *Application of Radiogenic Isotope Systems to Problems in Geology*. *Min. Assoc. Can. Short Course* 19, pp. 365–421.
- Kerrich, R., 1993. Perspectives on genetic models for lode gold deposits. *Miner. Deposita* 28, 362–365.
- Kerrich, R., Allison, I., 1978. Flow mechanisms in rocks: microscopic and mesoscopic structures, and their relation to physical conditions of deformation in the crust. *Geosci. Can.* 5, 110–118.
- Kerrich, R., Cassidy, K.F., 1994. Temporal relationships of lode gold mineralization to accretion, magmatism, metamorphism and deformation—Archean to present: a review. *Ore Geol. Rev.* 9, 263–310.
- Kerrich, R., Feng, R., 1992. Archean geodynamics and the Abitibi–Pontiac collision: implications for advection of fluids at transpressive collisional boundaries and the origin of giant quartz vein systems. *Earth-Sci. Rev.* 32, 33–60.
- Kerrich, R., Fryer, B.J., 1979. Archean precious metal hydrothermal systems. Dome Mine, Abitibi greenstone belt: II. REE and oxygen isotope relations. *Can. J. Earth Sci.* 16, 440–458.
- Kerrich, R., Fryer, B.J., 1981. The separation of rare elements from abundant base metals in Archean lode gold deposits: implications of low water/rock source regions. *Econ. Geol.* 76, 160–166.
- Kerrich, R., Fyfe, W.S., 1981. The gold–carbonate association: source of CO<sub>2</sub> and CO<sub>2</sub>-fixation reactions in Archean lode gold deposits. *Chem. Geol.* 33, 265–294.
- Kerrich, R., Fyfe, W.S., 1988a. The formation of gold deposits with particular reference to Archean greenstone belts and Yellowknife. *Contrib. Geol. Northwest Territories*, Yellowknife 3, 37–61.
- Kerrich, R., Fyfe, W.S., 1988b. Archean vein gold deposits: II. Hydrothermal systems and models of origin. *Contrib. Geol. Northwest Territories* 3, 63–95.
- Kerrich, R., King, R., 1993. Hydrothermal zircon and baddeleyite in Val d'Or Archean mesothermal gold deposits: Characteristics, compositions and fluid inclusion properties. *Can. J. Earth Sci.* 30, 2334–2351.
- Kerrich, R., Watson, R., 1984. The Macassa mine Archean lode gold deposit, Kirkland Lake, Ontario: Geology, patterns of alteration, and hydrothermal regimes. *Econ. Geol.* 79, 1104–1130.
- Kerrich, R., Wyman, D., 1990. Geodynamic setting of mesothermal gold deposits: An association with accretionary tectonic regimes. *Geology* 18, 882–885.
- Kerrich, R., Wyman, D., 1993. The mesothermal gold–lamprophyre association: significance for an accretionary geodynamic setting, supercontinental cycles, and metallogenic processes. *Mineral. Petrol.* 49, 125–178.
- Kerrich, R., Fyfe, W.S., Gomman, B.E., Allison, I., 1977. Local modification of rock chemistry by deformation. *Contrib. Mineral. Petrol.* 65, 183–190.
- Kesler, S.E., 1990. Nature and composition of mineralizing solutions. In: Robert, F., Sheahan, P.A., Green, S.B. (Eds.), *Greenstone Gold and Crustal Evolution*. NUNA Conference Volume, pp. 86–90.
- King, R.W., 1988. Geochemical characteristics of tourmaline from Superior Province Archaean lode gold deposits; implications for source regions and processes. *Geol. Soc. Aust. Abstr.* 23, 445–447.
- King, R.W., Kerrich, R., 1987. Fluorapatite fenitization and gold

- enrichment in sheeted trondjemites within the Destor-Porcupine fault zone, Taylor Township, Ontario. *Can. J. Earth Sci.* 24, 479–502.
- King, R.W., Kerrich, R., 1989a. Chromian-dravite associated with ultramafic hosted Archean lode gold deposits. *Can. Mineral.* 5, 240–252.
- King, R.W., Kerrich, R., 1989b. Strontium isotope compositions of tourmaline from lode gold deposits of the Archean Abitibi greenstone belt (Ontario–Quebec, Canada): Implications for source reservoirs. *Chem. Geol.* 79, 225–240.
- Kishida, A., Kerrich, R., 1987. Hydrothermal alteration zoning and gold concentration at the Kerr Addison Archean lode gold deposit, Kirkland Lake, Ontario. *Econ. Geol.* 82, 649–690.
- Knight, J.T., Groves, D.I., Ridley, J.R., 1993. District-scale structural and metamorphic controls on Archean lode-gold mineralization in the amphibolite facies Coolgardie Goldfield, Western Australia. *Mineral. Deposita* 28, 436–456.
- Knipe, S.W., Foster, R.P., Stanley, C.J., 1994. Role of sulphide surfaces in sorption of precious metals from hydrothermal fluids. *Inst. Min. Metall. Trans., Section B* 101, B83–B88.
- Kogiso, T., Tatsumi, Y., Nakano, S., 1997. Trace element transport during dehydration processes in the subducted oceanic crust: 1. Experiments and implications for the origin of ocean island basalts. *Earth Planet. Sci. Lett.* 148, 193–205.
- Kontak, D.J., Kerrich, R., 1997. An isotopic (C, O, Sr) study of vein gold deposits in the Meguma Terrane, Nova Scotia; implications for source reservoirs. *Econ. Geol.* 92, 161–180.
- Kontak, D.J., Smith, P.M., Kerrich, R., Williams, P.F., 1990. An integrated model for Meguma Group lode gold deposits, Nova Scotia, Canada. *Geology* 18, 238–242.
- Koons, P.O., Craw, D., 1991. Gold mineralization as a consequence of continental collision; an example from the Southern Alps, New Zealand. *Earth Planet. Sci. Lett.* 103, 1–9.
- Koons, P.O., Craw, D., Cox, S.C., Upton, P., Templeton, A.S., Chamberlain, C.P., 1998. Fluid flow during active oblique convergence: A Southern Alps model from mechanical and geochemical observations. *Geology* 26, 159–162.
- Korzhinskii, D.S., 1970. Theory of Metasomatic Zoning. Oxford Univ. Press, London, 162 p.
- Kyser, T.K., 1987. Equilibrium fractionation factors for stable isotopes. In: Kyser, T.K. (Ed.), Stable isotope geochemistry of low temperature fluids. *Min. Assoc. Can. Short Course* 13, pp. 1–84.
- Kyser, T.K., Kerrich, R., 1990. Geochemistry of fluids in tectonically active crustal regions. In: Nesbitt, B.E. (Ed.), Fluids in Tectonically Active Regimes of the Continental Crust. *Min. Assoc. Can. Short Course* 19, pp. 133–230.
- Kyser, T.K., Kerrich, R., 1991. Retrograde exchange of hydrogen isotopes between hydrous minerals and water at low temperatures. In: Taylor, H.P., O’Neil, J.R., Kaplan, J.R. (Eds.), Stable isotope geochemistry: a tribute to Samuel Epstein. *Geochem. Soc. Spec. Publ.* 3, 409–422.
- Lambert, I.B., Phillips, G.N., Groves, D.L., 1984. Sulphur isotope compositions and genesis of Archean gold mineralization, Australia and Zimbabwe. In: Foster, R.P. (Ed.), Gold ’82. *Geol. Soc. Zimbabwe, Spec. Publ.* No. 1.
- Landefeld, L.A., 1988. The geology of the Mother Lode gold belt, Sierra Nevada, Foothills Metamorphic Belt, California. *Bicentennial Gold ’88, Extended Abstracts, Geol. Soc. Aust. Abstr.*, 22: 167–172.
- Lesher, C.M., Phillips, G.N., Groves, D.I., Campbell, I.H., 1991. Immobility of REE and most high field-strength elements and first transition series metals during Archean gold-related hydrothermal alteration of metabasalts at the Hunt mine, Western Australia. In: Ladiera, E.A. (Ed.), *Proceedings of Brazil Gold 91*. Balkema, Rotterdam, pp. 327–334.
- Letnikov, F.A., Vilor, N.V., 1990. Gold in the Hydrothermal Process. *Geol. Dep. Univ. Extension, Univ. Western Australia* Publ. 19, 110 p.
- Ludden, J., Hubert, C., Gariepy, C., 1986. The tectonic evolution of the Abitibi greenstone belt of Canada. *Geol. Mag.* 123, 153–166.
- Madu, B.E., Nesbitt, B.E., Muehlenbachs, K., 1990. A mesothermal gold-stibnite-quartz vein occurrence in the Canadian Cordillera. *Econ. Geol.* 85, 1260–1268.
- McCuaig, T.C., 1996. The genesis and evolution of lode gold mineralization and mafic host lithologies in the late-Archean Norseman Terrane, Yilgarn Block, Western Australia, Ph.D. Thesis unpublished, University of Saskatchewan, 328 pp.
- McCuaig, T.C., Kerrich, R., Groves, D.I., Archer, N., 1993. The nature and dimensions of regional and local gold-related hydrothermal alteration in tholeiitic metabasalts in the Norseman Goldfields: the missing link in a crustal continuum of gold deposits. *Mineral. Deposita* 28, 420–435.
- McKeag, S.A., Craw, D., 1989. Contrasting fluids in gold-bearing quartz vein systems formed progressively in a rising metamorphic belt; Otago Schist, New Zealand. *Econ. Geol.* 84, 22–33.
- McNaughton, N.J., Barley, M.E., Cassidy, K.F., Golding, S.D., Groves, D.I., Ho, S.E., Hronsky, J.M.A., Sang, J.H., Turner, J.V., 1990. Carbon isotope studies. In: Ho, S.E., Groves, D.I., Bennett, J.M. (Eds.), *Gold deposits of the Archean Yilgarn Block, Western Australia: Nature, Genesis and Exploration Guides*. *Geol. Dep. Univ. Extension, Univ. Western Australia* Publ. 20, pp. 246–251.
- McNaughton, N.J., Cassidy, K.F., Dahl, N., de Laeter, J.R., Golding, S.D., Groves, D.I., Ho, S.E., Mueller, A.G., Perring, C.S., Sang, J.H., Turner, J.V., 1992. The source of ore components in lode-gold deposits of the Yilgarn Block, Western Australia. In: Glover, J.E., Ho, S.E. (Eds.), *The Archean: Terrains Processes and Metallogeny*. *Geol. Dep. Univ. Extension, Univ. Western Australia* Publ. 22, pp. 351–363.
- McNaughton, N.J., Groves, D.I., Witt, W.K., 1993. The source of lead in Archean lode gold deposits of the Menzies–Kalgoorlie Kambalda region, Yilgarn Block, Western Australia. *Mineral. Deposita* 28, 495–502.
- McNeil, A.M., Kerrich, R., 1986. Archean lamprophyre dykes and gold mineralization, Matheson, Ontario: the conjunction of LILE-enriched mafic magmas, deep crustal structures and Au concentration. *Can. J. Earth Sci.* 23, 324–343.
- Michard, A., 1989. Rare earth element systematics in hydrothermal fluids. *Geochim. Cosmochim. Acta* 53, 745–750.
- Michard, A., Albarade, F., 1986. The REE content of some hydrothermal fluids. *Chem. Geol.* 55, 52–60.
- Mikucki, E.J., Groves, D.I., 1990. Gold transport and depositional

- models. In: Ho, S.E., Groves, D.I., Bennett, J.M. (Eds.), Gold deposits of the Archaean Yilgarn Block, Western Australia: Nature, Genesis and Exploration Guides. Geol. Dep. Univ. Extension, Univ. Western Australia Publ. 20, pp. 278–284.
- Mikucki, E.J., Heinrich, C.A., 1990. Vein- and mine-scale wall-rock alteration and gold mineralization in the Archaean Mount Charlotte deposit, Kalgoorlie, Western Australia. In: An International Conference on Crustal Evolution, and Exploration in the Eastern Goldfields, Extended Abstract, AGSO, Record 54, pp. 135–140.
- Mikucki, E.J., Ridley, J.R., 1993. The hydrothermal fluid of Archean lode gold deposits at different metamorphic grades: compositional constraints from ore and wall rock alteration assemblages. *Mineral. Deposita* 28, 469–481.
- Mikucki, E.J., Groves, D.I., Cassidy, K.F., 1990. Wall rock alteration in sub-amphibolite facies gold deposits. In: Ho, S.E., Groves, D.I., Bennett, J.M. (Eds.), Gold deposits of the Archaean Yilgarn Block, Western Australia: Nature, Genesis and Exploration Guides. Geol. Dep. Univ. Extension, Univ. Western Australia Publ. 20, pp. 60–78.
- Miller, L.D., Goldfarb, R.J., Gehrels, G.E., Snee, L.W., 1994. Genetic links among fluid cycling, vein formation, regional deformation, and plutonism in the Juneau gold belt, southeastern Alaska. *Geology* 22, 203–206.
- Moorbath, S., Taylor, P.N., 1981. Isotopic evidence for continental growth in the Precambrian. In: Kröner, A. (Ed.), Precambrian Plate Tectonics. Dev. in Precambrian Geology 4. Elsevier, Amsterdam, pp. 491–525.
- Morasse, S., Wasteneys, H.A., Cormier, M., Helmstaedt, H., Mason, R., 1995. A pre-2686 Ma intrusion-related gold deposit at the Kiena Mine, Val d'Or, Quebec, southern Abitibi Subprovince. *Econ. Geol.* 90, 1310–1321.
- Morrison, G.W., Rose, W.J., Jaireth, S., 1991. Geological and geochemical controls on the silver content (fineness) of gold in gold-silver deposits. *Ore Geol. Rev.* 6, 333–364.
- Muehlenbachs, K., 1986. Alteration of the oceanic crust and the  $^{18}\text{O}$  history of seawater. *Rev. Mineral.* 16, 425–444.
- Mueller, A.G., Groves, D.I., 1991. The classification of Western Australian greenstone-hosted gold deposits according to wall rock-alteration mineral assemblages. *Ore Geol. Rev.* 6, 291–331.
- Mueller, A.G., de Laeter, J.R., Groves, D.I., 1991a. Strontium isotope systematics of hydrothermal minerals from epigenetic Archean gold deposits in the Yilgarn Block, Western Australia. *Econ. Geol.* 86, 780–809.
- Mueller, A.G., Groves, D.I., Delor, C.P., 1991b. The Savage Lode magnesian skarn in the Marvel Loch gold-silver mine, Southern Cross greenstone belt, Western Australia: Part II: Pressure-temperature estimates and constraints on fluid sources. *Can. J. Earth Sci.* 28, 686–705.
- Naden, J., Shepherd, T.J., 1989. Role of methane and carbon dioxide in gold deposition. *Nature* 342, 793–795.
- Neall, F.B., Phillips, G.N., 1987. Fluid-wall rock interaction in an Archean hydrothermal gold deposit: a thermodynamic model for the Hunt mine, Kambalda. *Econ. Geol.* 82, 1679–1694.
- Nesbitt, B.E., 1988. Gold deposit continuum; a genetic model for lode Au mineralization in the continental crust. *Geology* 16, 1044–1048.
- Nesbitt, B.E., 1995. Crustal paleo-hydrogeological mapping as a tool in exploration for mineral deposits. *J. Geochem. Explor.* 54, 153–165.
- Nesbitt, B.E., Muehlenbachs, K., 1989. Origins and movement of fluids during deformation and metamorphism in the Canadian Cordillera. *Science* 245, 733–736.
- Nesbitt, B.E., Muehlenbachs, K., 1991. Melange- and sediment-hosted gold-bearing quartz veins, Hodgkinson gold field, Queensland, Australia; a discussion. *Econ. Geol.* 86, 195–197.
- Nesbitt, B.E., Murowchick, J.B., Muehlenbachs, K., 1986. Dual origin of lode deposits in the Canadian Cordillera. *Geology* 14, 506–509.
- Nesbitt, B.E., Muehlenbachs, K., Murowchick, J.B., 1989. Genetic implications of stable isotope characteristics of mesothermal Au deposits and related Sb and Hg deposits in the Canadian Cordillera. *Econ. Geol.* 84, 1489–1506.
- Neumayer, P., Cabri, L.J., Groves, D.I., Mikucki, E.J., Jackman, A.J., 1993a. The mineralogical distribution of gold and relative timing of gold mineralization in two Archean settings of high metamorphic grade in Australia. *Can. Mineral.* 31, 711–722.
- Neumayer, P., Groves, D.I., Ridley, J.R., Koning, C.D., 1993b. Syn-amphibolite-facies Archaean lode-gold mineralization in the Mt. York district, Pilbara Block, Western Australia. *Mineral. Deposita* (in press).
- O'Hanley, D.S., Kyser, T.K., Wicks, F.J., 1989. Evidence from lizardite/chrysotile serpentinites for proton exchange without recrystallization. *Geol. Soc. Am. Abstr. Prog.* 32, A13.
- O'Neil, J.R., 1986. Theoretical and experimental aspects of isotope fractionations. In: Valley, J.W., Taylor Jr., H.P., O'Neil, J.R. (Eds.), Stable Isotopes in High Temperature Geological Processes. Min. Soc. Amer., Rev. Mineral. 16, 1–40.
- Oberthür, T.U., Mumm, A.S., Vetter, U., Simon, K., Amanor, J.A., 1996. Gold mineralization in the Ashanti belt of Ghana: genetic constraints of the stable isotope geochemistry. *Econ. Geol.* 91, 289–301.
- Ohmoto, H., 1986. Stable isotope geochemistry of ore deposits. In: Valley, J.W., Taylor Jr., H.P., O'Neil, J.R. (Eds.), Stable Isotopes in High Temperature Geological Processes. Min. Soc. Amer., Rev. Mineral. 16, 491–560.
- Ohmoto, H., Goldhaber, M.B., 1997. Sulfur and carbon isotopes. In: Barnes, H.L. (Ed.), *Geochemistry of Hydrothermal Ore Deposits*. Wiley, New York, pp. 435–486.
- Ohmoto, H., Rye, R.O., 1979. Isotopes of Sulphur and Carbon. In: Barnes, H.L. (Ed.), *Geochemistry of Hydrothermal Ore Deposits*. Wiley, New York, pp. 509–567.
- Oversby, V.M., 1975. Lead isotope systematics and ages of Archean acid intrusives in the Kalgoorlie-Norseman area, Western Australia. *Geochim. Cosmochim. Acta* 39, 1107–1125.
- Pan, Y., Fleet, M.E., 1995. The late Archean Hemlo gold deposit, Ontario, Canada: a review and synthesis. *Ore Geol. Rev.* 9, 455–488.
- Pan, Y., Fleet, M.E., 1996. Rare earth element mobility during

- prograde granulite facies metamorphism: significance for fluorine. *Contrib. Mineral. Petrol.* 32, 251–262.
- Pan, Y., Eilect, M.E., Barnett, R.L., 1994. Rare-earth mineralogy and geochemistry of the Mattagami Lake volcanicogenic massive sulphide deposit, Quebec. *Can. Mineral.* 32, 133–147.
- Pearce, J.A., Peate, D.W., 1995. Tectonic implications of the composition of volcanic arc magmas. *Annu. Rev. Earth Planet. Sci.* 23, 251–285.
- Penczak, R.S., Mason, R., 1997. Metamorphosed Archean epithermal Au–As–Sb–Zn (Hg) vein mineralization at the Campbell mine, Northwestern Ontario. *Econ. Geol.* 92, 696–719.
- Perring, C.S., Barley, M.E., 1990. KIRb ratios. In: Ho, S.E., Groves, D.I., Bennett, J.M. (Eds.), *Gold deposits of the Archean Yilgarn Block, Western Australia: Nature, Genesis and Exploration Guides*. Geol. Dep. Univ. Extension, Univ. Western Australia Publ. 20, pp. 263–267.
- Perring, C.S., Groves, D.I., Shellabear, J.N., 1990. Ore geochemistry. In: Ho, S.E., Groves, D.I., Bennett, J.M. (Eds.), *Gold deposits of the Archean Yilgarn Block, Western Australia: Nature, Genesis and Exploration Guides*. Geol. Dep. Univ. Extension, Univ. Western Australia Publ. 20, pp. 93–101.
- Perring, C.S., McNaughton, N.J., 1990. Proterozoic remobilization of ore metals within Archean gold deposits: lead-isotope evidence from Norseman, Western Australia. *Aust. J. Earth Sci.* 37, 369–372.
- Perring, C.S., McNaughton, N.J., 1992. The relationship between Archean gold mineralization and spatially associated minor intrusions at the Kombalda and Norseman gold camps, Western Australia: Lead isotope evidence. *Mineral. Deposita* 27, 10–22.
- Peters, S.G., 1993a. Nomenclature, concepts and classification of oreshoots in vein deposits. *Ore Geol. Rev.* 8, 3–22.
- Peters, S.G., 1993b. Formation of oreshoots in mesothermal gold-quartz vein deposits: examples from Queensland, Australia. *Ore Geol. Rev.* 8, 277–301.
- Peters, S.G., Golding, S.D., 1989. Geologic, fluid inclusion, and stable isotope studies of granitoid-hosted gold-bearing quartz veins, Charters Towers, Northeastern Australia. In: Keays, R.R., Ramsay, W.R.H., Groves, D.I. (Eds.), *The Geology of Gold Deposits: the Perspective in 1988*. Econ. Geol. Monograph 6, pp. 260–273.
- Peters, S.G., Golding, S.D., Dowling, K., 1991. Melange- and sediment-hosted gold-bearing quartz veins, Hodgkinson gold field, Queensland, Australia: reply. *Econ. Geol.* 86, 197–200.
- Pettke, T., Diamond, L.W., 1997. Oligocene gold quartz veins at Brusson, NW Alps: Sr isotopes trace the source of ore-bearing fluid over a 10-km depth. *Econ. Geol.* 92, 389–406.
- Phillips, G.N., 1993. Metamorphic fluids and gold. *Miner. Mag.* 57, 365–374.
- Phillips, G.N., de Nooy, D., 1988. High-grade metamorphic processes which influence Archean gold deposits, with particular reference to Big Bell, Australia. *J. Meta. Geol.* 6, 95–114.
- Phillips, G.N., Groves, D.I., Kerrich, R., 1997. Factors in the formation of the giant Kalgoorlie gold deposit. *Ore Geol. Rev.*, in press.
- Phillips, G.N., Groves, D.I., Neall, F.B., Donnelly, T.H., Lambert, I.B., 1986. Anomalous sulphur isotope compositions in the Golden Mile, Kalgoorlie. *Econ. Geol.* 81, 2008–2015.
- Phillips, G.N., Hughes, M.J., 1996. The geology and gold deposits of the Victorian gold province. *Ore Geol. Rev.* 11, 255–302.
- Phillips, G.N., Powell, R., 1993. Link between gold provinces. *Econ. Geol.* 88, 1084–1098.
- Pickthorn, W.J., Goldfarb, R.J., Leach, D., 1987. Comment on ‘dual origins of lode gold deposits in the Canadian Cordillera’. *Geology* 15, 471–472.
- Platt, J., England, P.C., 1993. Convective removal of lithosphere beneath mountain belts: Thermal and mechanical consequences. *Amer. J. Sci.* 293, 307–336.
- Polat, A., Kerrich, R., 1997. Geodynamic controls on gold mineralization in greenstone belts of the Archean Superior Province. *Geol. Soc. Am. Abstr. Prog.* A–444.
- Poulsen, K.H., Card, K.D., Franklin, J.M., 1992. Archean tectonic and metallogenic evolution of the Superior Province of the Canadian Shield. *Precamb. Res.* 58, 25–54.
- Powell, R., Will, T.M., Phillips, G.N., 1991. Metamorphism in Archean greenstone belts: calculated fluid compositions and implications for gold mineralization. *J. Metal Geol.* 9, 141–150.
- Richards, J.P., Kerrich, R., 1993. The Porgera gold mine, Papua New Guinea: Magmatic hydrothermal to epithermal evolution of an alkalic-type precious metal deposit. *Econ. Geol.* 88, 1017–1052.
- Ridley, J.R., 1990. Constraints from alteration assemblages on gold-bearing hydrothermal fluid composition and source. In: Ho, S.E., Groves, D.I., Bennett, J.M. (Eds.), *Gold deposits of the Archean Yilgarn Block, Western Australia: Nature, Genesis and Exploration Guides*. Geol. Dep. Univ. Extension, Univ. Western Australia Publ. 20, pp. 268–272.
- Ridley, J.R., 1993. The relations between mean rock stress and fluid flow in the crust, with reference to vein- and lode-style gold deposits. *Ore Geol. Rev.* 8, 23–37.
- Ridley, J., Mikucki, E.J., Groves, D.I., 1996. Archean lode-gold deposits; fluid flow and chemical evolution in vertically extensive hydrothermal systems. *Ore Geol. Rev.* 10, 279–293.
- Robert, F., 1994. Vein fields in gold districts: the example of Val d'Or, southeastern Abitibi subprovince, Quebec, in, *Current Research 1994-C*. Geol. Surv. Canada, pp. 295–302.
- Robert, F., 1995. Diverse gold mineralization styles in Precambrian greenstone terranes in Canada. In: *Precambrian '95*, 126.
- Robert, F., Brown, A.C., 1986a. Archean gold-bearing quartz veins at the Sigma mine, Abitibi greenstone belt, Quebec: Part I. Geologic relations and formation of the vein system. *Econ. Geol.* 81, 578–592.
- Robert, F., Brown, A.C., 1986b. Archean gold-bearing quartz veins at the Sigma mine, Abitibi greenstone belt, Quebec: Part II. Vein paragenesis and hydrothermal alteration. *Econ. Geol.* 81, 593–616.
- Robert, F., Kelly, W.C., 1987. Ore-forming fluids in Archean gold-bearing quartz veins at the Sigma mine, Abitibi greenstone belt, Quebec, Canada. *Econ. Geol.* 82, 1464–1482.
- Robert, F., Bouillier, A.-M., Firdaous, K., 1995. Gold-quartz veins in metamorphic terranes and their bearing on the role of fluids in faulting. *J. Geophys. Res.* 100, 12861–12879.
- Roberts, R.G., 1988. Archean lode gold deposits. In: Roberts, R.G., Sheahan, P.A. (Eds.), *Ore Deposit Models*. Geosci. Can. 2, pp. 1–19.

- Roberts, R.J., 1986. The Carlin story. Rep. Nevada Bureau Mines Geol. 40, 71–80.
- Rock, N.M.S., Groves, D.I., Perring, C.S., Golding, S.D., 1989. Gold, lamprophyres, and porphyries; what does their association mean? In: Keays, R.R., Ramsay, W.R.H., Groves, D.I. (Eds.), *The Geology of Gold Deposits: the Perspective in 1988*. Econ. Geol. Monogr. 6, pp. 609–625.
- Roedder, E., 1984. Fluid inclusion evidence bearing on the environments of gold deposition. In: Foster, R.P. (Ed.), *Gold '82*. Geol. Soc. Zimbabwe, Spec. Publ. No. 1, pp. 129–163.
- Roedder, E., Bodnar, R.J., 1980. Geologic pressure determinations from fluid inclusion studies. Annu. Rev. Earth Planet. Sci. 8, 263–301.
- Roedder, E., Bodnar, R.J., 1997. Fluid inclusion studies of hydrothermal ore deposits. In: Barnes, H.L. (Ed.), *Geochemistry of Hydrothermal Ore Deposits*. Wiley, New York, pp. 657–698.
- Rogers, D.S., 1982. The geology of ore deposits of the number 8 Shaft area, Dome mine. In: Hodder, R.W., Petruk, W. (Eds.), *Geology of Canadian Gold Deposits*. Can. Inst. Min. Metall. Spec. Vol. 24, pp. 161–168.
- Romberger, S.B., 1986. The solution chemistry of gold applied to the origin of hydrothermal deposits. In: Clark, L.A. (Ed.), *Gold in the Western Shield*. Can. Inst. Min. Metall. Spec. Vol. No. 38, pp. 168–186.
- Romberger, S.B., 1990. The transport and deposition of gold in hydrothermal systems. In: Robert, F., Sheahan, P.A., Green, S.B. (Eds.), *Greenstone Gold and Crustal Evolution*, NUNA Conference Volume, pp. 61–66.
- Rutter, E.H., 1976. The kinetics of rock deformation by pressure solution. Phil. Trans. R. Soc. Lond. A 283, 203–219.
- Rye, R.O., 1987. Sulfur isotopic data. In: Roehler, H.W., Martin, P.L. (Eds.), *Geological investigations of the Vermillion Creek coal bed in the Eocene Niland Tongue of the Wasatch Formation, Sweetwater County, WY*. U.S. Geol. Surv. Prof. Pap., pp. 165–169.
- Rye, R.O., Ohmoto, H., 1974. Sulfur and carbon isotopes and ore genesis: a review. Econ. Geol. 69, 826–842.
- Rye, D.M., Rye, R.O., 1974. Homestake gold mine, South Dakota: I. Stable isotope studies. Econ. Geol. 69, 293–317.
- Rye, D.M., Doe, B.R., Delevaux, M.H., 1974. Homestake gold mine, South Dakota: II. Lead isotopes, mineralization ages, and source of lead in ores of the northern Black Hills. Econ. Geol. 69, 814–822.
- Sandiford, M., Keays, R.R., 1986. Structural and tectonic constraints on the origin of gold deposits in the Ballarat Slate Belt, Victoria. In: Keppie, J.D., Boyle, J.W., Haynes, S.J. (Eds.), *Turbidite Hosted Gold Deposits*. Geol. Assoc. Canada Spec. Pap. No. 32, pp. 15–24.
- Sandiford, M., Powell, R., 1991. Some remarks on high-temperature–low-pressure metamorphism in convergent orogens. J. Meta. Geol. 9, 333–340.
- Schidlowski, M., Eichmann, R., Junge, C.E., 1975. Precambrian sedimentary carbonates: carbon and oxygen isotope geochemistry and implications for the terrestrial oxygen budget. Precamb. Res. 2, 1–69.
- Schoell, M., Wellmer, F.W., 1981. Anomalous  $^{13}\text{C}$  depletion in early Precambrian graphites from Superior Province, Canada. Nature 290, 696–699.
- Scrimgeour, I., Sandiford, M., 1993. Early Proterozoic metamorphism at the Granites gold mine, Northern Territory: implications for the timing of fluid production in high temperature, low pressure terranes. Econ. Geol. 88, 1099–1113.
- Seward, T.M., 1973. Thio complexes of gold and the transport of gold in hydrothermal ore solutions. Geochim. Cosmochim. Acta 37, 370–399.
- Seward, T.M., 1991. The hydrothermal geochemistry of gold. In: Foster, R.P. (Ed.), *Gold Metallogeny and Exploration*. Blackie, pp. 37–62.
- Shelton, K.L., So, C.S., Chang, J.S., 1988. Gold-rich mesothermal vein deposits of the Republic of Korea; geochemical studies of the Jungwon gold area. Econ. Geol. 83, 1221–1237.
- Shelton, K.L., So, C.S., Haeussler, G.T., Lee, K.Y., Chi, S.J., 1990. Geochemical studies of the Tongyoung gold–silver deposits, Republic of Korea: Evidence of meteoric water dominance in a Te-bearing epithermal system. Econ. Geol. 85, 1114–1132.
- Shenberger, D.M., Barnes, H.L., 1989. Solubility of gold in aqueous sulphide solutions from 150 to 350 °C. Geochim. Cosmochim. Acta 53, 269–278.
- Sibson, R.H., 1985. A note on fault reactivation. J. Struct. Geol. 7, 751–754.
- Sibson, R.H., 1990. Faulting and fluid flow. In: Nesbitt, B.E. (Ed.), *Fluids in tectonically active régimes of the continental crust*. Min. Assoc. Can. Short Course 18, 93–132.
- Sibson, R.H., Robert, F., Poulsen, H., 1988. High angle faults, fluid pressure cycling and mesothermal gold–quartz deposits. Geology 16, 551–555.
- Smith, D.W., Craw, D., Koons, P.O., 1996. Tectonic hydrothermal gold mineralisation in the outboard zone of the Southern Alps, New Zealand. N.Z. J. Geol. Geophys. 39, 201–209.
- So, C.S., Yun, S.T., 1997. Jurassic mesothermal gold mineralization of the Samhwanghak Mine, Youngdong area, Republic of Korea: Constraints on hydrothermal fluid geochemistry. Econ. Geol. 92, 60–80.
- Spooner, E.T.C., Bray, C.J., Wood, P.C., Burrows, D.R., Callan, N.J., 1987. Au–quartz vein and Cu–Au–Ag–Mo–anhydrite mineralization, Hollinger–McIntyre Mines, Timmins, Ontario:  $^{13}\text{C}$  values (McIntyre) fluid inclusion gas chemistry, pressure (depth) estimation, and  $\text{H}_2\text{O}–\text{CO}_2$  phase separation as a precipitation and dilation mechanism. Ont. Geol. Surv. Misc. Paper 136, 35–56.
- Spooner, E.T.C., Robert, F., Crevier, M., Downes, M.J., 1989. Drilling the deep structure of a major Archean Au–quartz vein ore system: Sigma–Lamaque, Val d'Or, Quebec. Can. Cont. Dril. Prog. Rep. 89, 21–22.
- Starling, A., Gilligan, J.M., Carter, A.H.C., Saunders, R.A., 1989. High-temperature hydrothermal precipitation of precious metals on the surface of pyrite. Nature 340, 298–300.
- Strauss, H., 1986. Carbon and sulfur isotopes in Precambrian sediments from the Canadian Shield. Geochim. Cosmochim. Acta 50, 2653–2662.

- Stüwe, K., Sandiford, M., Powell, R., 1993a. Episodic metamorphism and deformation in low-pressure, high-temperature terranes. *Geology* 21, 829–832.
- Stüwe, K., Will, T.M., Zhou, S., 1993b. On the timing relationship between fluid production and metamorphism in metamorphic piles: some implications for the origin of post-metamorphic gold mineralisation. *Earth Planet. Sci. Lett.* 114, 417–430.
- Swager, C., 1993. Stratigraphy and structure in the Southeastern Goldfields Province. An international conference on crustal evolution, metallogeny and exploration of the Eastern Goldfields: extended abstracts, AGSO record 1993/94: 69–72.
- Taylor, H.P. Jr., 1974. The application of oxygen and hydrogen isotope studies to problems of hydrothermal alteration and ore deposition. *Econ. Geol.* 69, 843–883.
- Taylor, B.E., 1986. Magmatic volatiles: isotopic variations of C, H, and S. In: Valley, J.W., Taylor, H.P., O'Neil, J.R. (Eds.), *Stable isotopes in high temperature geologic processes*. Mineral. Soc. Amer. Rev. Mineral. 16, 185–226.
- Taylor, H.P., 1997. Oxygen and hydrogen isotope relationships in hydrothermal mineral deposits. In: Barnes, H.L. (Ed.), *Geochemistry of Hydrothermal Ore Deposits*, 3rd edn., Wiley, New York, pp. 229–303.
- Taylor, S.R., McLennan, S.M., 1985. *The Continental Crust: Its Composition and Evolution*. Blackwell, Oxford, 312 pp.
- Thode, H.G., Goodwin, A.M., 1983. Further sulphur and carbon isotope studies of late Archean iron formations of the Canadian Shield and the rise of sulphate reducing bacteria. *Precambrian Res.* 20, 337–356.
- Thompson, A.B., Connolly, J.A.D., 1992. Migration of metamorphic fluid: some aspects of mass and heat transfer. *Earth-Sci. Rev.* 32, 107–121.
- Travis, G.A., Woodall, R., Bartram, G.D., 1971. The geology of the Kalgoorlie gold field. In: Glover, J.E. (Ed.), *Proc. Symp. Archean Rocks*. Perth, 1970. *Geol. Soc. Aust., Spec. Publ.* 3, 175–190.
- Valley, J.W., 1986a. Stable isotope geochemistry of metamorphic rocks. *Rev. Mineral.* 16, 445–489.
- Valley, J.W., 1986b. Fluid-absent metamorphism in the Adirondacks. *LPI Techn. Rep.*, 86-04: 107–111.
- van Hees, E.H.P., Kesler, S.E., 1990. Geochemistry of fluid inclusions in gold, Porcupine camp, Ontario. In: Robert, F., Sheahan, P.A., Green, S.B. (Eds.), *Greenstone Gold and Crustal Evolution*. NUNA Conference Volume, 222.
- Vearncombe, J.R., 1993. Quartz vein morphology and implications for formation depth and classification of Archaean gold-vein deposits. *Ore Geol. Rev.* 8, 407–424.
- Veizer, J., Hoefs, J., Lowe, D.R., Thurston, P.C., 1989a. Geochemistry of Precambrian carbonates: II. Archean greenstone belts and Archean sea water. *Geochim. Cosmochim. Acta* 53, 859–871.
- Veizer, J., Hoefs, J., Ridder, R.H., Jensen, L.S., Lowe, D.R., 1989b. Geochemistry of Precambrian carbonates: I. Archean hydrothermal systems. *Geochim. Cosmochim. Acta* 53, 845–857.
- Vitryk, M.O., Krouse, H.R., Skakun, L.Z., 1994. Fluid evolution and mineral formation in the Beregovo gold-base metal deposit, Transcarpathia, Ukraine. *Econ. Geol.* 89, 547–565.
- Weaver, B.L., Tarney, J., 1993. Elemental depletion in Archean granulite-facies rocks. In: Atherton, M.P., Gribble, C.D. (Eds.), *Shiva Publishing*, Cheshire, UK, pp. 250–263.
- Weir, R.H., Kerrich, D.M., 1987. Mineralogic, fluid inclusion and stable isotope studies of several gold mines in the Mother Lode, Tuolumne and Mariposa counties, California. *Econ. Geol.* 82, 328–344.
- Whitehead, R.E.S., Davies, J.F., Cameron, R.A., Duff, D., 1981. Carbonate, alkali and arsenic anomalies associated with gold mineralization, Timmins area. *Ont. Geol. Surv. Misc. Pap.* 98, 318–333.
- Wilkins, C., 1993. A post-deformational, post-peak metamorphic timing for mineralization at the Archean Big Bell gold deposit, Western Australia. *Ore Geol. Rev.* 7, 439–483.
- Wilkinson, J.J., Johnston, J.D., 1996. Pressure fluctuations, phase separation, and gold precipitation during seismic fracture propagation. *Geology* 24, 395–398.
- Wilson, G.C., Rucklidge, J.C., 1987. Geology, geochemistry and economic significance of carbonaceous host rocks in gold deposits of the Timmins area. *Ont. Geol. Surv. Misc. Pap.* 136, 66–76.
- Witt, W.K., 1991. Regional metamorphic controls on alteration associated with gold mineralization in the Eastern Goldfields Province, Western Australia: Implications for the timing and origin of Archean lode-gold deposits. *Geology* 19, 982–985.
- Wood, S.A., Williams-Jones, A.E., 1994. The aqueous geochemistry of the rare-earth elements and yttrium: 4. Monazite solubility and REE mobility in exhalative massive sulphide-depositing environments. *Chem. Geol.* 115, 47–60.
- Wood, P.C., Burrows, D.R., Thomas, A.V., Spooner, E.T.C., 1986. The Hollinger-McIntyre Au-quartz vein system, Timmins, Ontario, Canada: Geological characteristics, fluid properties and light stable isotope geochemistry. In: Macdonald, A.J. (Ed.), *Gold '86. Konsult International*, pp. 56–80.
- Wyman, D.A., Kerrich, R., 1988. Archean lamprophyres, gold deposits and transcrustal structures: implications for greenstone belt gold metallogeny. *Econ. Geol.* 83, 454–459.
- Yardley, B.W.D., Banks, D.A., Bottrill, S.H., Diamond, L.W., 1993. Post-metamorphic gold-quartz veins from N.W. Italy: the composition and origin of the ore fluid. *Miner. Mag.* 57, 407–422.
- Zhang, X., Nesbitt, B.E., Muehlenbachs, K., 1989. Gold mineralization in the Okanagan Valley, Southern British Columbia: fluid inclusion and stable isotope studies. *Econ. Geol.* 84, 410–424.
- Zweng, P.L., Martenson, J.K., Dalrymple, G.B., 1993. Thermochronology of the Camflo Gold Deposit, Malartic, Quebec: implications for magmatic underplating and the formation of gold-bearing quartz veins. *Econ. Geol.* 88, 1700–1721.